High Energy Density Experiments: Relativistic particle beams and magnetic field generation in high intensity laser-plasma interactions

Karl Krushelnick

Center for Ultrafast Optical Science (CUOS), University of Michigan, Ann Arbor

and

Laboratoire d’Optique Appliquée (LOA), ENSTA, Paris

Outline

Relativistic HEDP relevant to laboratory astrophysics?

High intensity lasers

- ultra-high magnetic fields
  - dynamics/reconnection
- particle beams
  - probes of high fields
  - positron beams (towards electron positron jets?)
  - relativistic beam instabilities

Table-top experiments?

Outline

- Magnetic fields in laser produced plasmas
- **Part 1:** Ultra-high fields from short pulse interactions
- **Part 2:** Magnetic fields in hohlraums
  - Long-pulse (ns) interactions
  - Driven magnetic reconnection
- **Part 3:** Relativistic beams from laser produced plasmas
  - Relativistic probing
  - Positron beams
  - Weibel instability

Summary

- Ultra high magnetic fields (~ 1GGauss) are produced during high intensity (> 10^{19}W/cm^2) laser plasma interactions.

- Lower fields produced by long (nanosecond) pulses are shown to greatly affect the dynamics of the interaction (reconnection and jet formation)

- Relativistic particle beams generated in plasmas may offer a unique experimental environment for investigating plasma physics relevant for astrophysics

History of laser intensity

(courtesy G. Mourou)

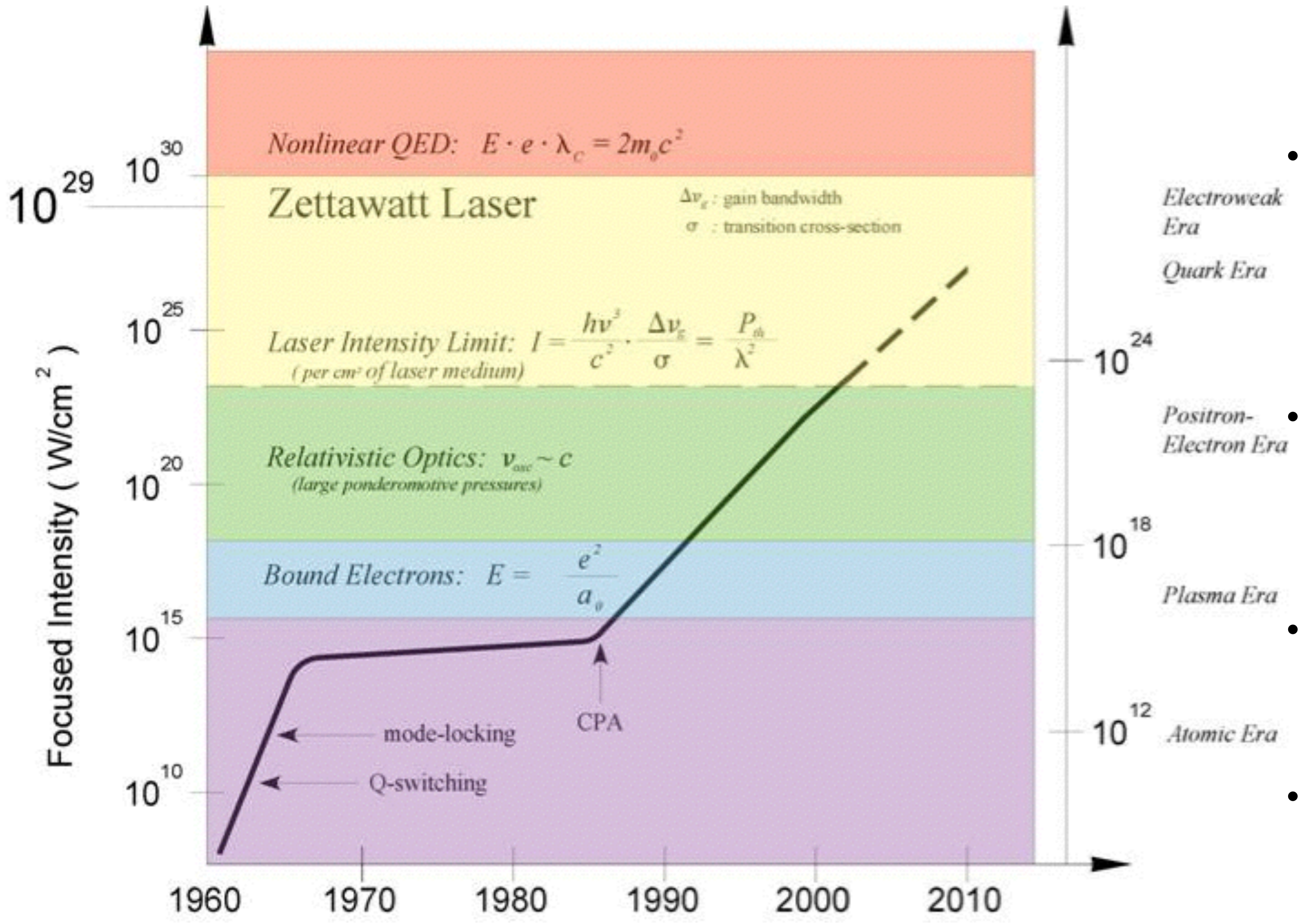

- Terawatt = 10^{12} W
  (Total electrical power generated in the world ~ 5 T W)
- Petawatt = 10^{15} W
  (Total sunlight on earth ~ 100 PW)
- Exawatt = 10^{18} W
  (ELI?)
- Zettawatt = 10^{21} W

High power/intensity laser systems

(power > 100TW, from C. Barty LLNL)

2010 ICUIL World Map of Ultrahigh Intensity Laser Capabilities

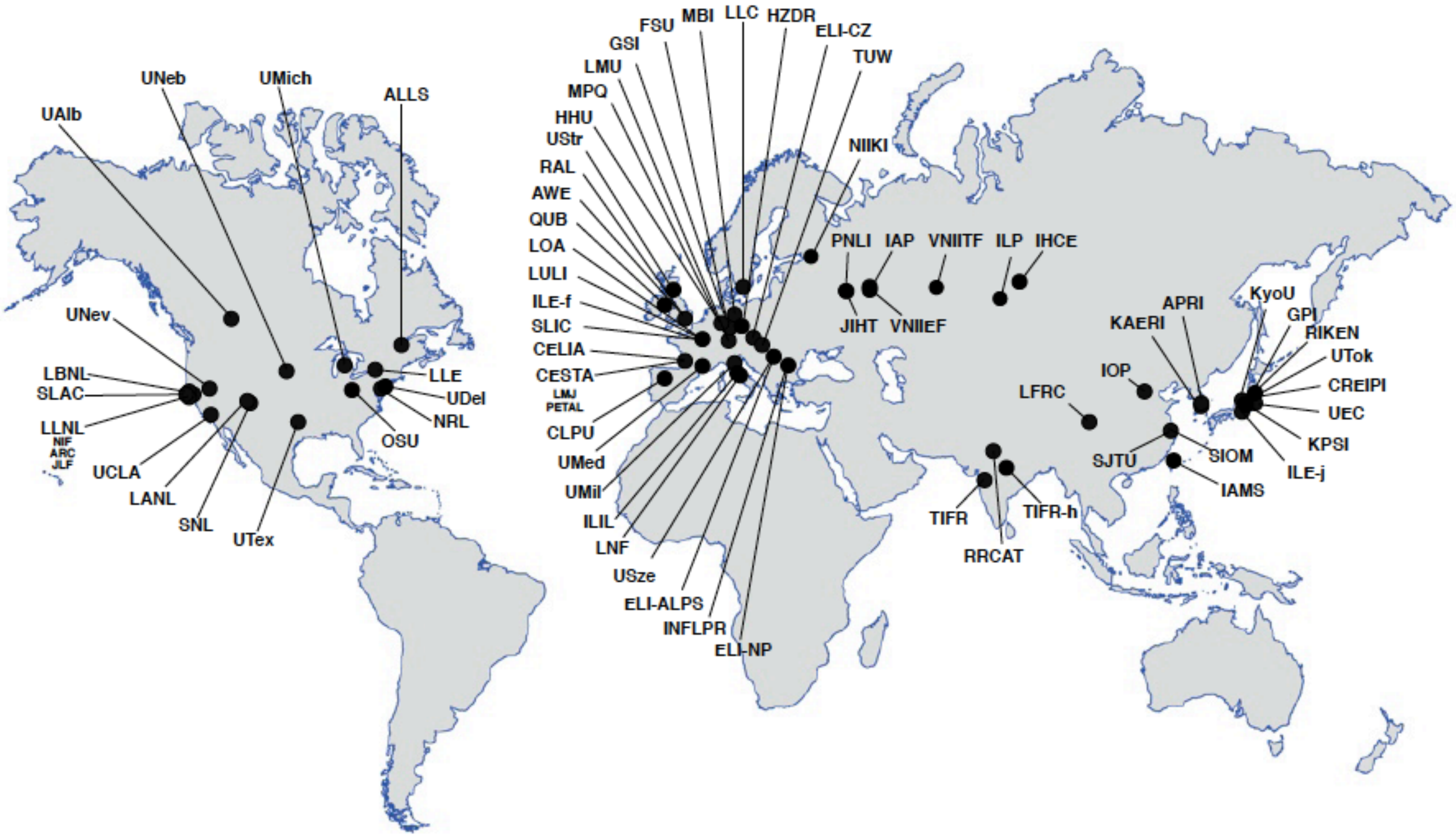

HERCULES Laser systems at Michigan enables 300 TW pulses

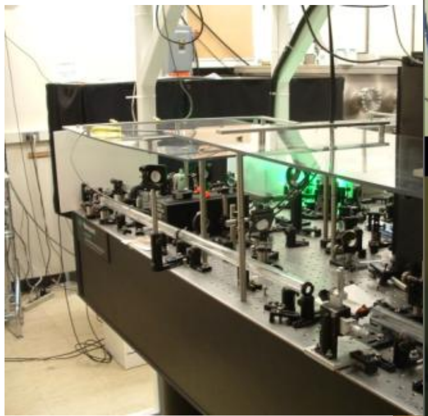

Pulse duration 30 fs
Repetition rate 0.1 Hz
Wavelength 810 nm

Petawatt scale compressor and beamlines (< 15 J, 30 fsec)

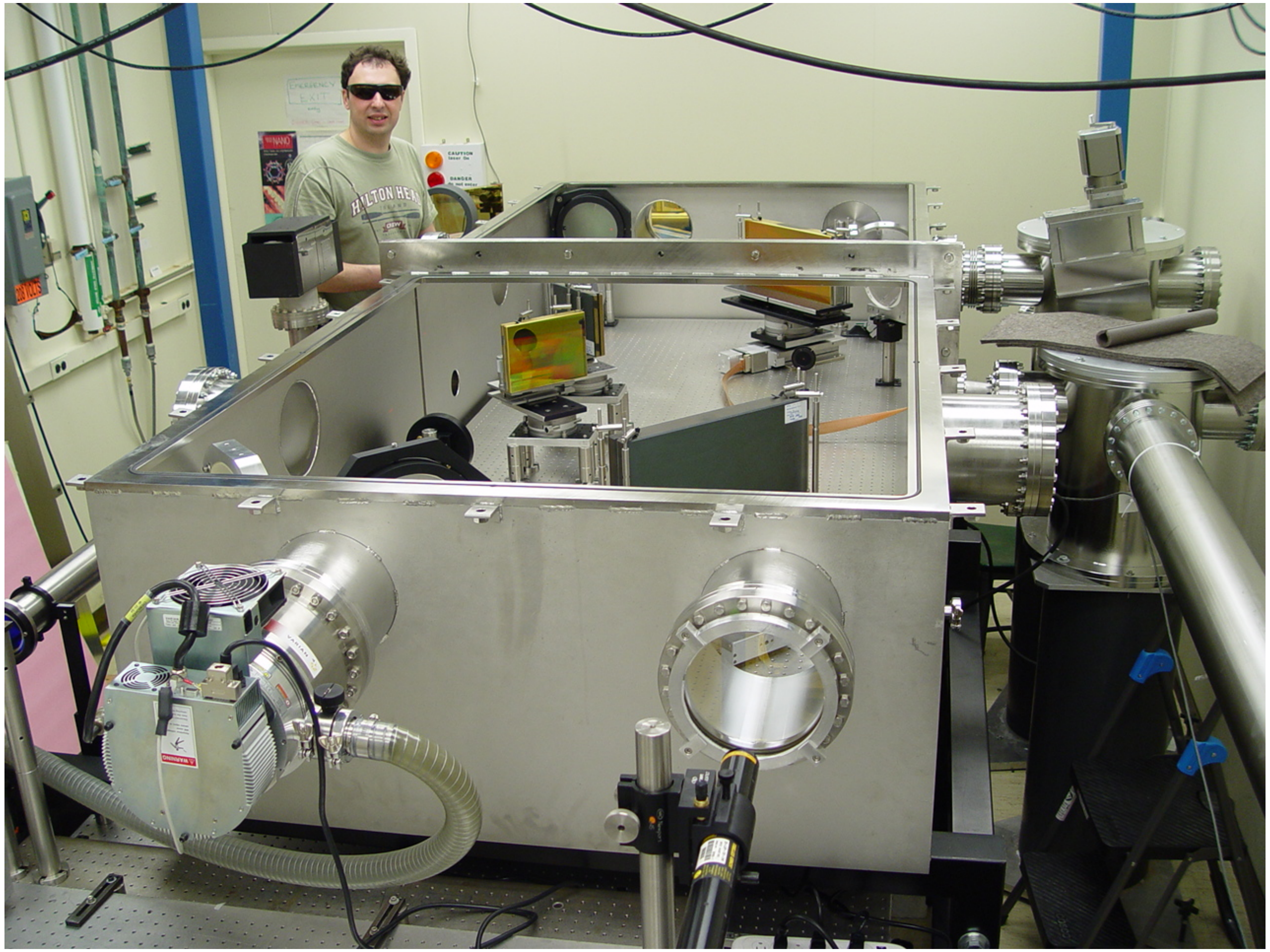

At high laser intensities photon-particle and particle-particle interactions become relativistic

High field interaction is dominated by electron coupling via Lorentz force

$$\underline{F} = \underline{E} + \underline{v}\times\underline{B}$$

10^{15} 10^{16} 10^{17} 10^{18} 10^{19} 10^{20} 10^{21} 10^{22} 10^{23} W/cm^2

atomic processes
collisional absorption
non-linear optics

relativistic electrons
nuclear processes
γ-production
ultrahigh E/B fields

e^+e^- plasmas
pion production
relativistic protons
QED

Typical parameters > 10^{20} W/cm^2	
Electric fields	10^{12} V/m
Magnetic fields	100's MG
Pressure	Gbar
Temperature	keV or 10^7 K
Acceleration	10^{21} g
Density	Nc or solid

Part 1: Mechanisms of magnetic field generation in intense laser plasma interactions

A. Non parallel temperature and density gradients.

$$\frac{\partial \mathbf{B}}{\partial t} = -\nabla \times \mathbf{E}$$

$$\frac{\partial \mathbf{B}}{\partial t} = -\nabla \times \left(\frac{\nabla p_e}{n_e e} \right) = \frac{k_e \nabla T_e \times \nabla n_e}{n_e e}$$

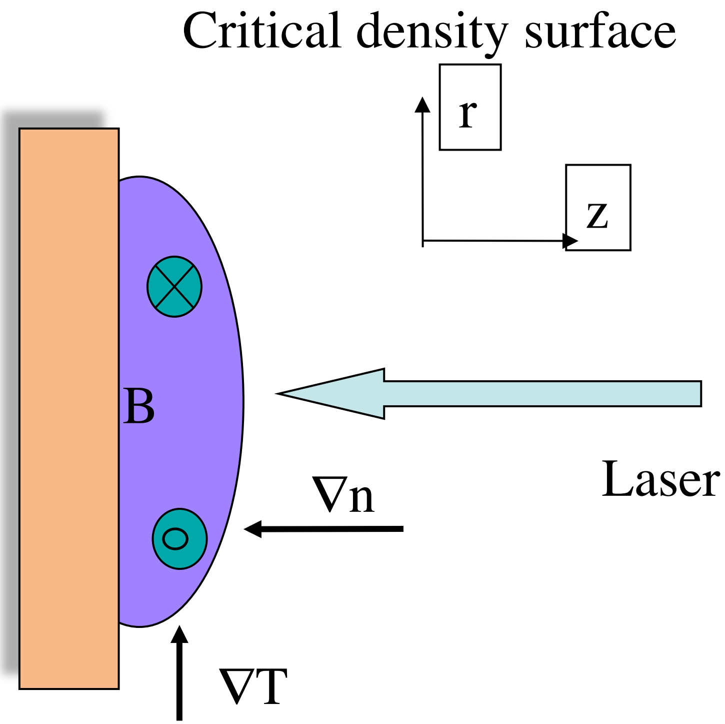

B. DC currents generated by the spatial and temporal variation of the ponderomotive force of the incident laser pulse $\mathbf{B}_{dc} \sim \mathbf{B}_{laser}^*$

R.N.Sudan, Phys. Rev. Lett., ***70,*** *3075 (1993)*

C. Current due to fast electrons generated during the interaction (Weibel instability)

Short pulse laser plasma interactions

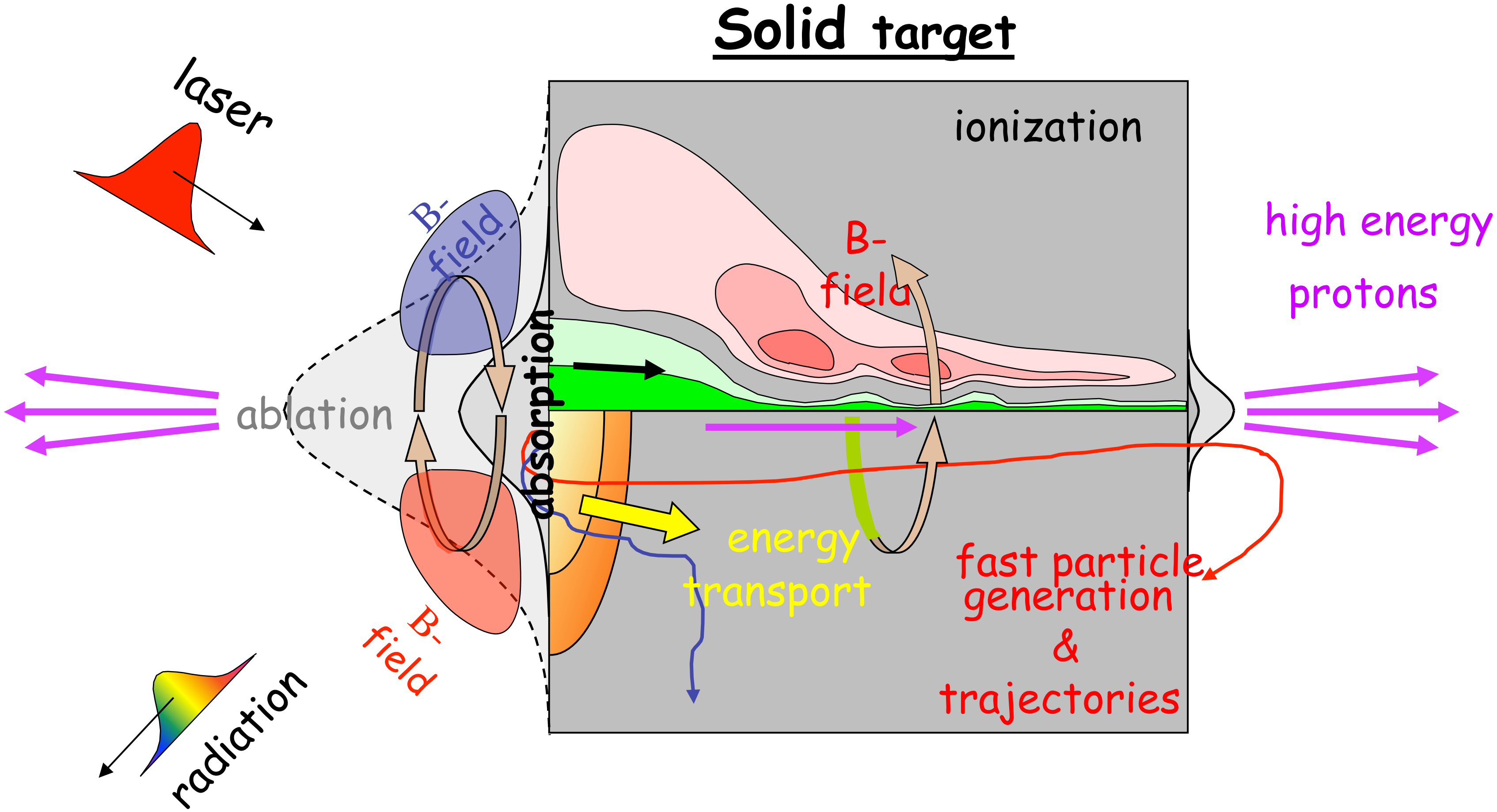

Mechanisms of magnetic field generation in high power laser plasma interactions

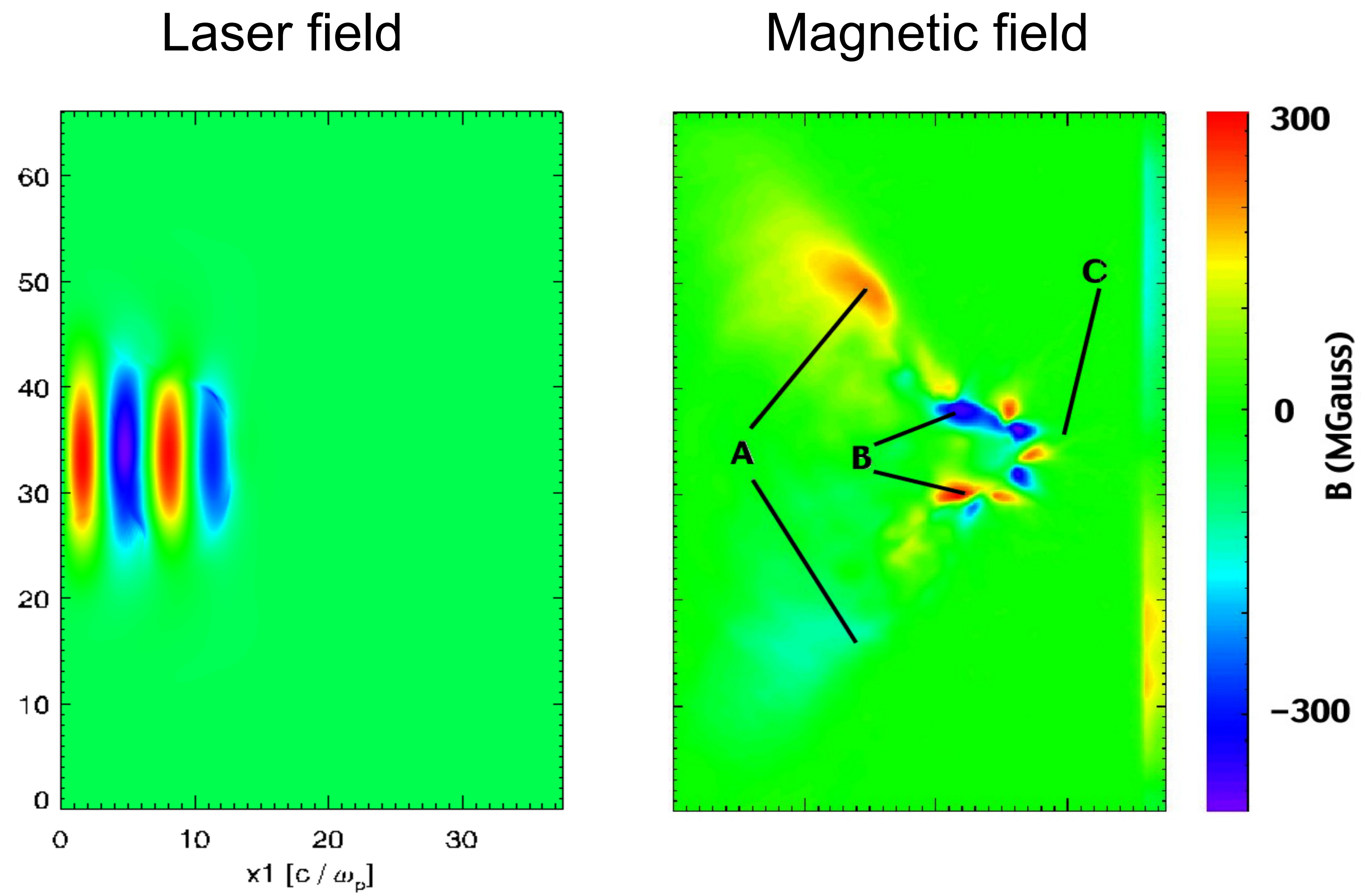

Experimental schematic

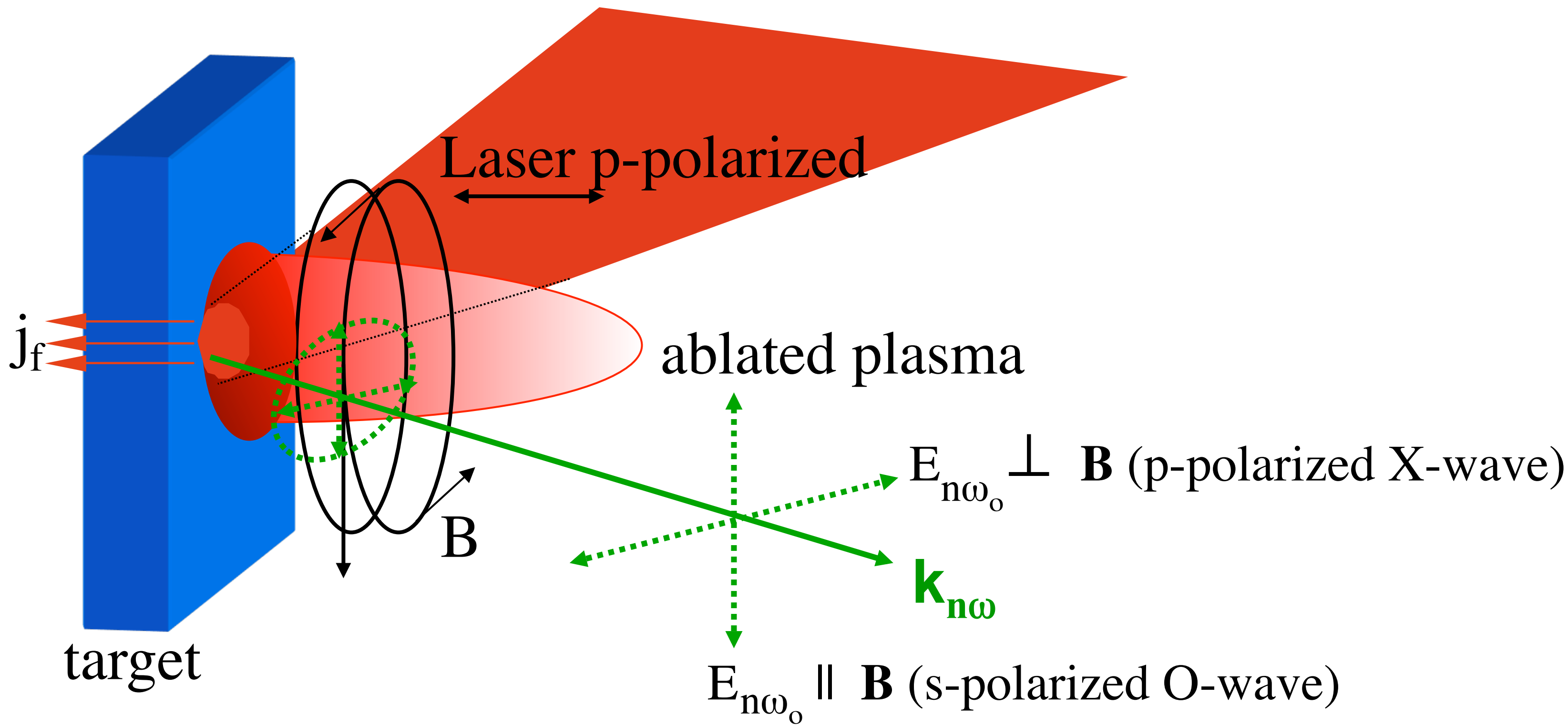

EM wave propagation in magnetized plasma

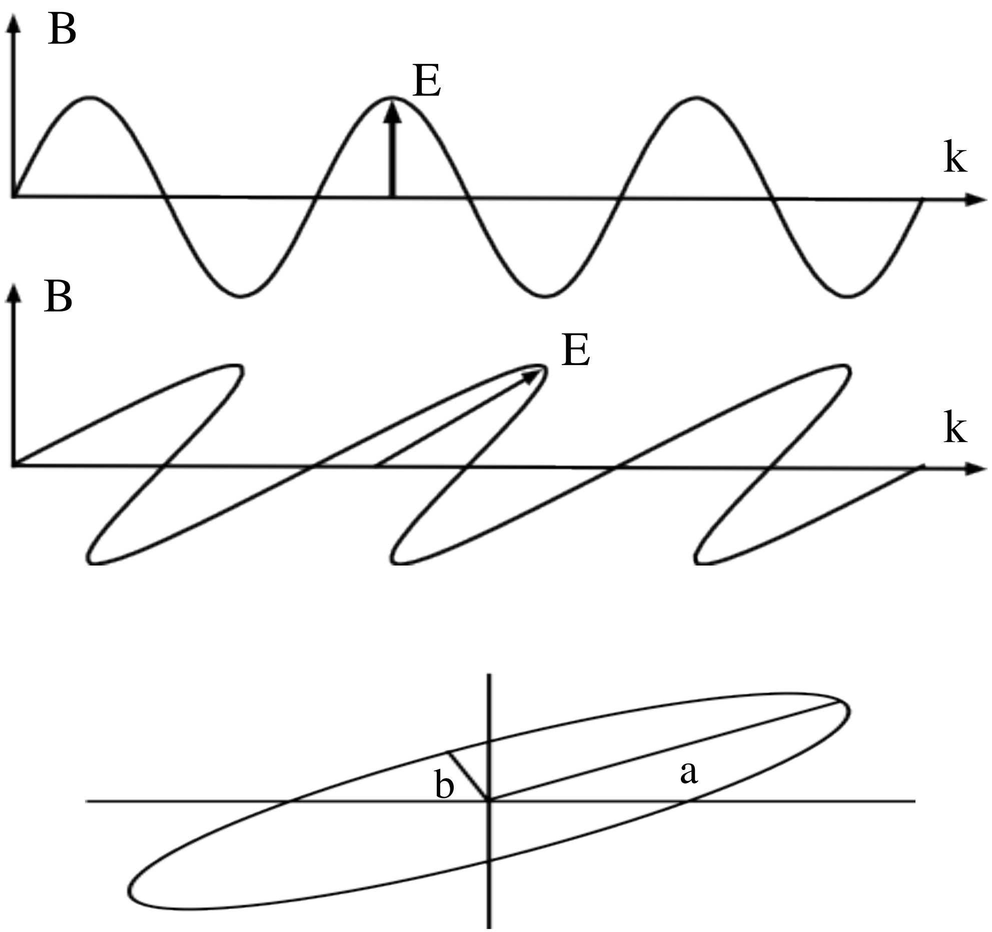

- Ordinary Wave (O)

$$\mu_O^2 = 1 - \frac{\omega_{pe}^2}{\omega_0^2}$$

- Extraordinary Wave (X)

$$\mu_X^2 = 1 - \frac{\frac{\omega_{pe}^2}{\omega_0^2}\left(1 - \frac{\omega_{pe}^2}{\omega_0^2}\right)}{1 - \frac{\omega_{pe}^2}{\omega_0^2} - \frac{\omega_{ce}^2}{\omega_0^2}}$$

- Ellipticity

$$\frac{b}{a} = 2.49 \text{ x } 10^{-21} \lambda_{\mu m}^3 \int n B_{MG}^2 dl$$

X-Wave cutoffs

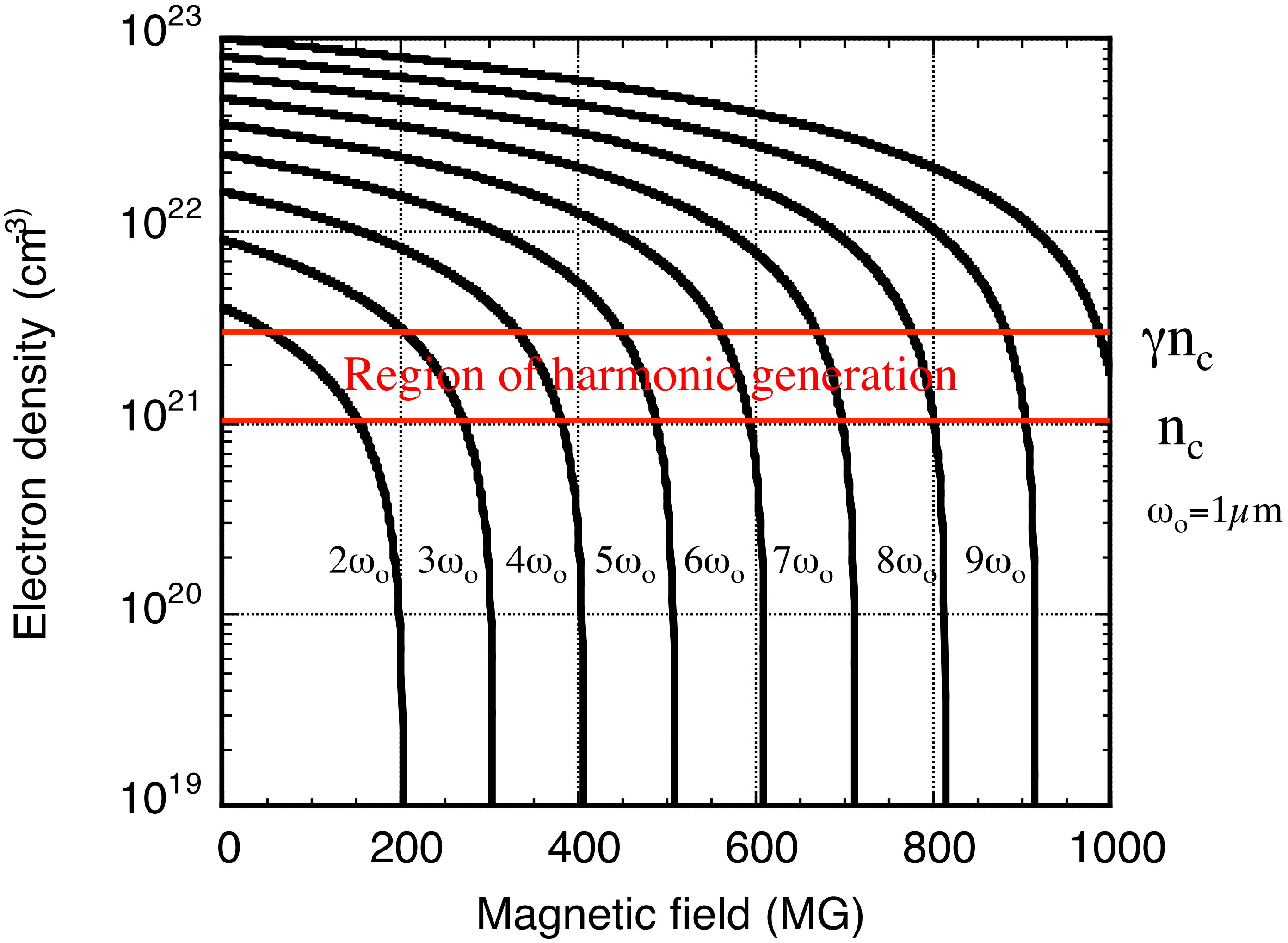

VULCAN laser system
(Rutherford Appleton Lab in UK)

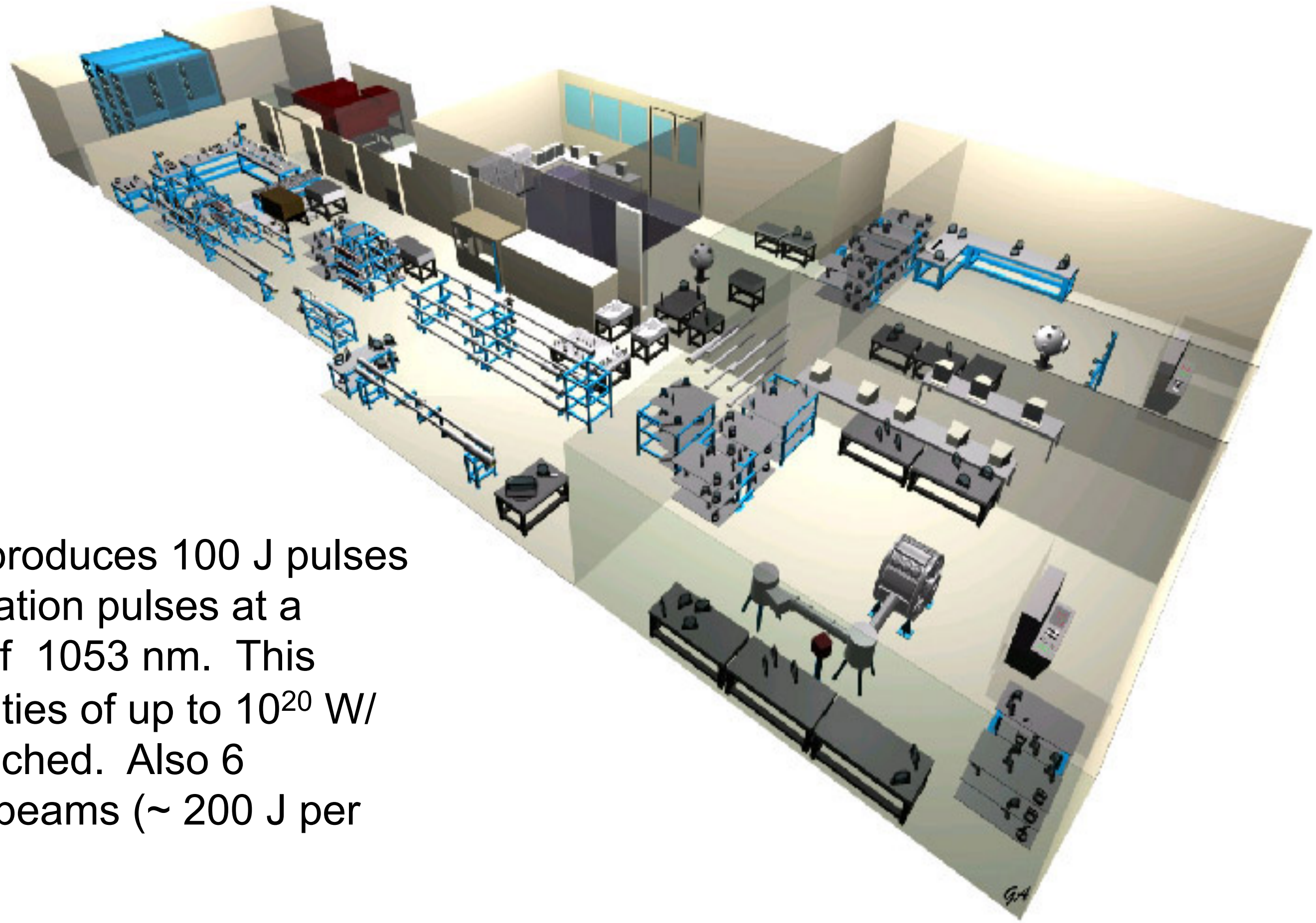

Vulcan CPA produces 100 J pulses in 1 psec duration pulses at a wavelength of 1053 nm. This allows intensities of up to 10^{20} W/cm^2 to be reached. Also 6 nanosecond beams (~ 200 J per beam).

Observation of cutoffs – fields at least 400 MG

(Tatarakis *et al. Nature*, 415, 280 (2002))

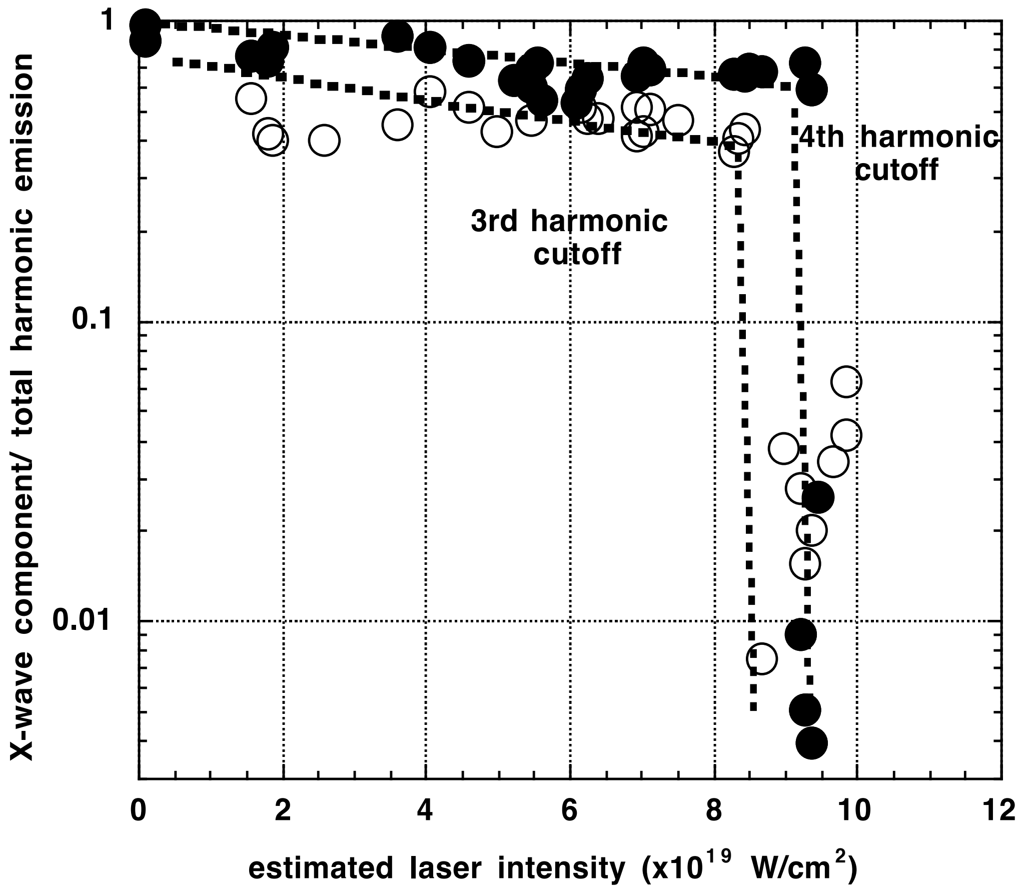

High Order Harmonic Generation
(I ~ 10^{20} W/cm^2)

- Relativistic nonlinear motion of critical surface gives rise to odd and even harmonics

- Need well defined reflective surface

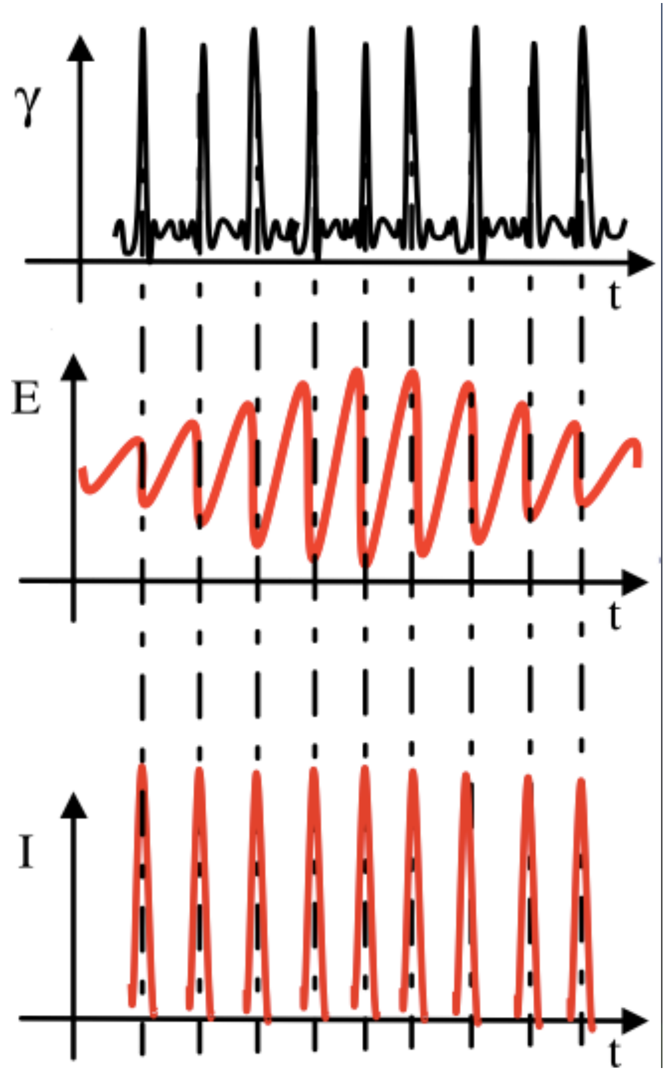

Harmonics of the laser frequency are emitted at very high orders

(up to 4000th recently, Dromey et al., PRL 2008)

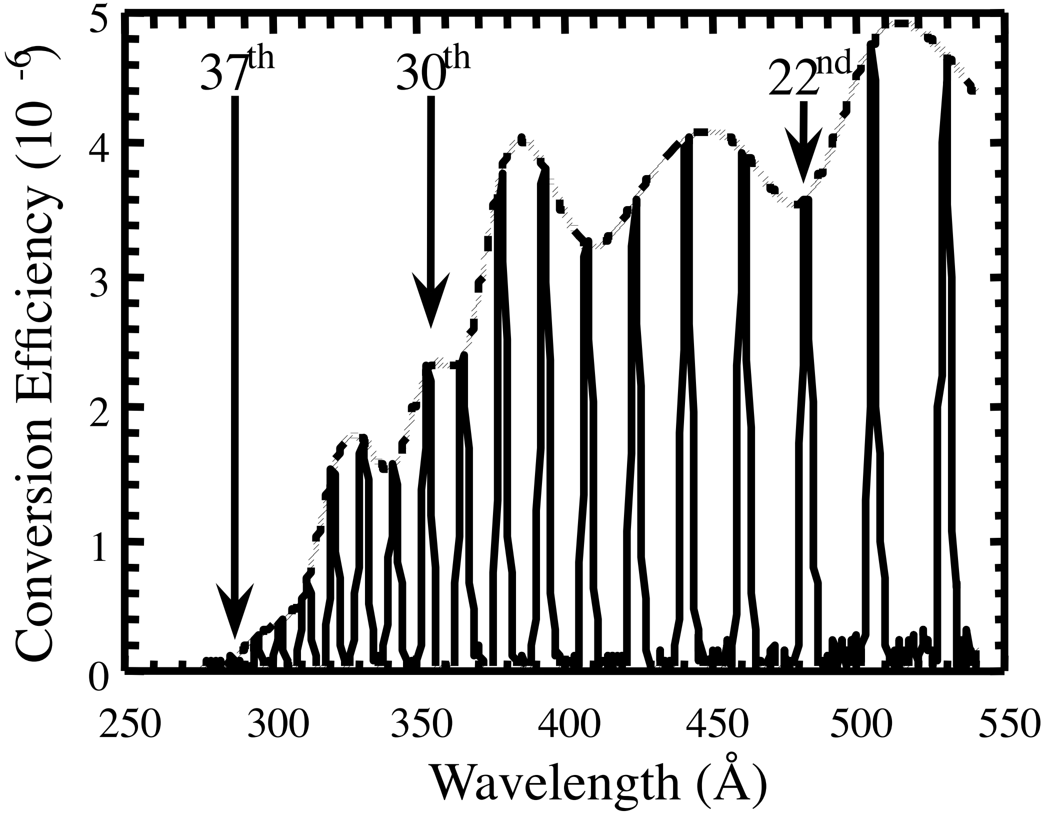

XUV-Polarimetry of High Harmonics

Measured Polarisation of the Harmonics:

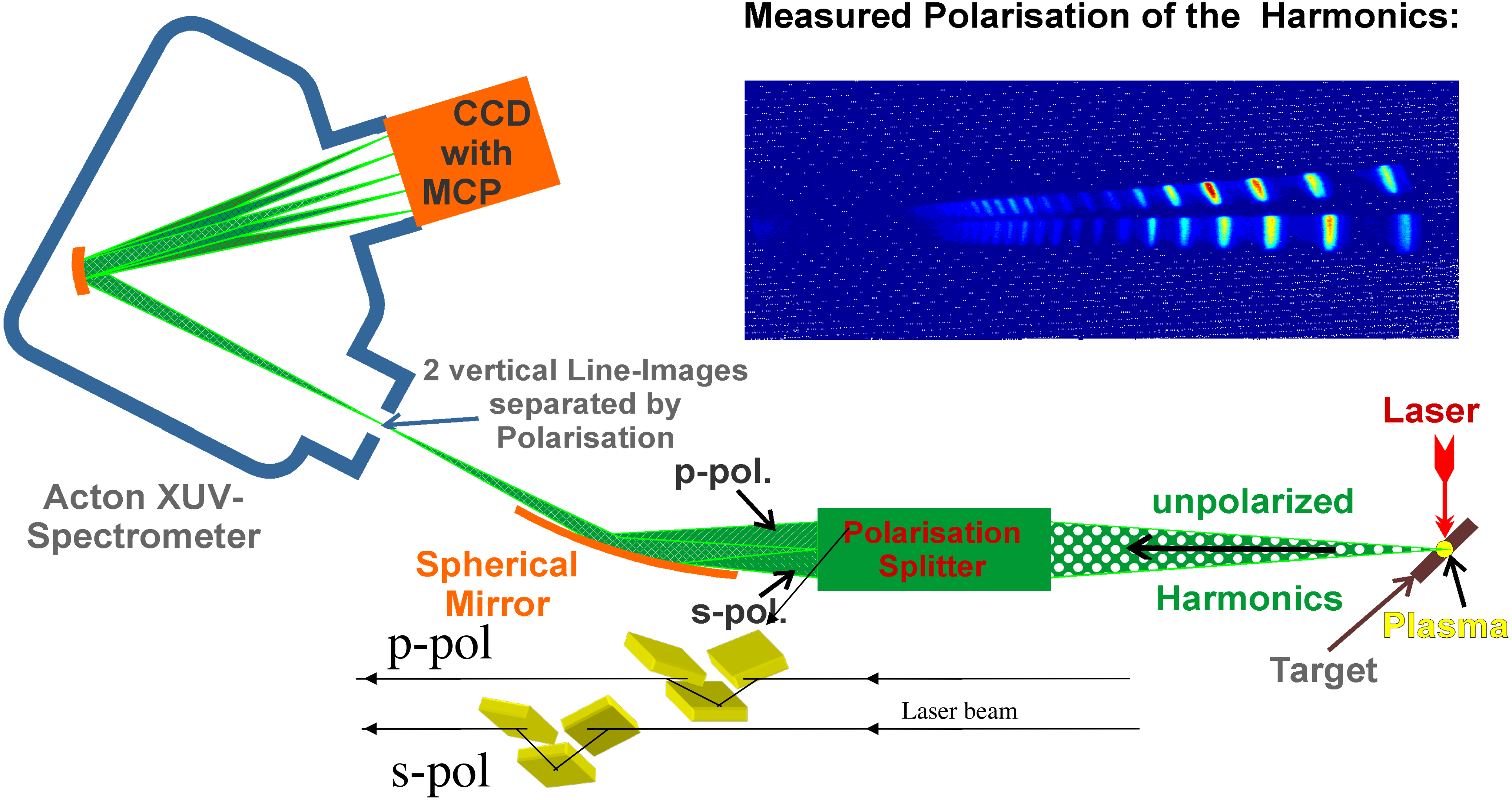

Harmonic depolarization follows λ^3 scaling

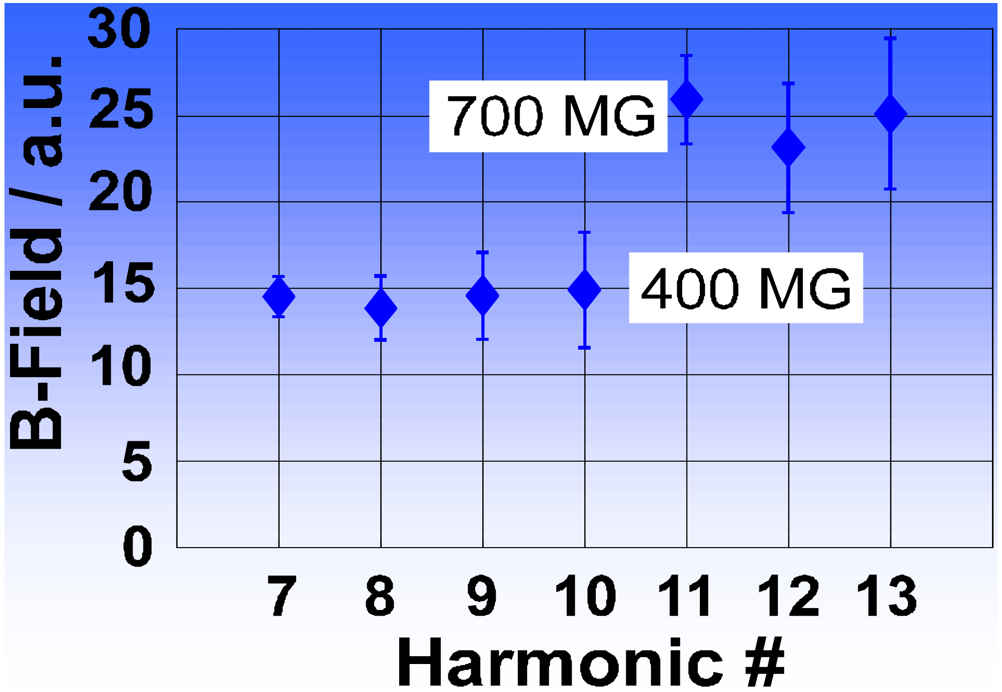

$$\frac{b}{a} = 2.49 \text{ x } 10^{-21} \lambda_{\mu m}^{3} \int n B_{MG}^{2} dl$$

b/a is the induced ellipticity

• this suggests that fields in the higher density regions of plasma are up to 0.7 ± 0.1 Gigagauss (Wagner et al., PRE, 2004)

Large B-fields - Summary

- measurements of high order harmonics can provide useful information about the physics of high intensity laser interactions with high density plasmas

- polarimetry measurements of harmonic emission imply the generation of magnetic fields approaching ~ 1 GigaGauss

ALSO OTHER RECENT MEASUREMENTS

- spatially resolved measurements agree with simulations that magnetic field asymmetries are produced from 45 degree angles of incidence (Gopal et al., PoP 2008)

- temporally resolved measurements suggest that the growth rate of the magnetic field is ~ $I^{1/2}$ suggesting the ponderomotive force is the principal field generation mechanism

Large scale differences are found in the magnetic fields in various systems

B (Gauss)

10^{-5}	Galactic magnetic fields
6×10^{-1}	Earth's magnetic field
4×10^{3}	Sunspot magnetic fields
10^{5}	Tokamak confinement fields for fusion
10^{6}	Pulsed laboratory magnets (msec)
10^{7}	Explosive compression of magnetic fields in plasmas (4 - 8 μsec)

7×10^{8} Intense laser-produced magnetic fields

10^{9}	neutron star atmospheres
10^{14-15}	magnetic pulsars ("magnetars")

Such laser-produced fields approach those observable in astrophysical phenomena

In the center of the Crab nebula a pulsar (neutron star) rotates with a speed of
30 times per second. The blue color shows the area where electrons spin in the huge magnetic field.

Photon bubble instability

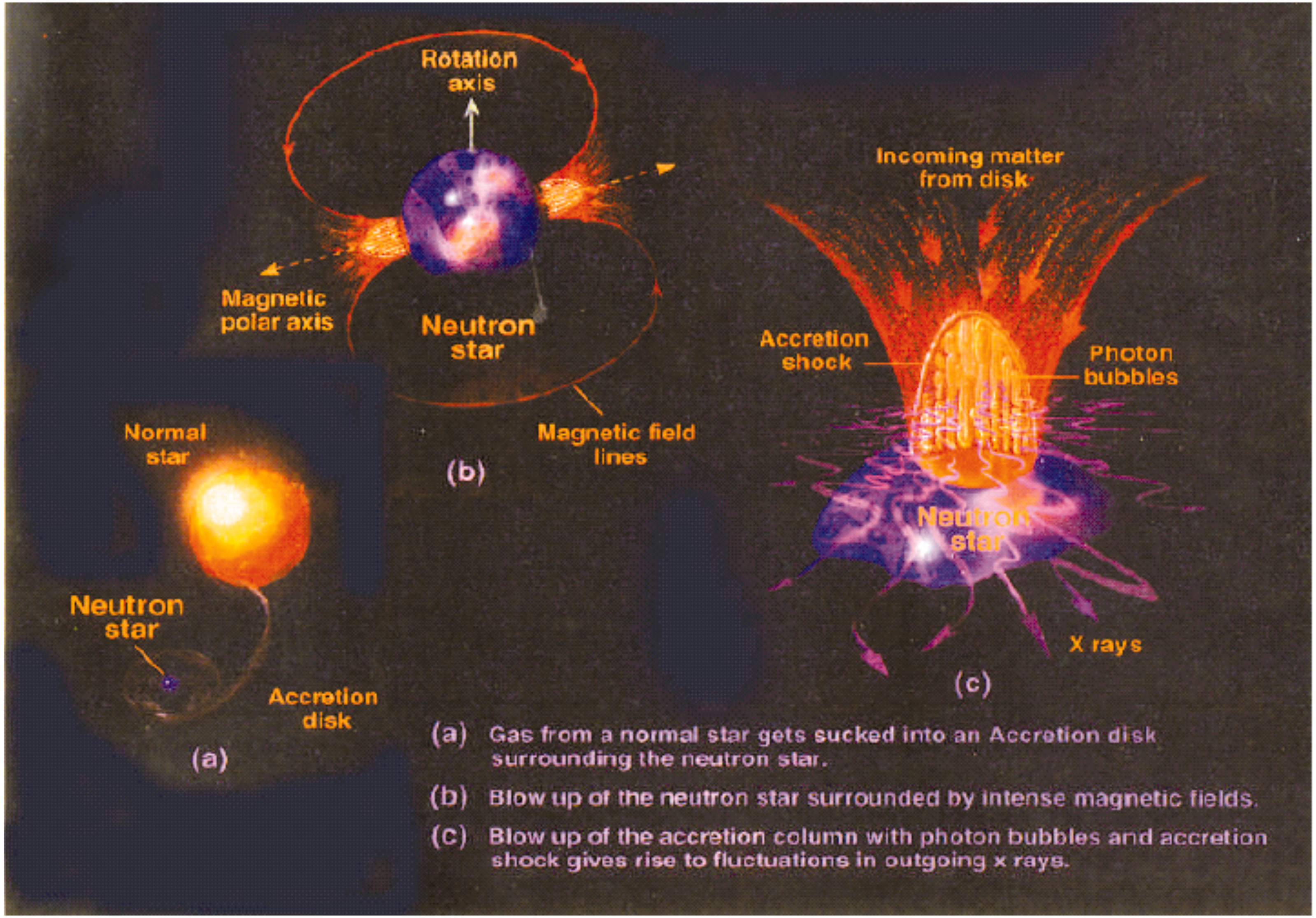

Neutron stars in the lab?
- experiment suggested by Richard Klein (UC Berkeley)

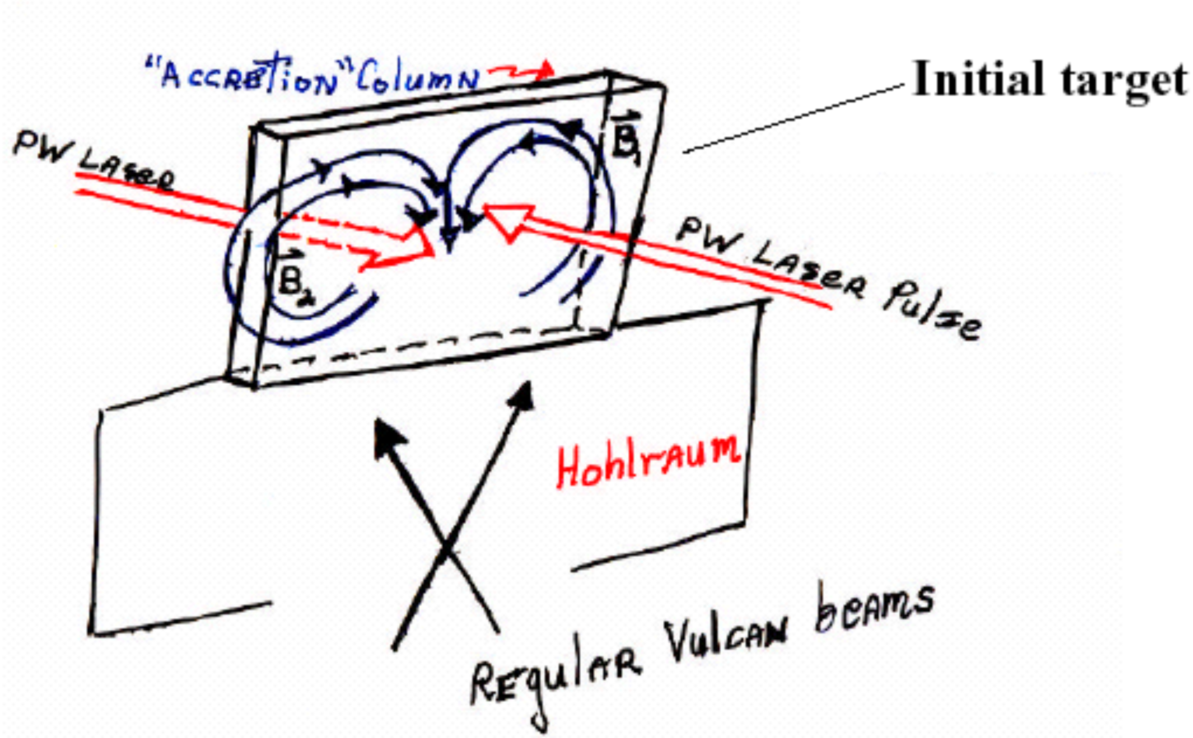

Split beam configuration

Part 2: Reconnection in HEDP fields
Dual-beam laser-solid interaction geometry

- consider the plasma created by two laser beams focused in close proximity to each other
- the role of the magnetic field on the plasma dynamics and heating
- self-organization of the magnetic field topology

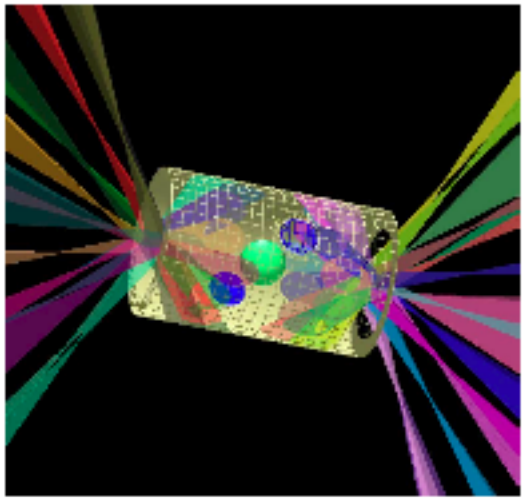

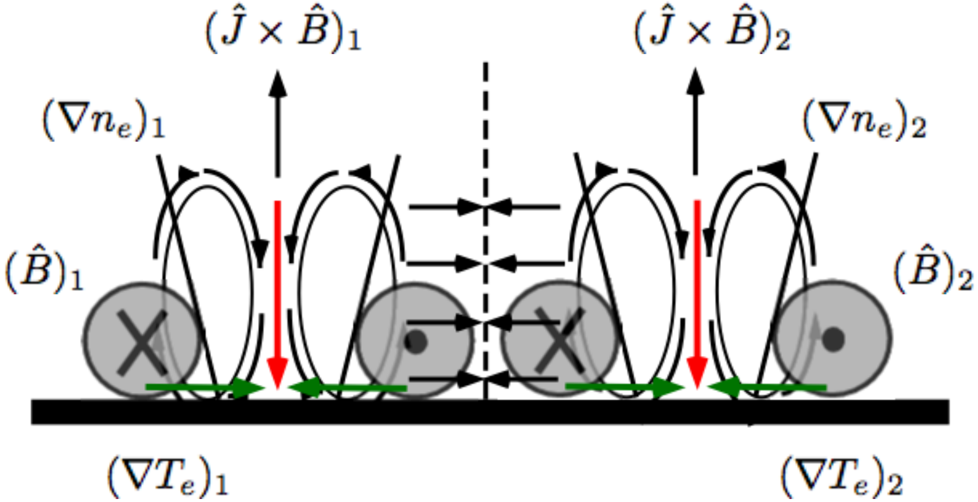

Inertial confinement fusion

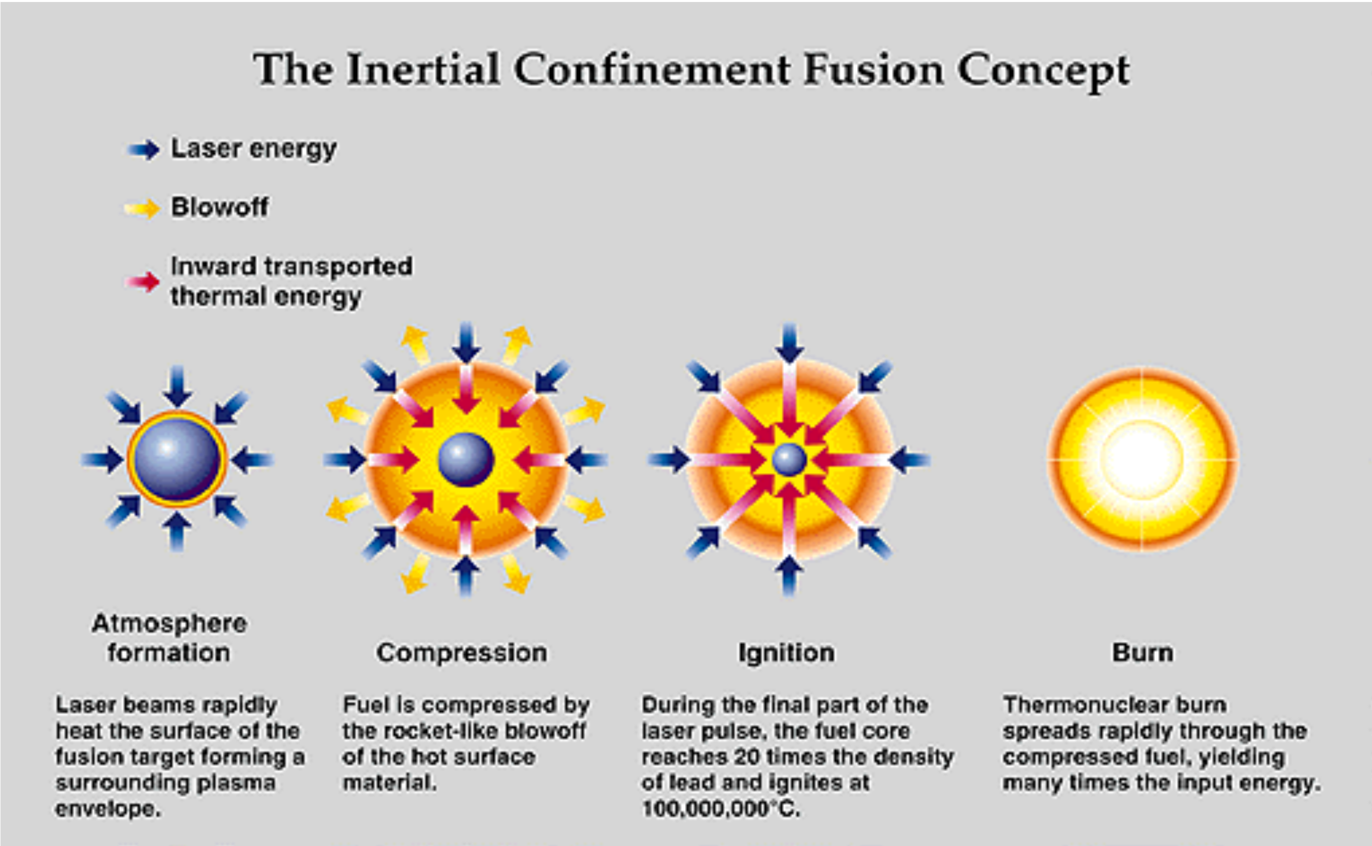

Can use lasers or X-rays from a z-pinch as driver for implosion of DT pellets

Many large scale facilities for ICF are under construction throughout the world

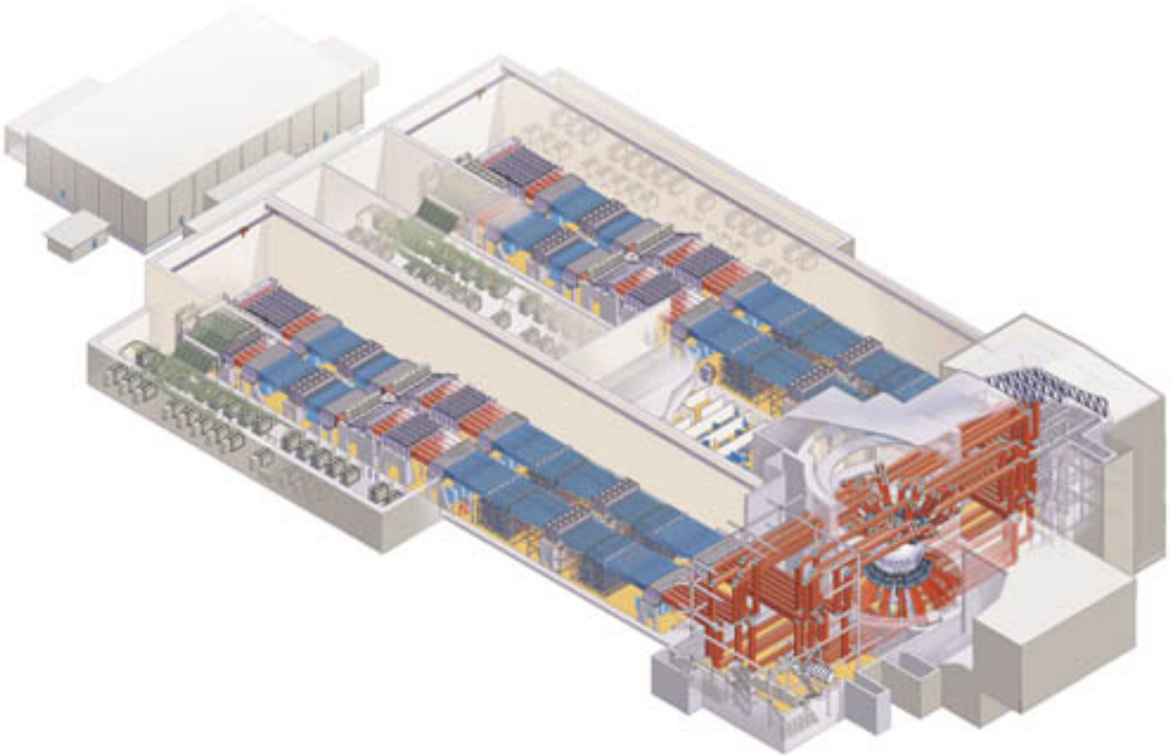

<u>Ignition scale lasers</u>

National Ignition facility (NIF), USA

Laser Megajoule (LMJ), France

<u>Petawatt lasers</u>

- Orion (AWE) UK
- OmegaEP (Rochester), USA
- FIREX, JAPAN
- LIL Petawatt, France
- LULI 2000, Ecole Polytechnique, France

Long-pulse (ns) solid target interactions
Magnetic field generation: dual beam geometry

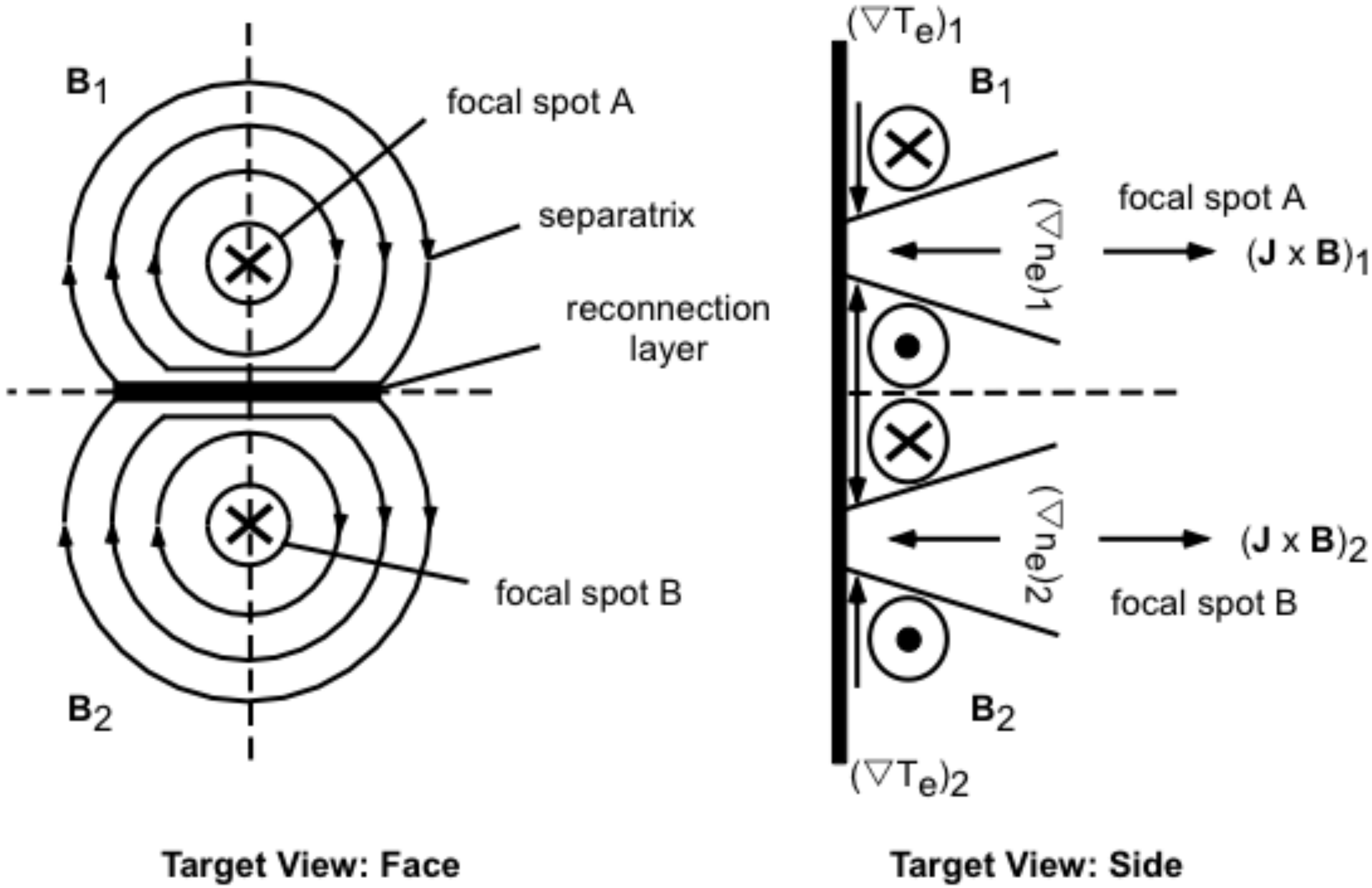

First experiment - objectives

- create the dual beam solid target interaction geometry
  - consider focal spot separation
  - consider target-Z effects (Al, Au)
- observe the generated plasma dynamics
- characterize the plasma parameter evolution
- evidence for a driven magnetic reconnection?
- <u>Main diagnostic – particle beam probing</u>

Proton deflectometry has been developed as a quantitative technique for plasma probing

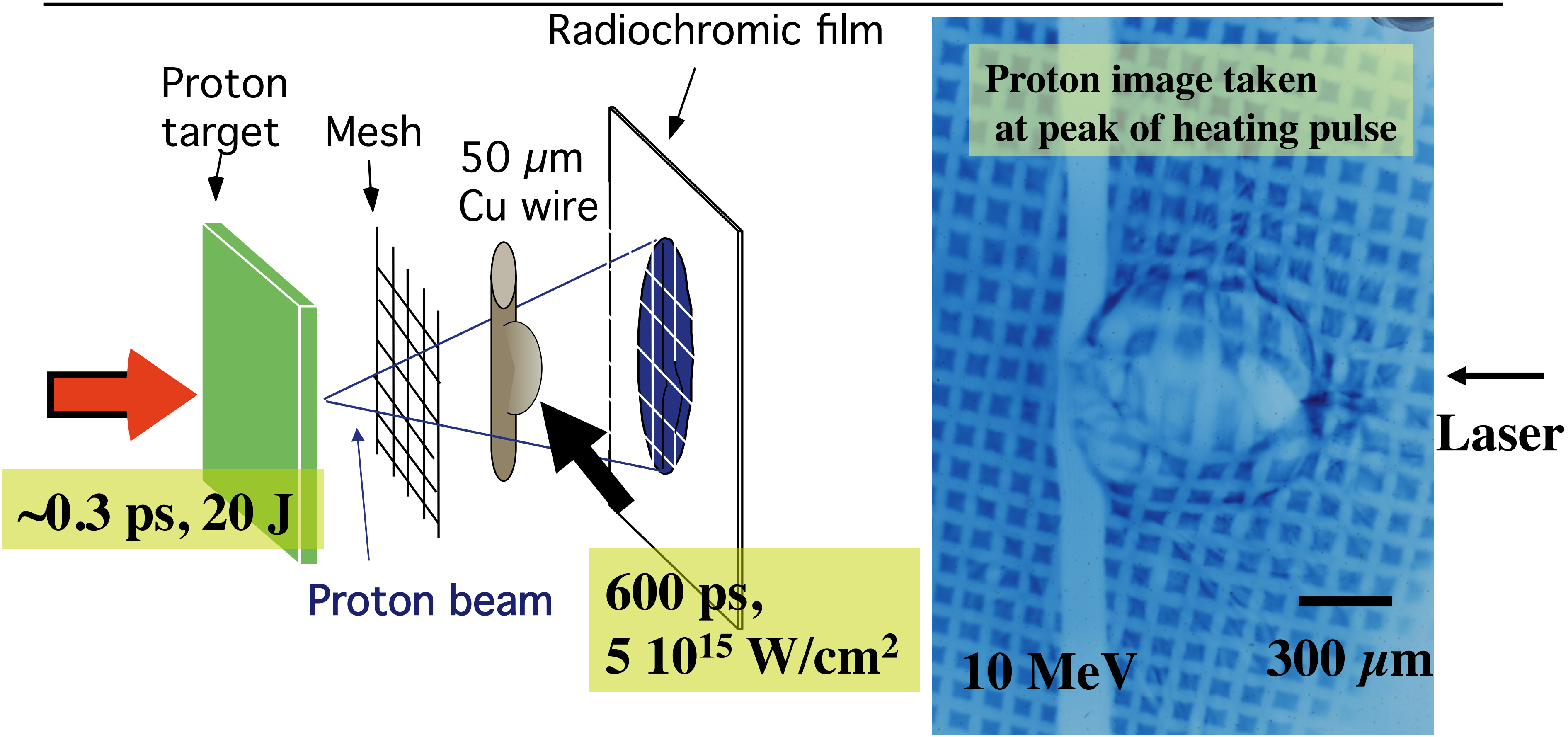

Pre-imposing a regular pattern on the beam allows a direct measurement of the proton deflection due to e.m. fields in the plasma

Queen's University Belfast

Proton probing of intense laser solid interaction

Borghesi et al., Queen's University Belfast

Field associated to expanding proton front
(~3 MeV) See L.Romagnani *et al*, PRL, 2005

Effect of azimuthal B-field around propagation axis ?

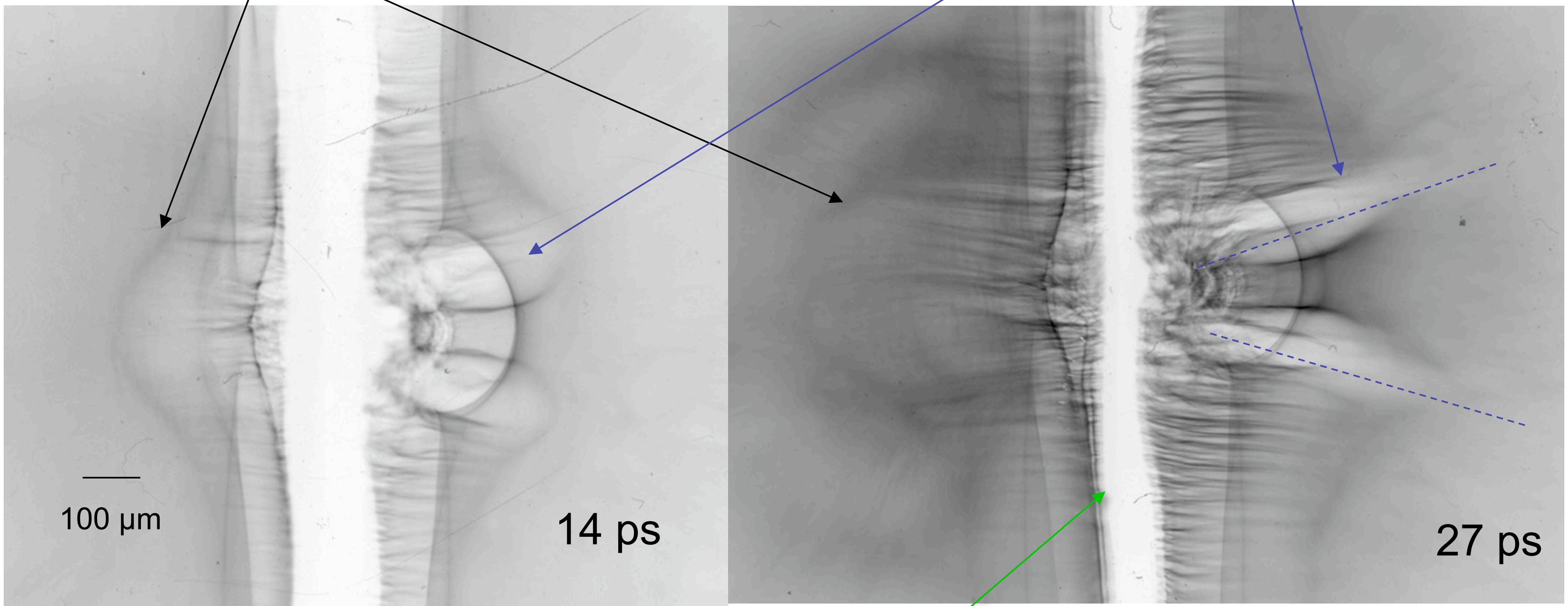

Fast growing, fine filaments (e.m.instability driven by returning hot electrons)

Proton beam probes measure B and E fields in HEDP plasmas (Willingale et al., PRL 2011)

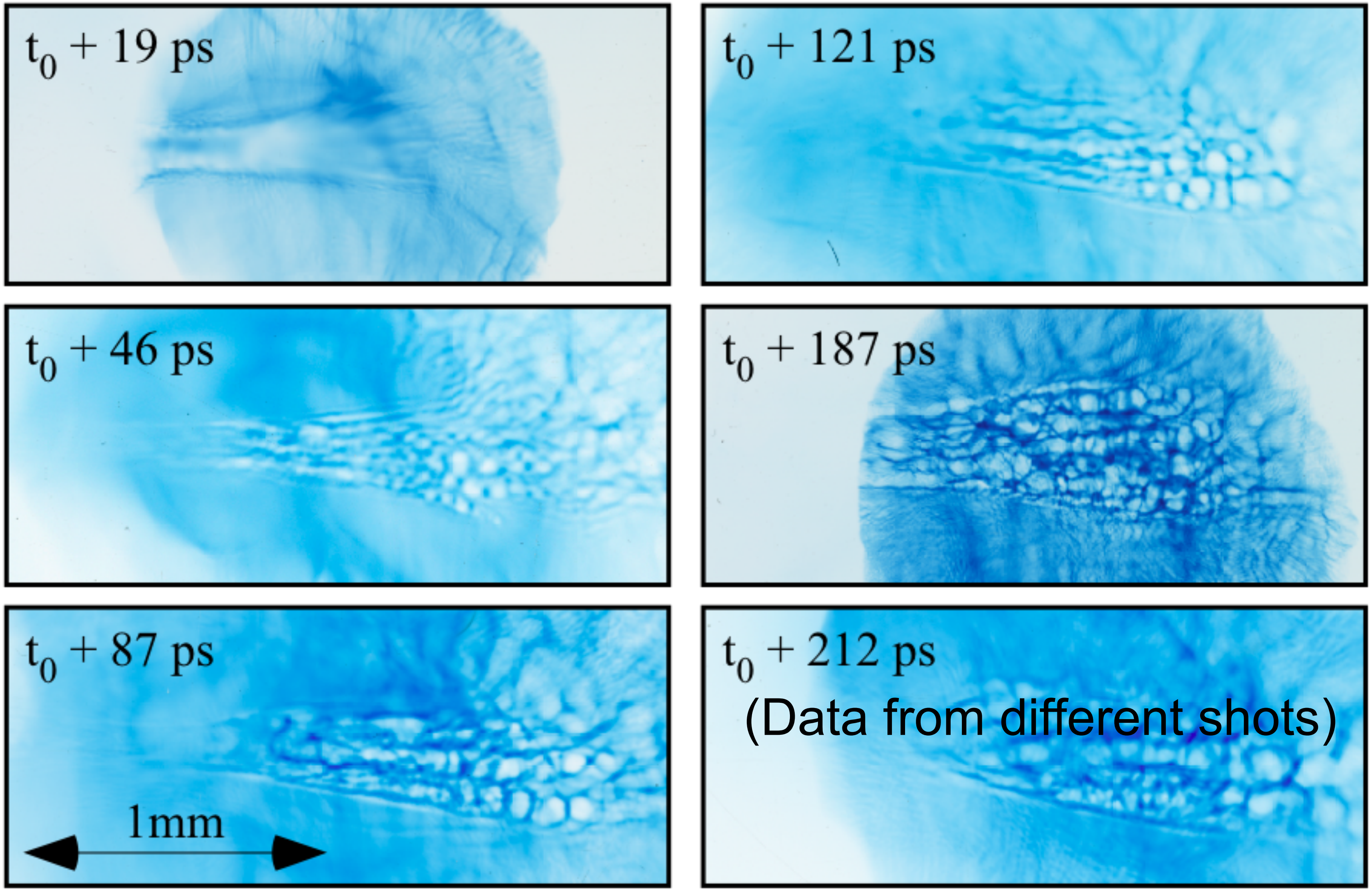

Unique diagnostic correlates with simulations of currents in plasma

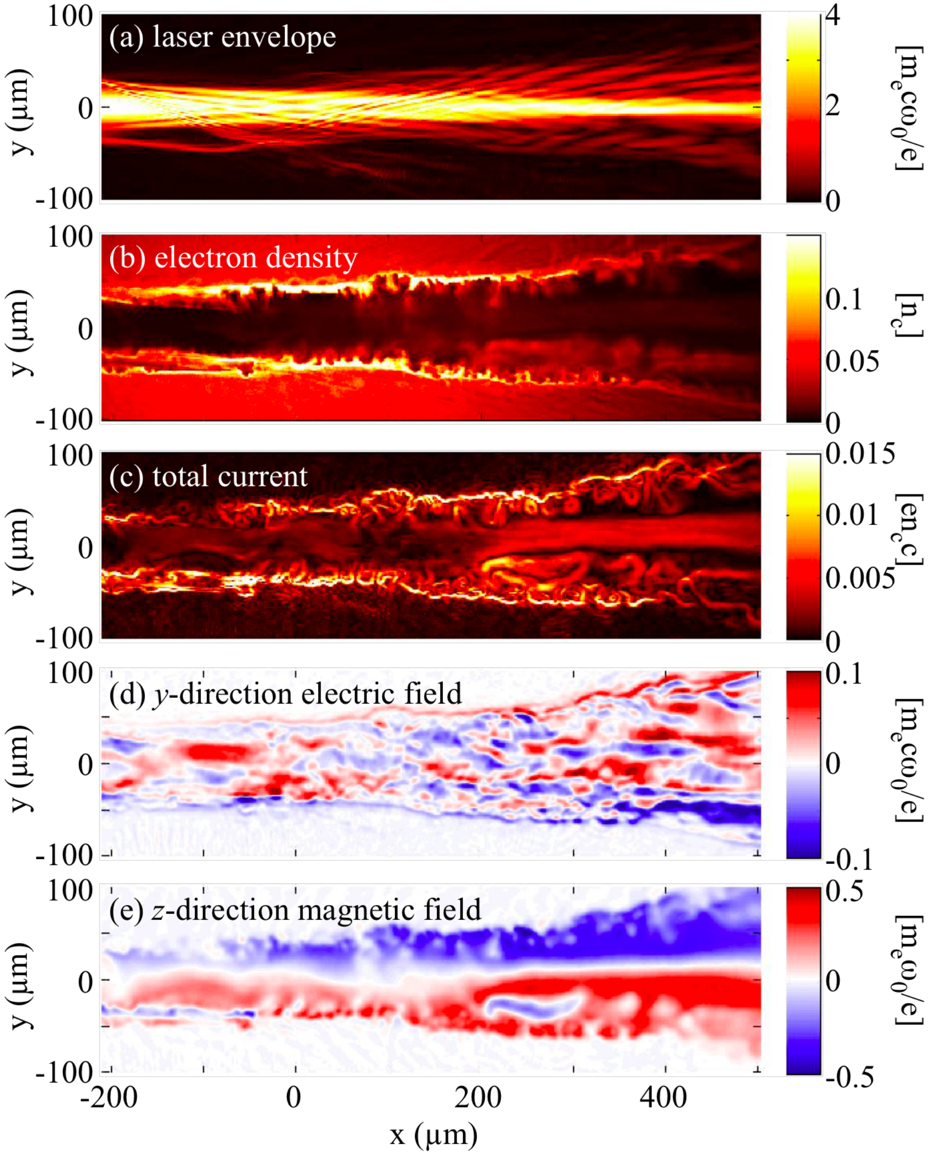

11 ps

15 ps

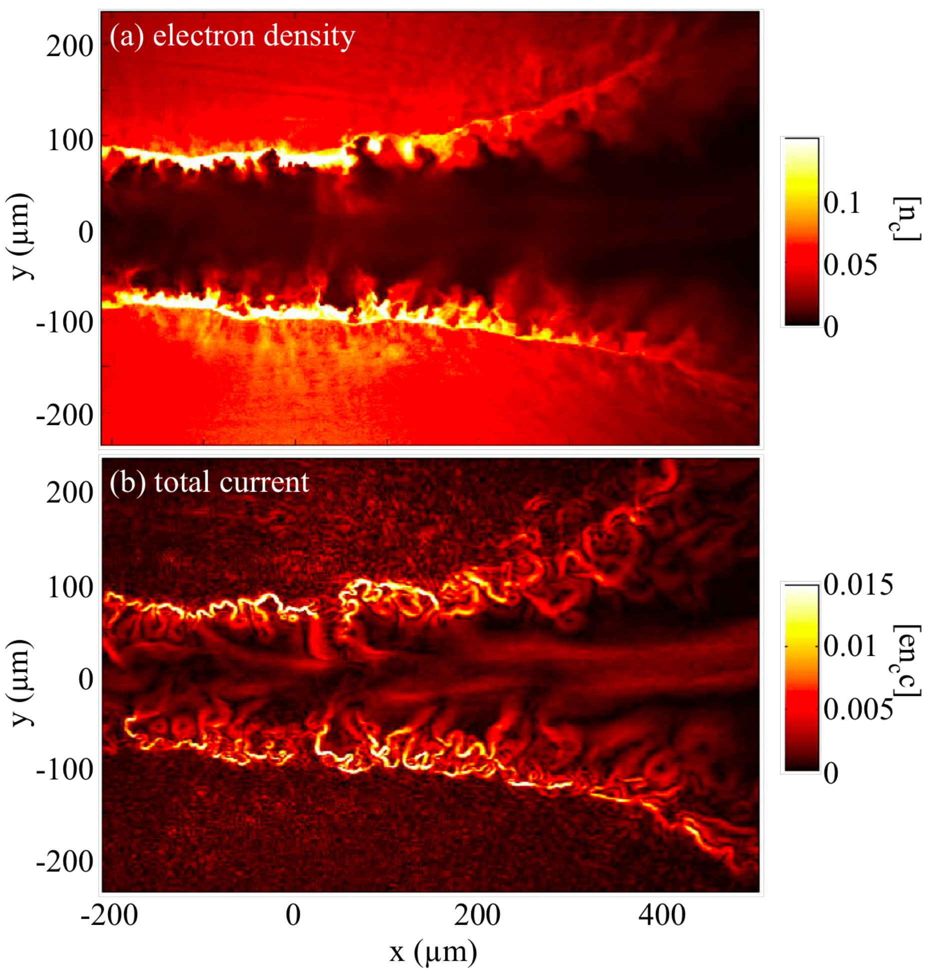

Experiment

Experiment
Main Target

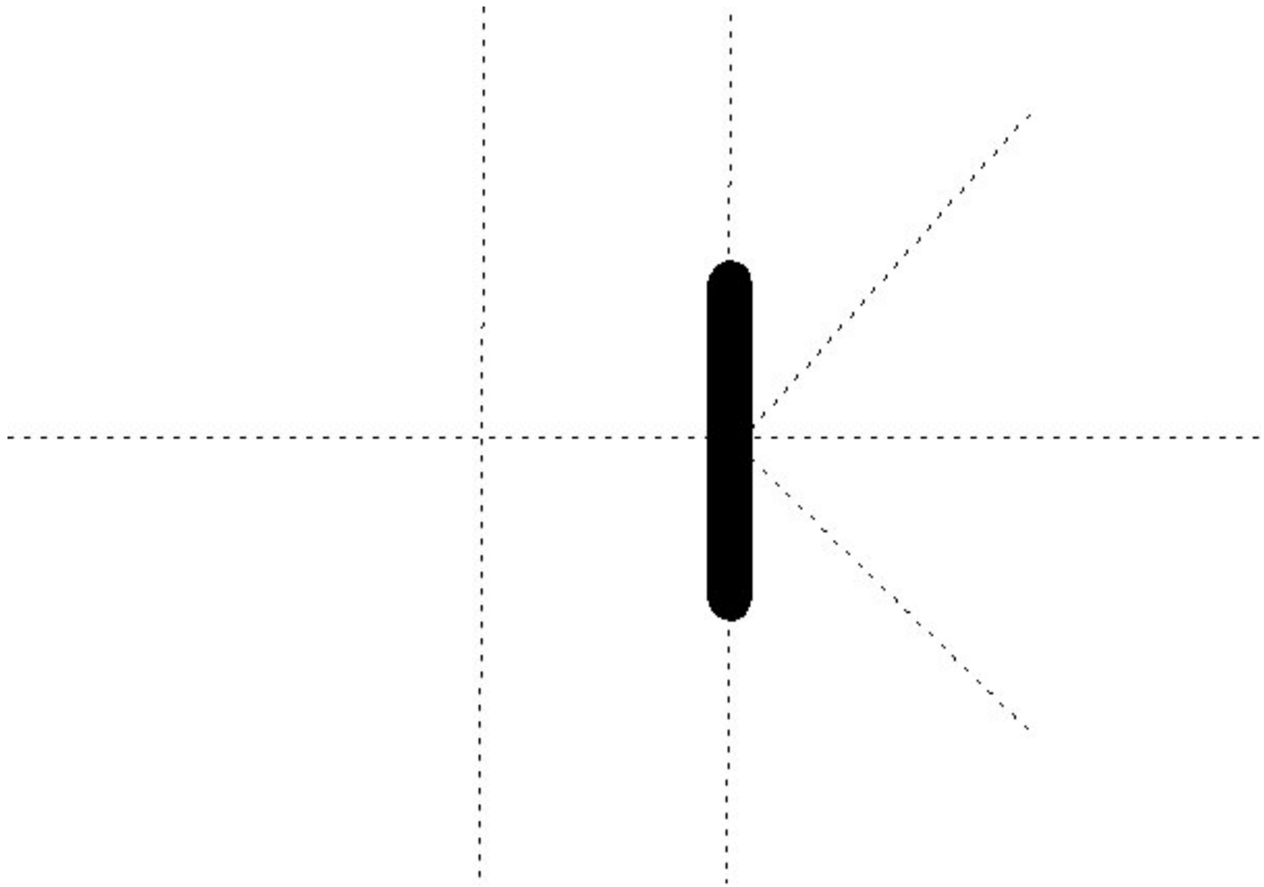

target foils: CH, Al, Au
3 x 5mm, 25 - 100μm

Experiment
Heater Beams

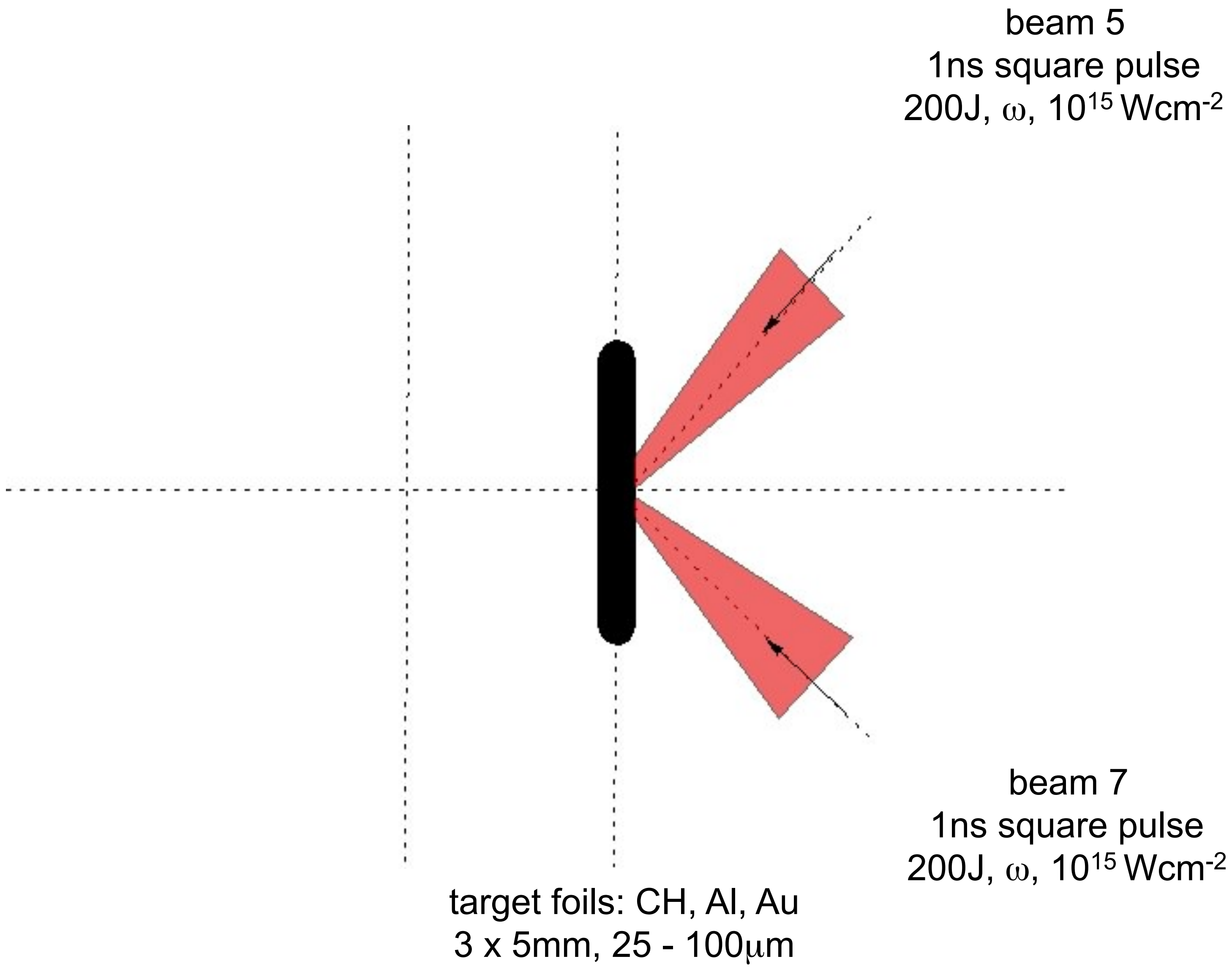

Experiment
Transverse 4ω Probe Beam

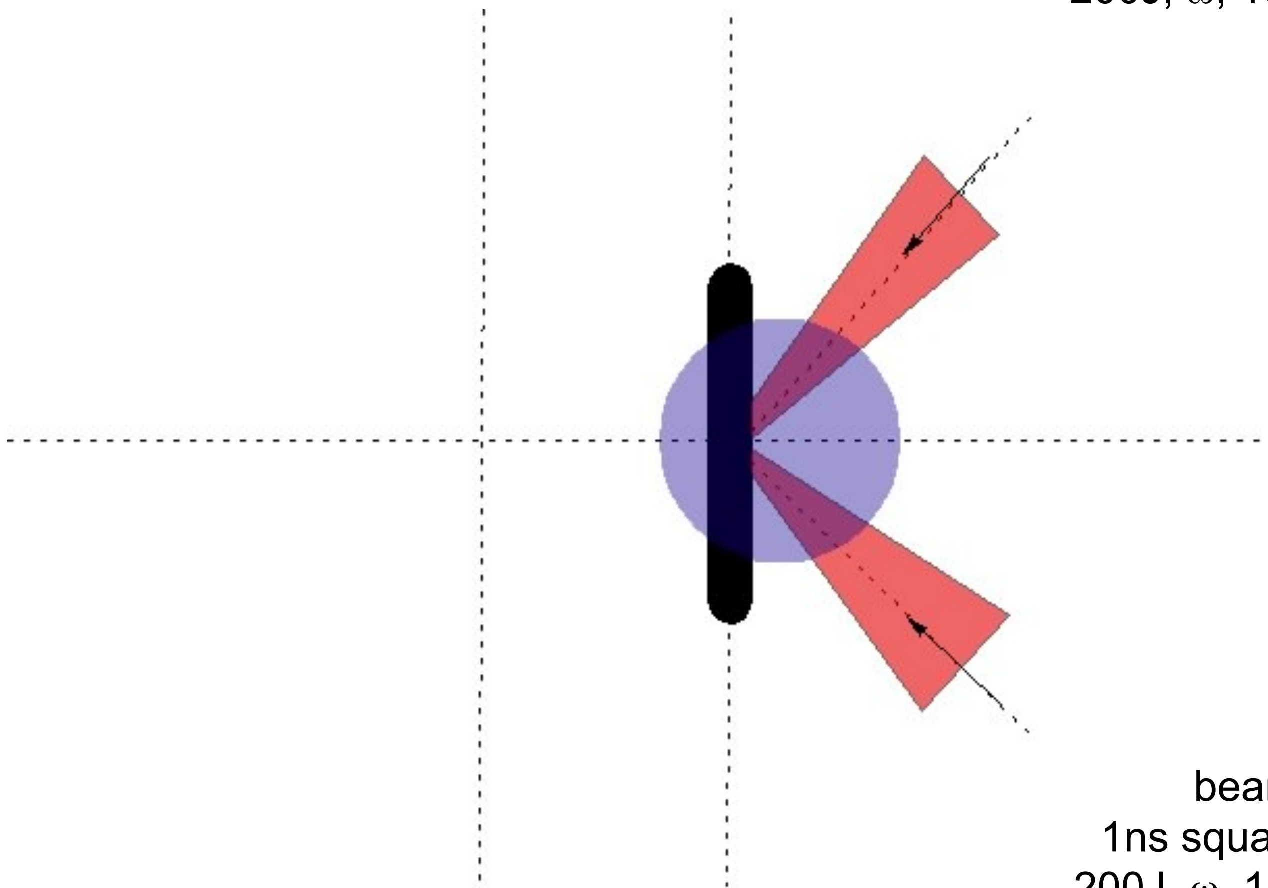

Experiment
Rear-Projection Proton Imaging

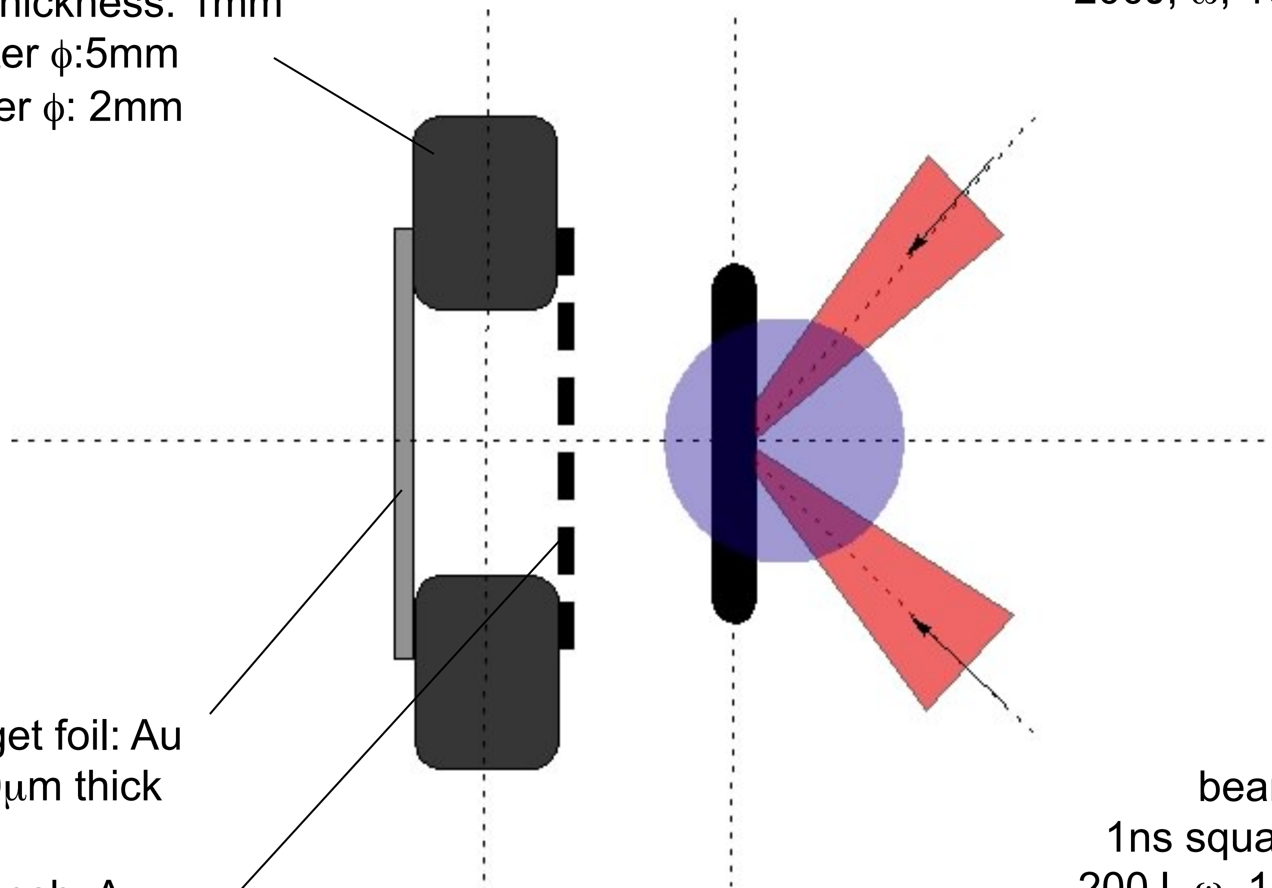

Experiment
Rear-Projection Proton Imaging

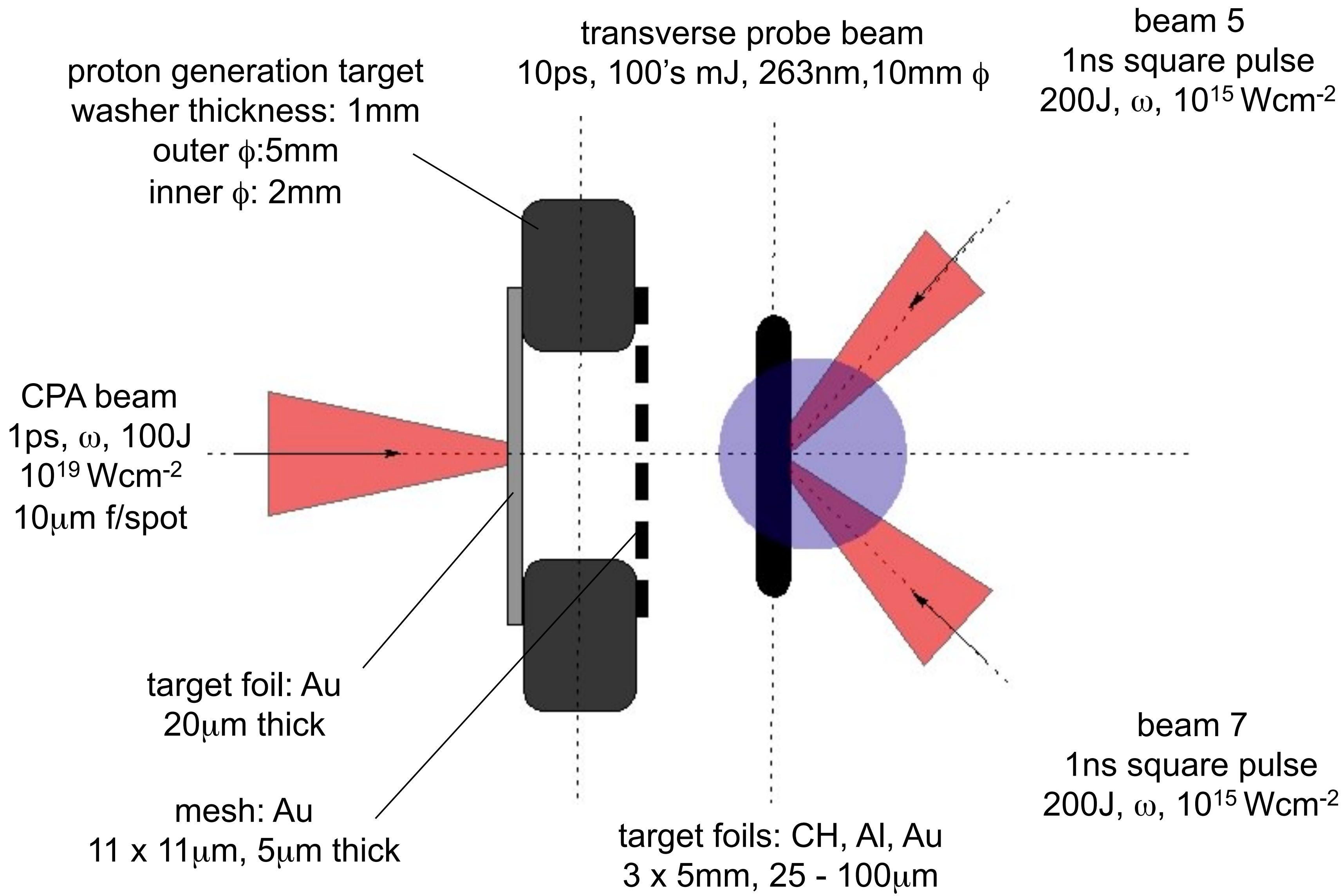

Experiment
Rear-Projection Proton Imaging

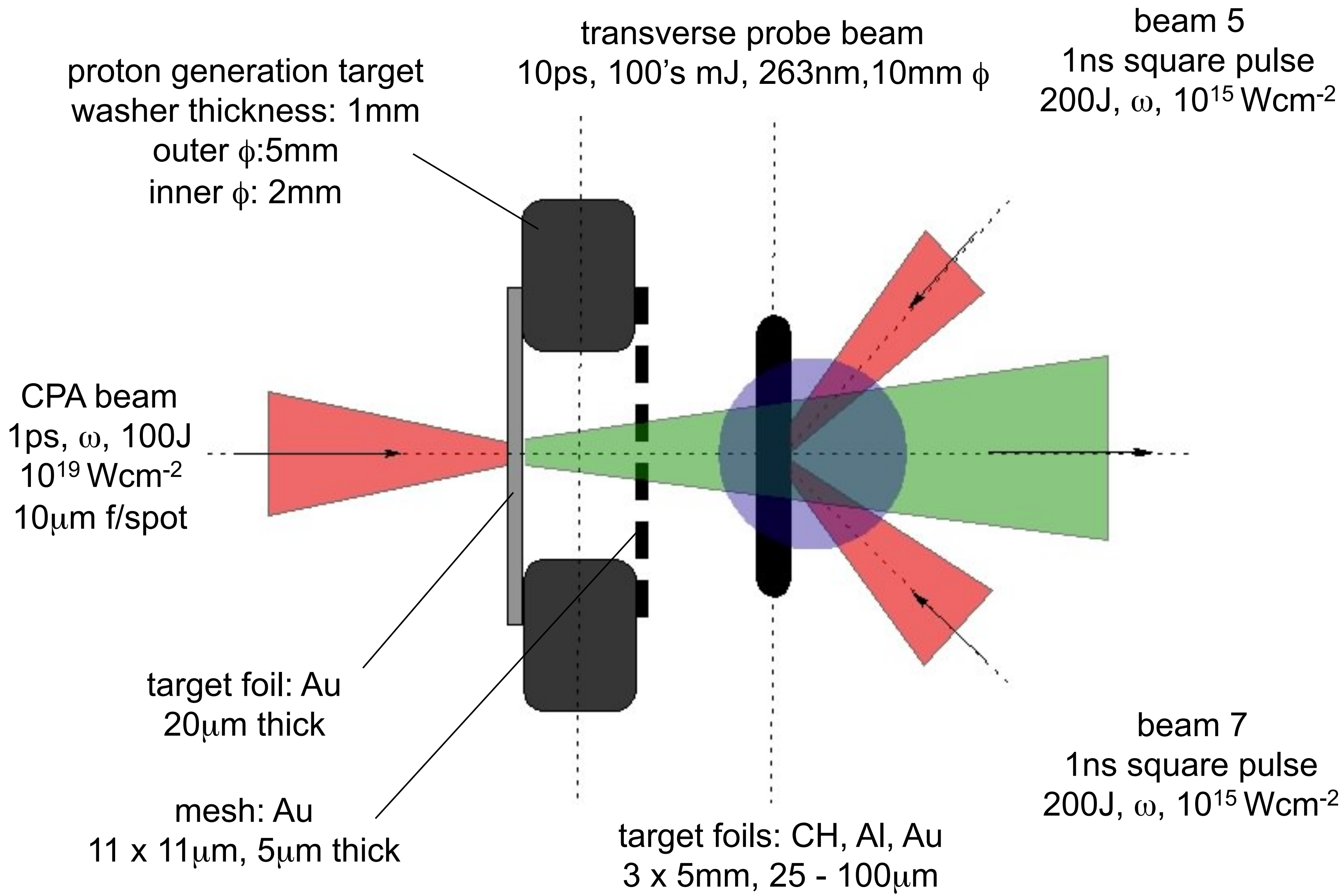

Experiment
Rear-Projection Proton Imaging

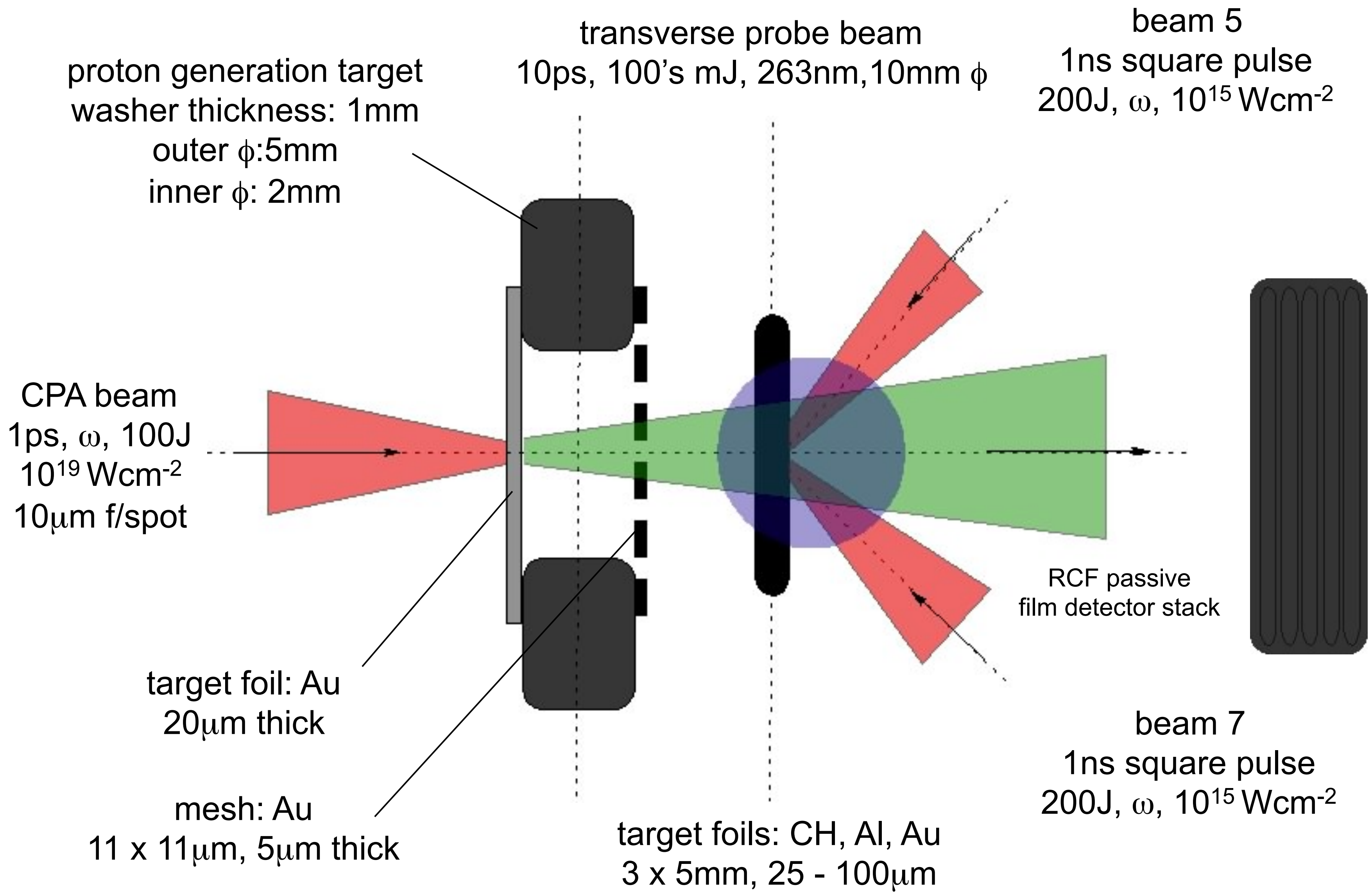

Experiment
Collective (4ω) Thomson Scattering

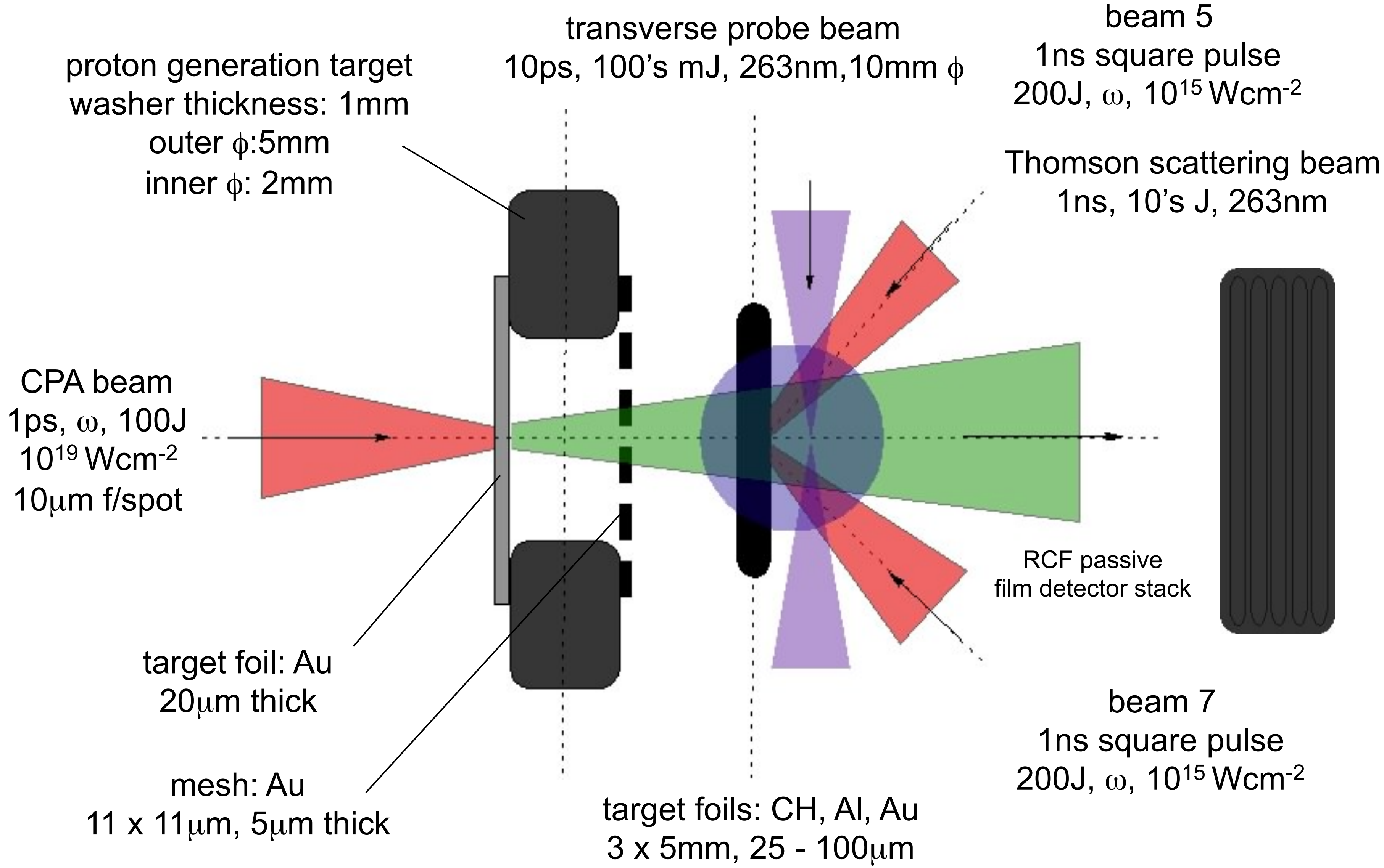

Experiment
Time-Integrated X-ray Pinhole Imaging

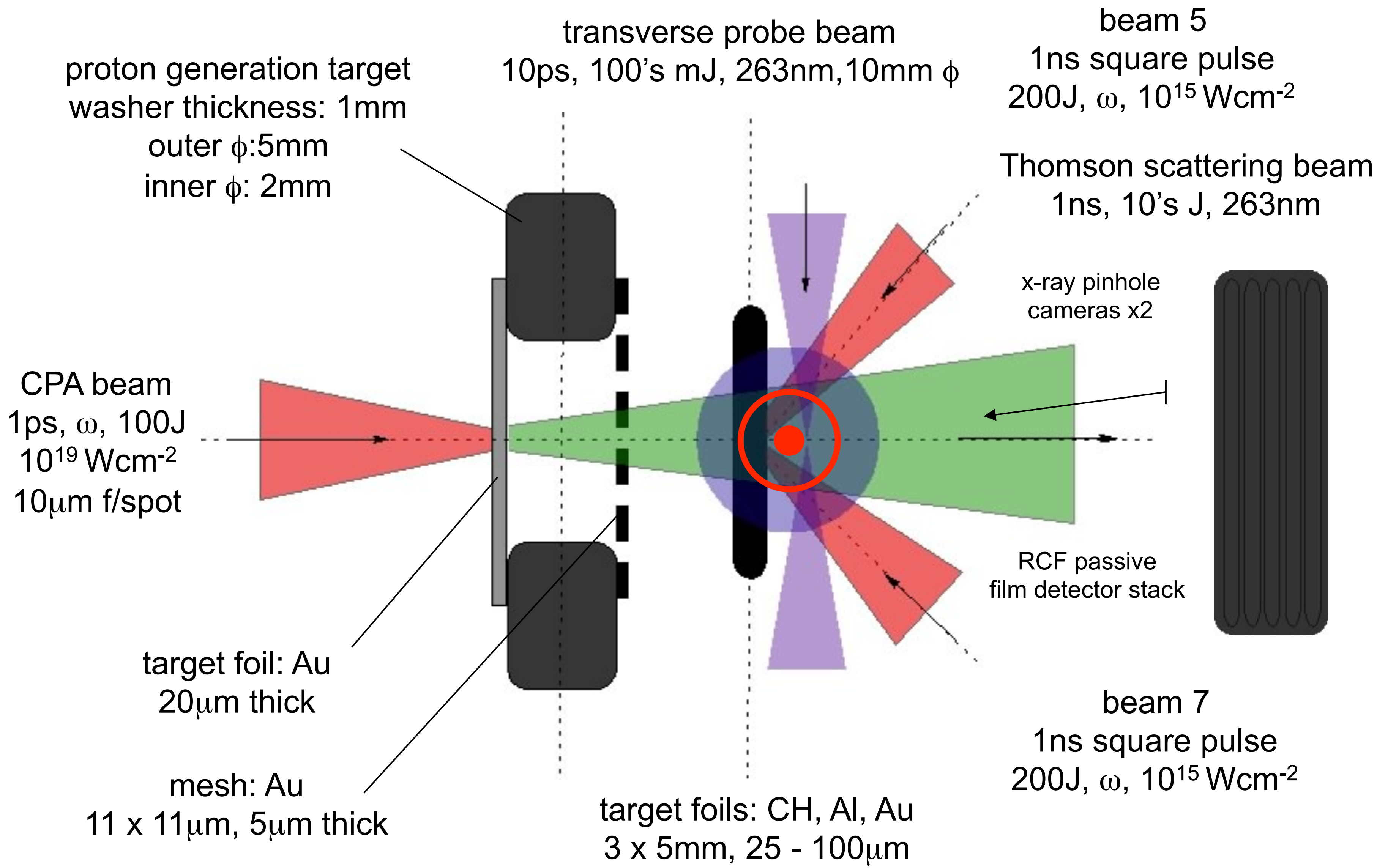

Experiment
VULCAN Target Area West (TAW)

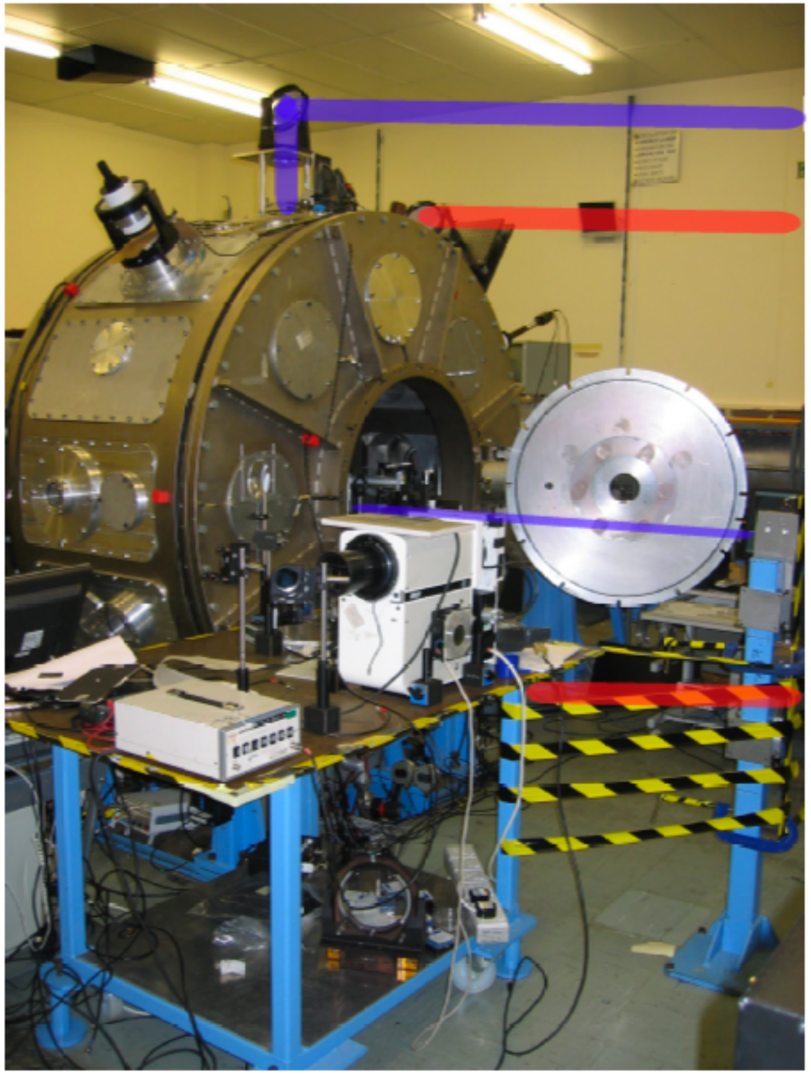

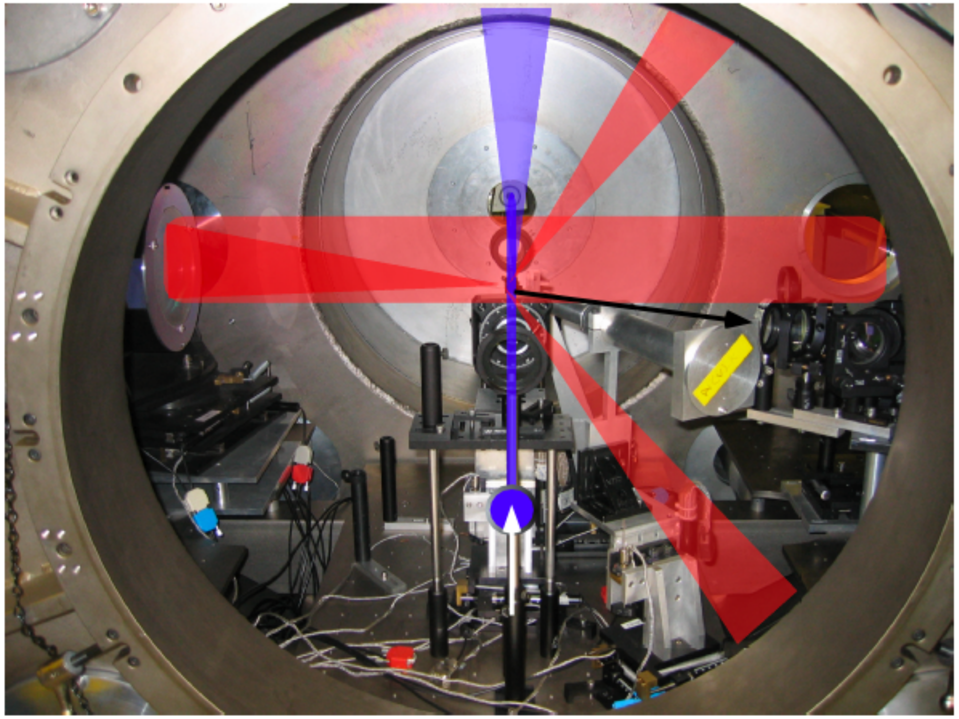

VULCAN TAW interaction chamber

Plasma dynamics: Al target

Rear projection proton imaging (fields ~ 1 MGauss)

(P. N. Nilson et al., Physical Review Letters 2006)

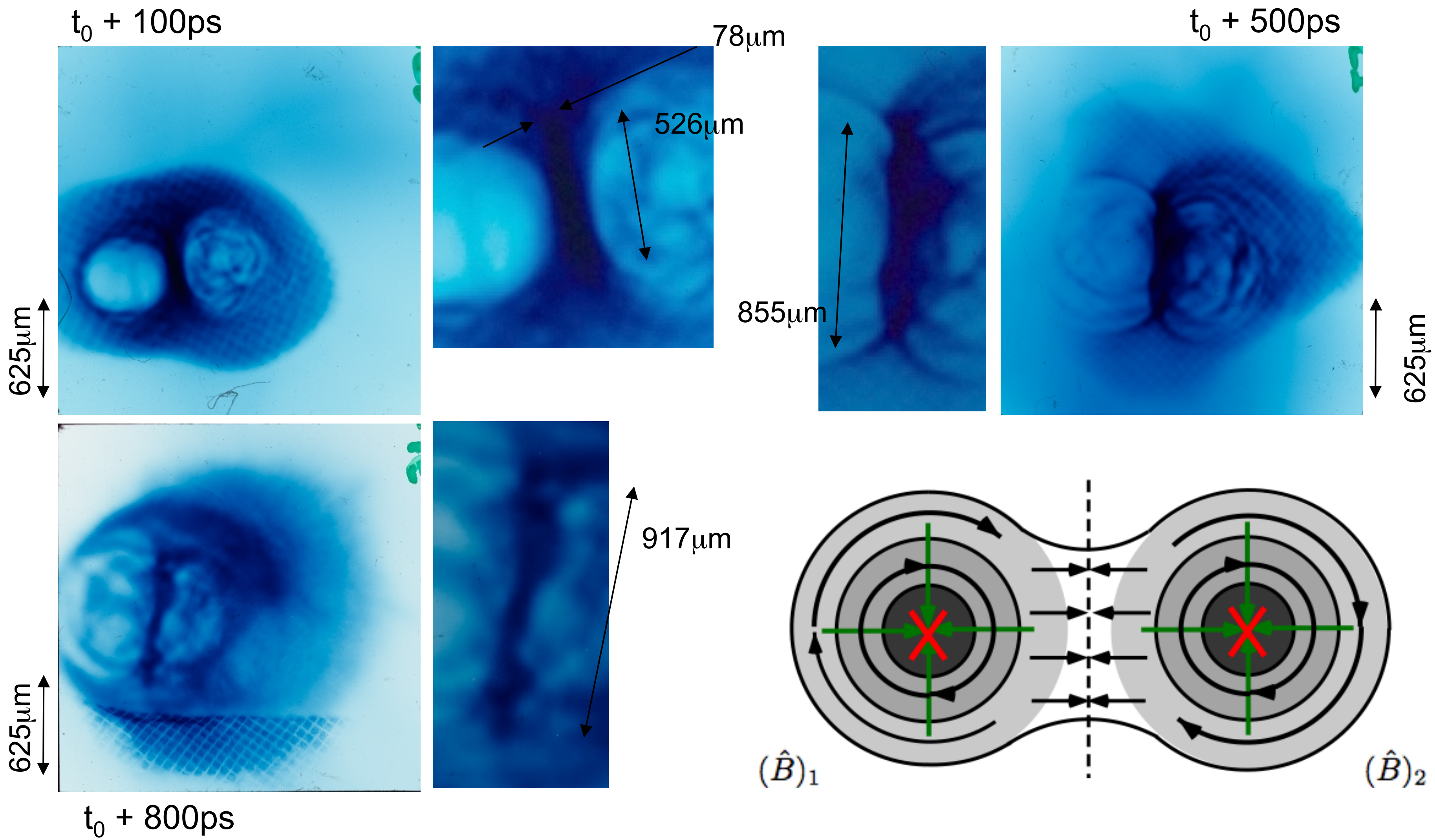

Plasma dynamics: Al target

4ω transverse probe beam

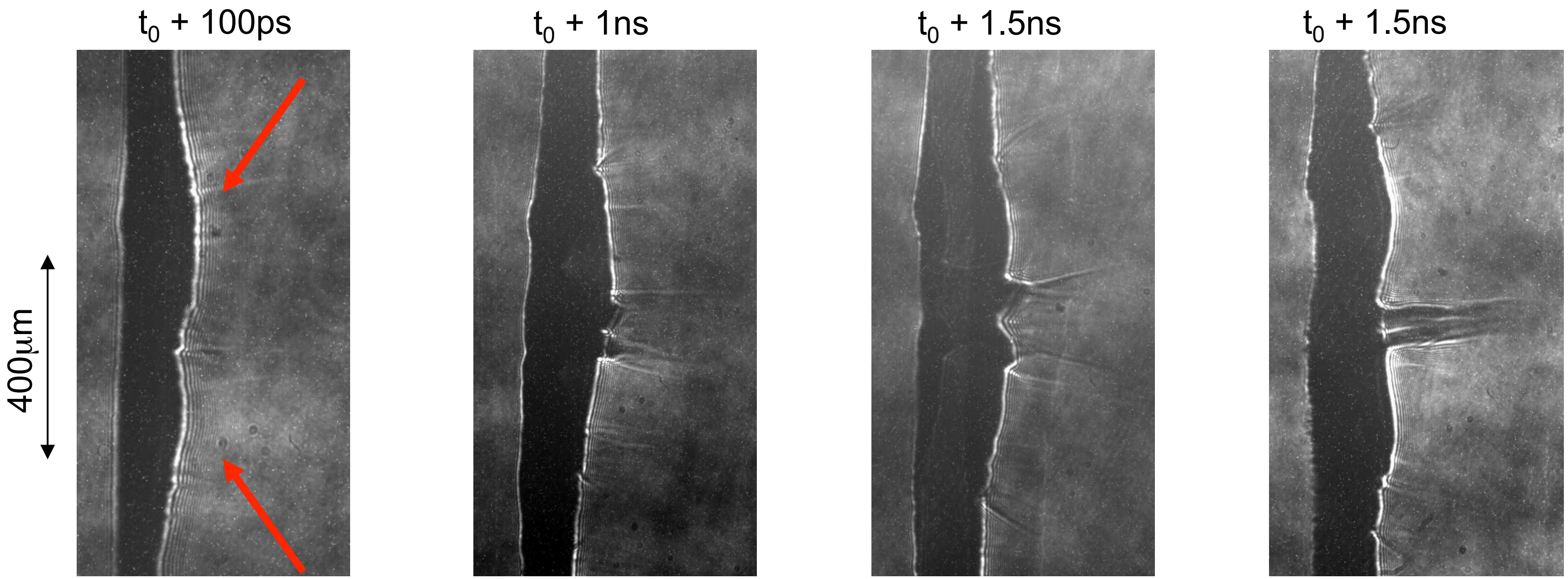

- filamentary structures
- jet-like structures
- highly collimated flows
- $n_e \sim 10^{20}$ cm^{-3}
- $v_{perp} \sim 5.0 \times 10^2$ kms^{-1}

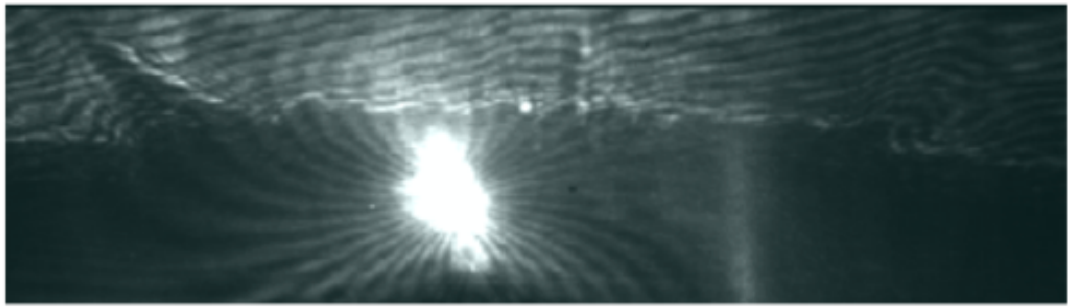

Plasma dynamics: Au target

4ω transverse probe beam & X-ray imaging

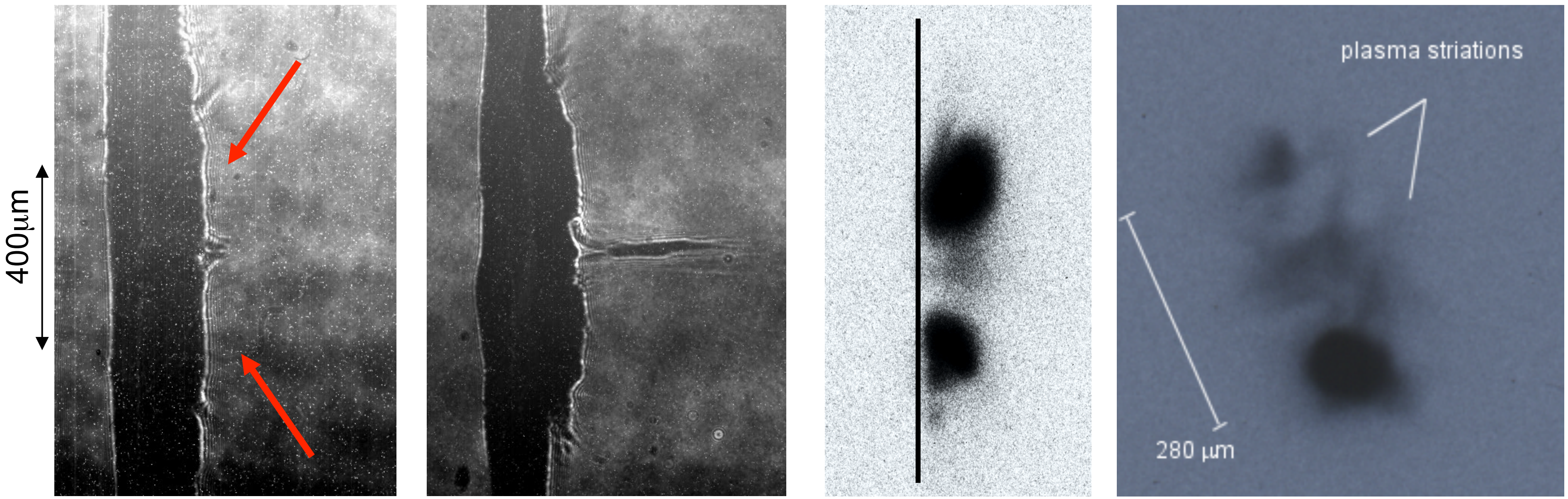

t_0 + 1ns t_0 + 2.5ns

- central plasma flow velocity, $v_{perp} \sim 2.6 \times 10^2$ kms^{-1}
- greater collimation in the Au plasmas compared to Al
- importance of radiative cooling

ref: Farley *et al.*, Radiative Jet Experiments, PRL **83**, 10 (1999)

Electron temperature: Al Target

Time-resolved collective Thomson scattering (4ω)

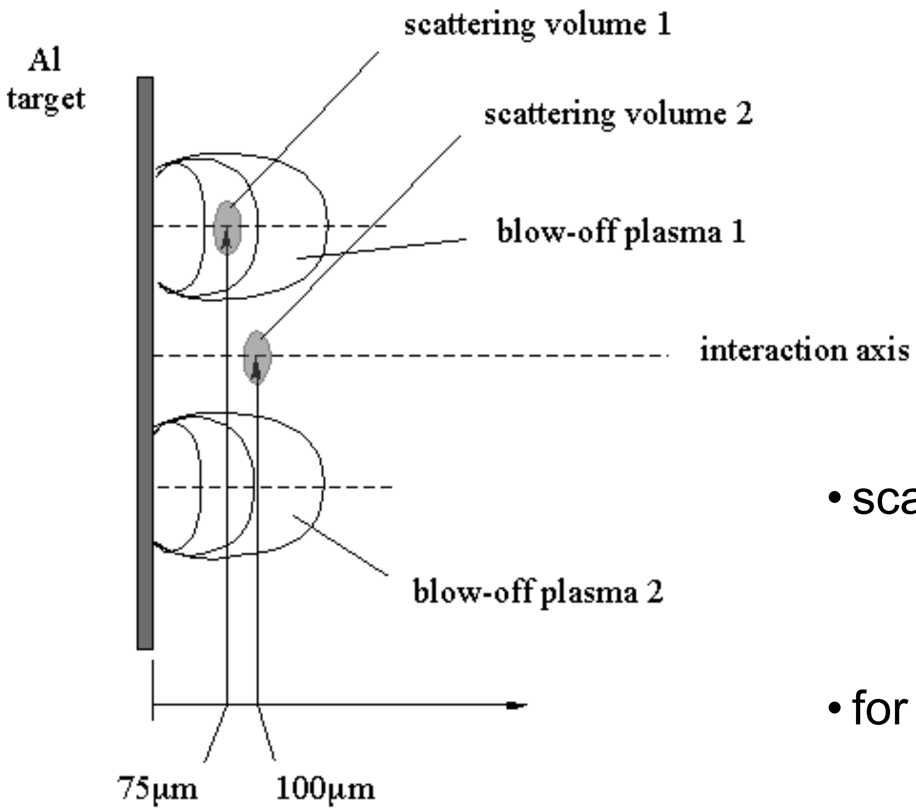

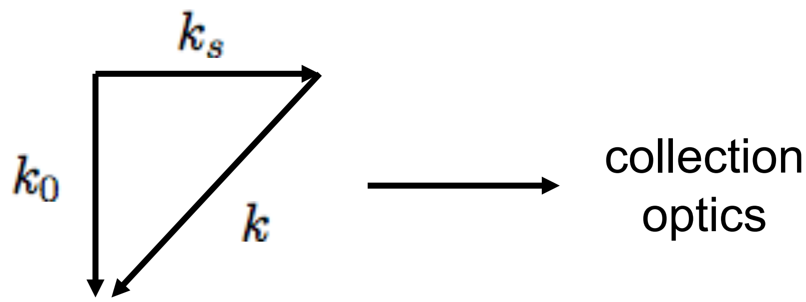

- scattering parameter, $\alpha = \dfrac{1}{k_B \lambda_D} \approx 2$

- for an ion mass, M, ion temperature, T_i, and specific heat ratio, Γ_i,

$$\left(\frac{\omega_{ia}}{k_{ia}}\right)^2 \approx \frac{T_e}{M}\left(\frac{\bar{Z}}{1+(k_{ia})\lambda_D^2}+\Gamma_i\frac{T_i}{T_e}\right) \approx \frac{T_e}{M}\left(\frac{\bar{Z}}{1+(k_{ia}\lambda_D)^2}\right)$$

Electron temperature: Al Target

Time-resolved collective Thomson scattering (4ω)

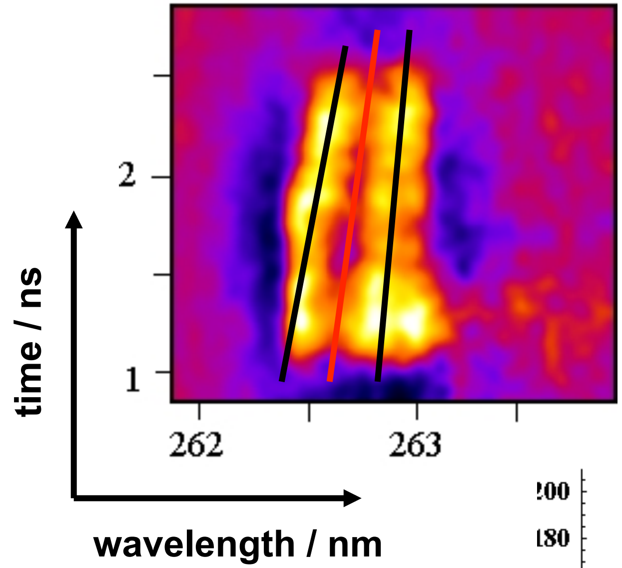

- scattering volume 1: single laser-ablated plume
- estimated electron temperature,

$$T_e \approx 0.5 - 1keV$$

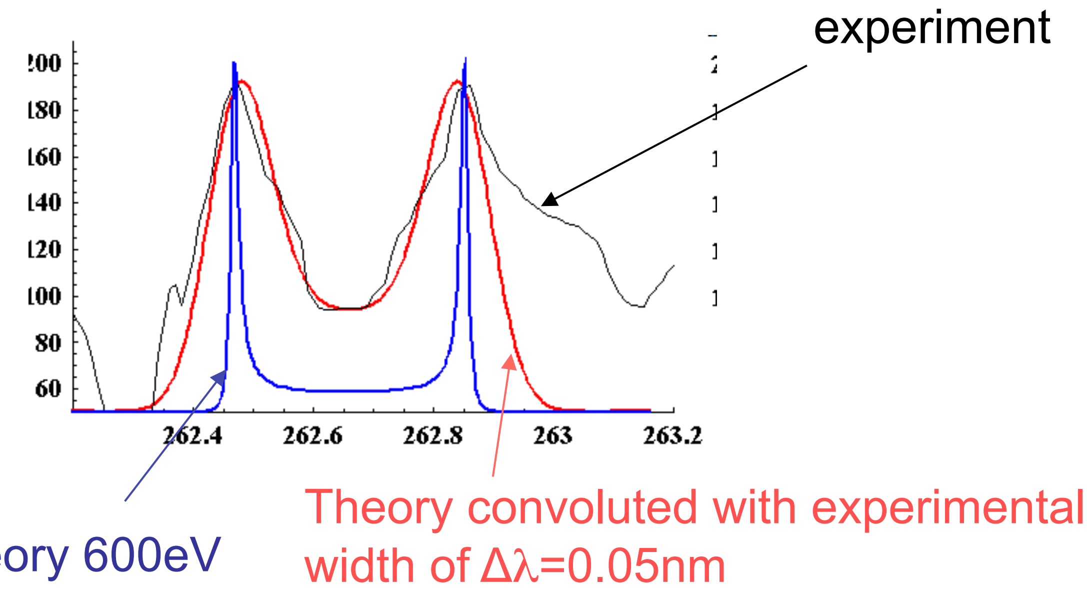

Electron temperature: Al target

Time-resolved collective Thomson scattering (4ω)

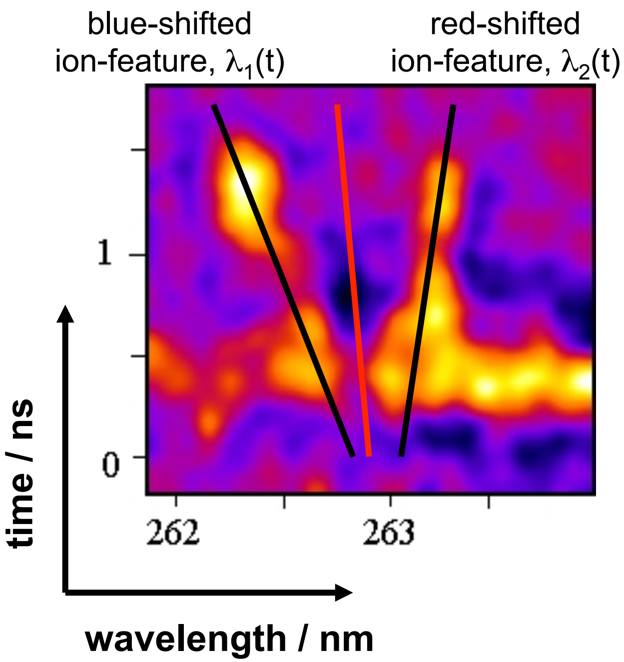

- scattering volume 2: interaction region
- asymmetry in the wavelength shift
- scattering volume: accelerated toward detector

$$(t_0 + 0.8ns) \rightarrow 0.22nm \rightarrow v_{exp} \approx 2.0 \times 10^7 cms^{-1}$$

$$(t_0 + 1.3ns) \rightarrow 0.30nm \rightarrow v_{exp} \approx 2.7 \times 10^7 cms^{-1}$$

- increasing wavelength separation infers heating

Questions

- role of T_i in the central plasma?
- source of energy resulting in large T_e?

Plasma heating source

- **Ohmic heating**

$$J^2/\sigma \rightarrow (\mu s) \rightarrow \sigma \approx T^{3/2}$$

- **Stagnation heating:**

a problem for equilibration timescales between electrons and ions

$$\tau_{ee} \approx 10ps \qquad \tau_{ii} \approx 100ps \qquad \tau_{ei} \approx 10ns$$

- **Driven reconnection:**

strong electron heating is a signature of reconnection

detailed microphysics and heating mechanisms are at still not well understood

Plasma Heating Source Parameters

- Energy considerations

$$\int \frac{B^2}{2\mu_0} dV \rightarrow \frac{3n_e k_B T_e}{2}$$

$$n_e \approx 10^{19-20} cm^{-3}$$

$$\boxed{5keV \rightarrow (1-2)MG}$$

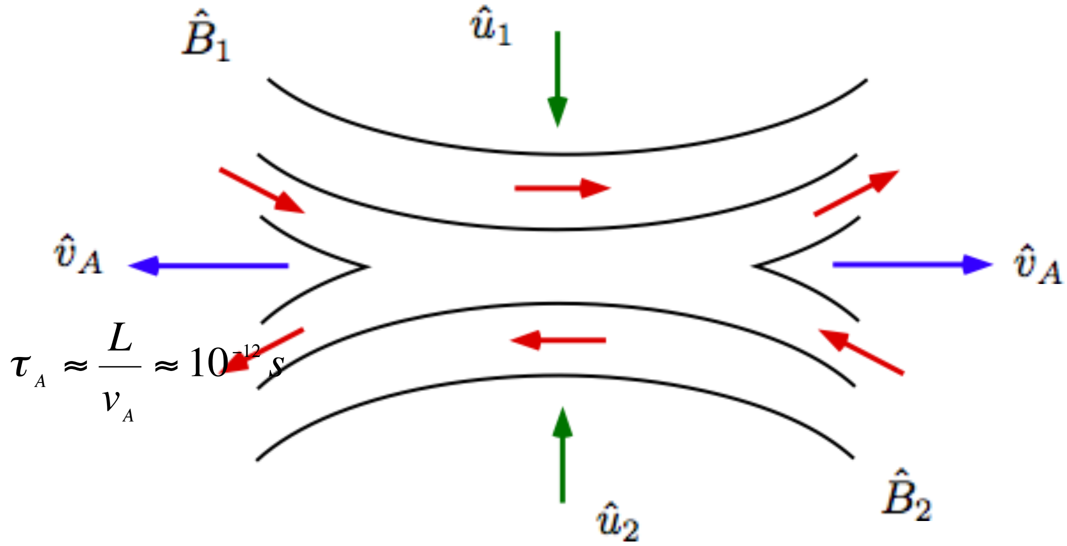

- Sweet-Parker Model

$$\tau_A \approx \frac{L}{v_A} \approx 10^{-12} s$$

$$\tau_R \approx \frac{\mu_o L^2}{\eta} \approx 10^{-6} s$$

$$\boxed{M_{dr} \approx (\tau_A \tau_R)^{1/2} \approx 10^{-9} s = \text{nanoseconds}}$$

<u>**Explained by Fox et al. PRL (theory/ simulation):**</u>

- "pile-up" of B-fields lead to enhanced reconnection time

Monoenergetic proton source - LLE/MIT

The proton source is a laser-driven glass capsule filled with D_2 and ^3He gas

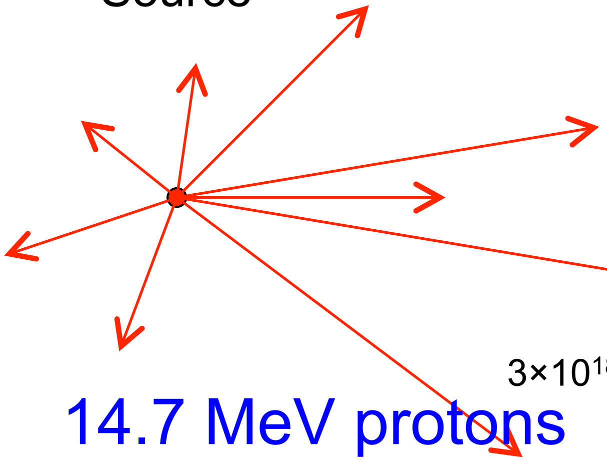

Heating of the gas during implosion leads to nuclear fusion production:

$$D + {}^3He \rightarrow {}^4He + p\ (14.7\ \text{MeV})$$

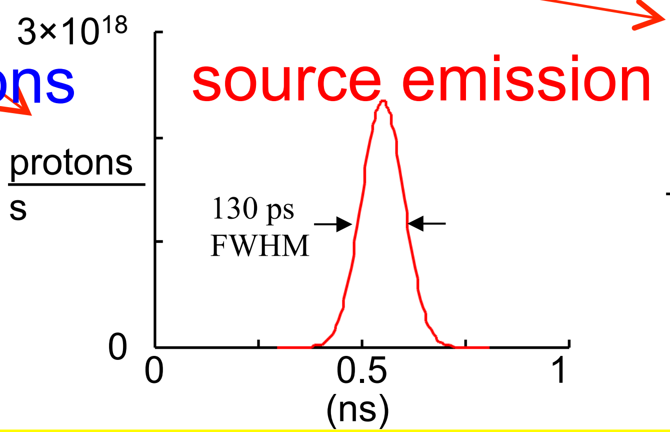

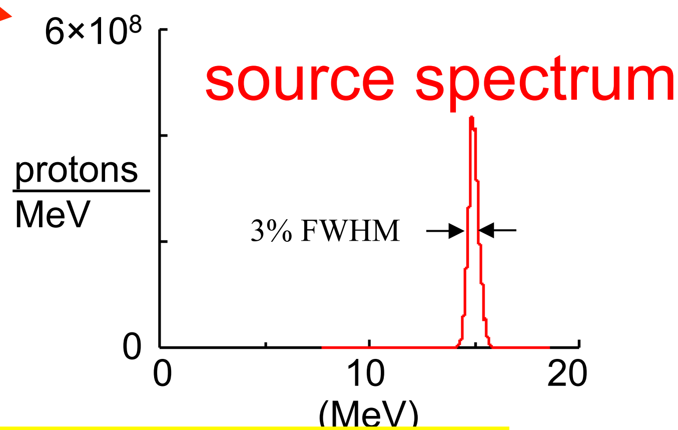

Emission of 14.7 MeV D^3He protons is pulsed, monoenergetic, and isotropic

Li and Petrasso PRL 2006

Radiographs of laser-generated plasma bubbles on opposite sides of a foil prove that deflecting fields are *B* rather than *E*

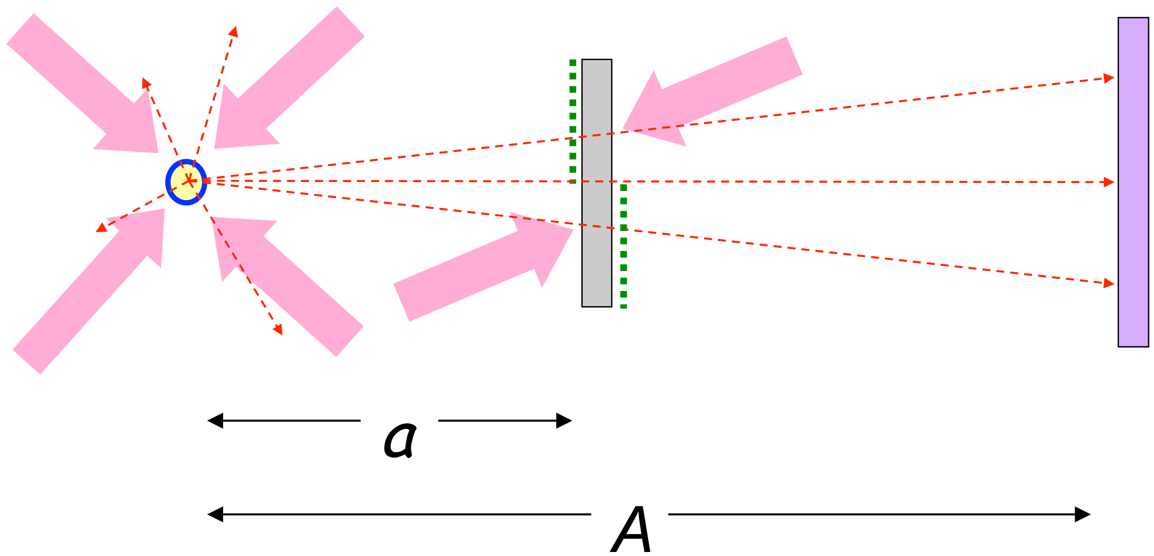

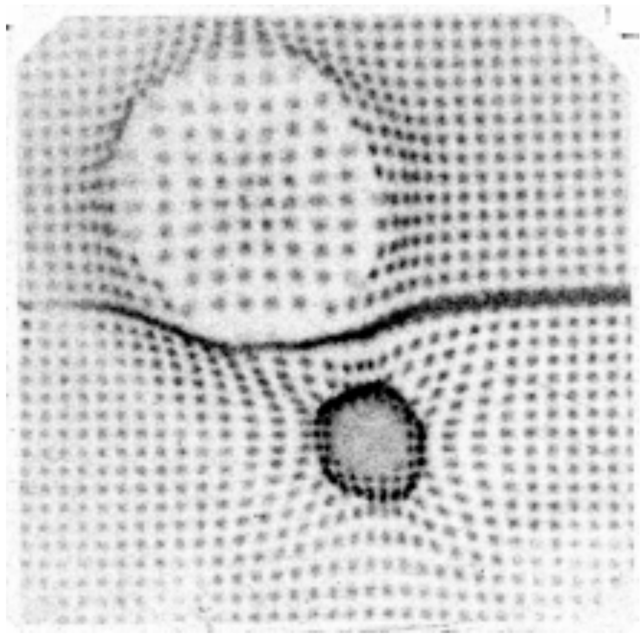

OMEGA shot 46535

$$\boldsymbol{\xi} = -\frac{qa(A-a)}{A\, m_p \mathbf{v_p}} \int \mathbf{B} \times d\ell$$

Petrasso et al POP 2008

Data and LASNEX simulations are similar with the laser on, but diverge afterwards

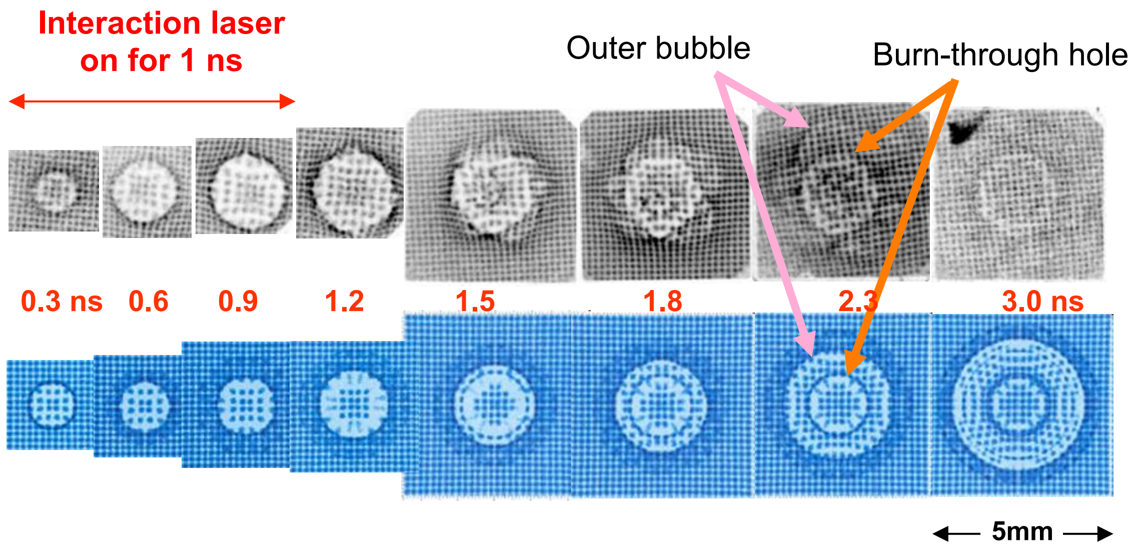

LASNEX+LSP by R. Town

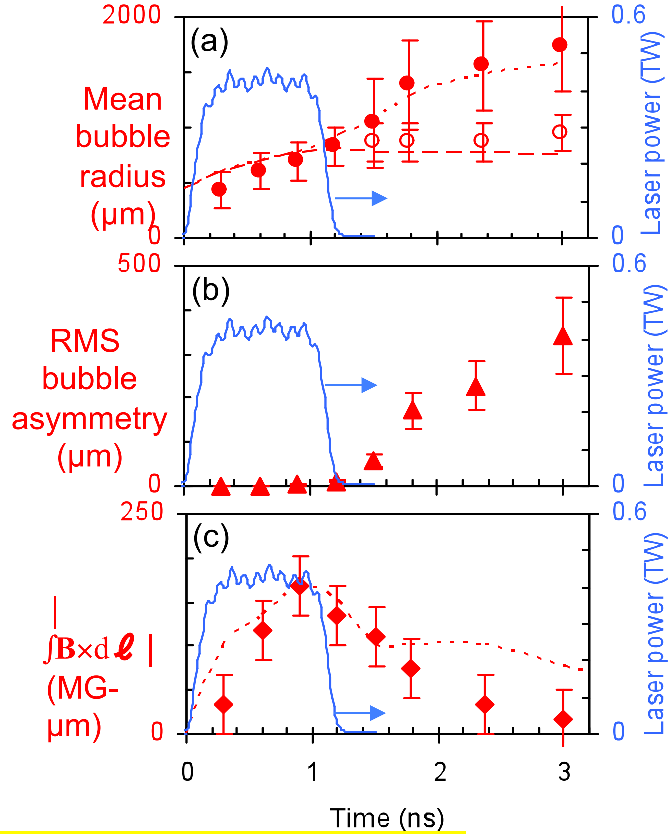

2D code LASNEX produces credible simulations of the hydrodynamics and field growth as long as the laser was on, failing only when 3D instabilities appeared.

Li and Petrasso PRL 2007a

Magnetic reconnection from multiple spots observed

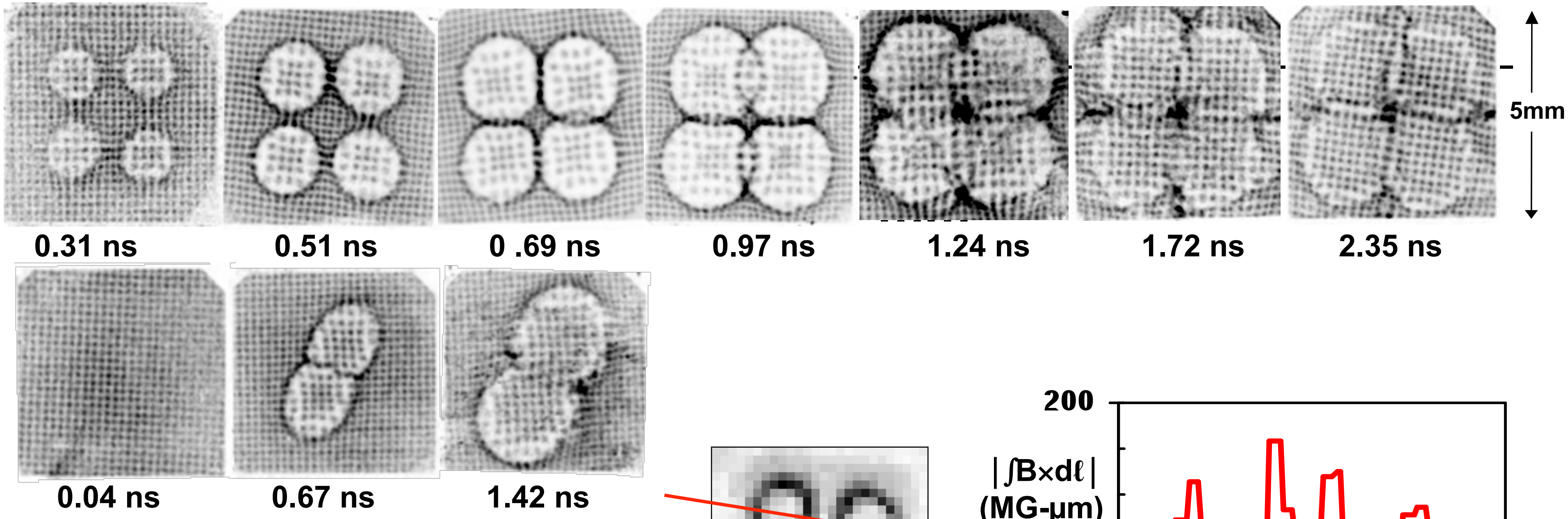

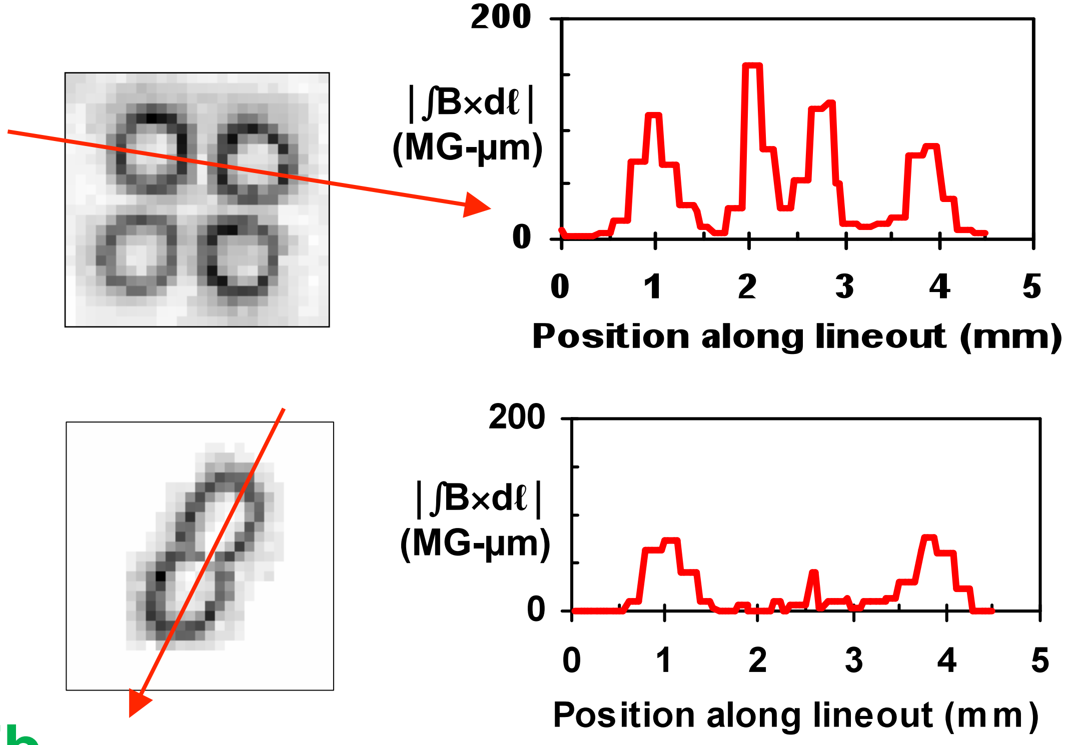

> 95% field strength was reduced in the region where bubbles overlap

Li and Petrasso PRL 2007b

Radiography of a cone-in-shell capsule implosion reveals field topology and capsule compression

Rygg et al., Science 2008

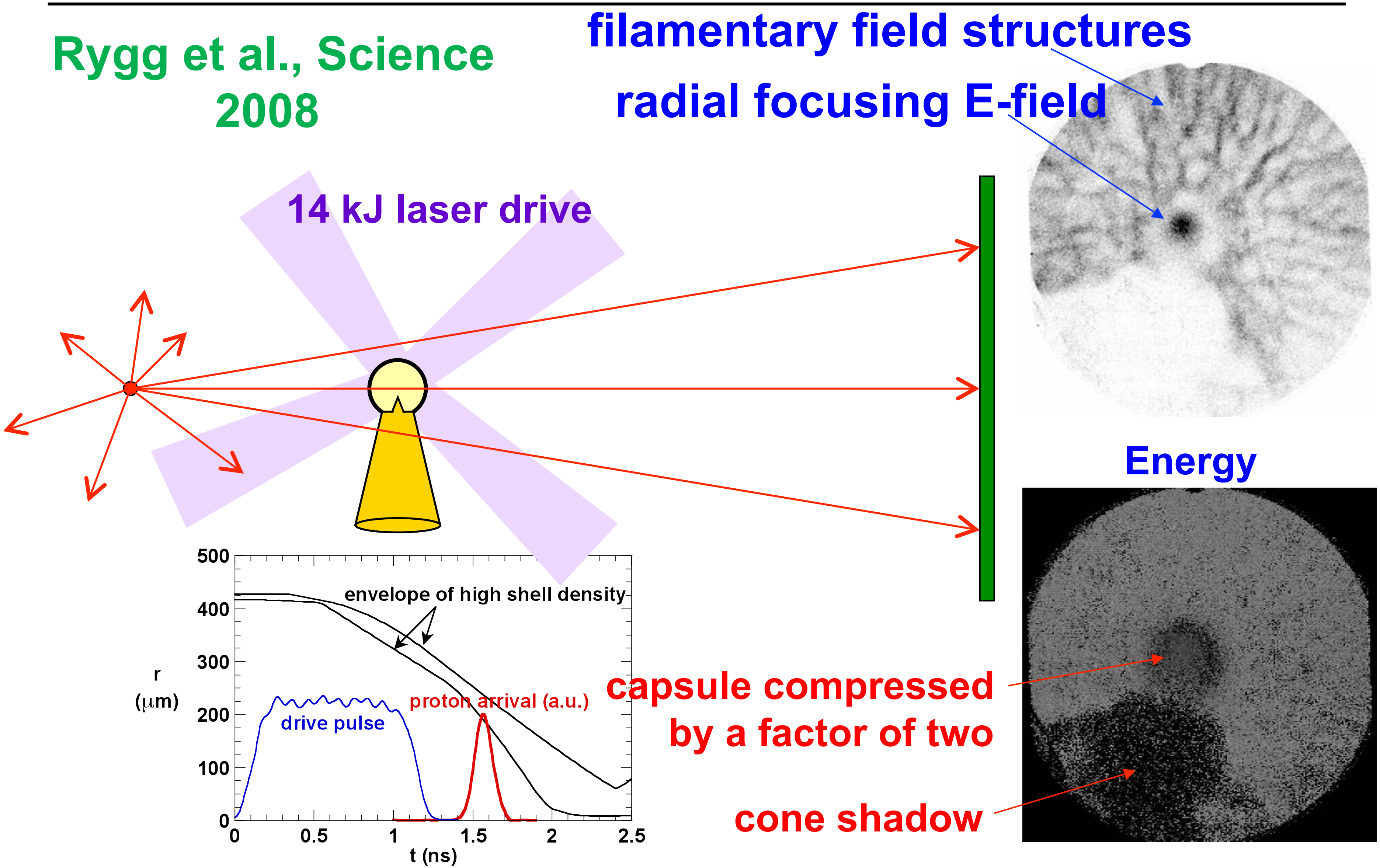

B-field dynamics - Summary

- the interaction between laser-ablated plasmas in two beam long pulse (ns) interaction geometries with planar mid- and high-Z solid targets has been studied
- characterized the ablation dynamics and plasma outflows using transverse optical probing
- observed B-field null formation using rear-projection proton probing
- measured strong electron heating via Thomson scattering
- the plasma dynamics and estimated reconnection rates appear faster than Sweet & Parker
- Effect of B-field pileup due to fast dynamics ?
- Other experimental configurations??

Part 3: Relativistic particle beams
Problem: Electron accelerators

Conventional accelerators have limits to electric fields from the threshold for electrical breakdown in material (E_{acc} ~ 20 MeV/m)

low electric fields

↓

long acceleration lengths

↓

large structures

↓

Huge Cost (Billions of $)

SLAC

2 miles

Solution?

(Tajima and Dawson PRL 1979)

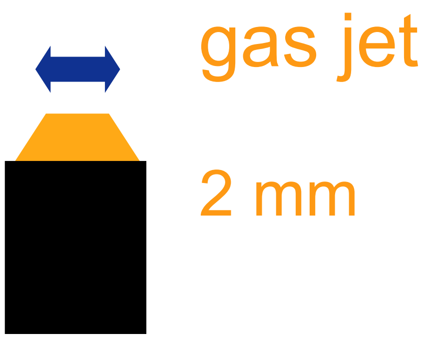

- plasmas are already ionized and accelerating fields are limited only by the plasma density (> 100 GeV/m)

- plasmas can support longitudinal electric fields moving close to the speed of light (relativistic plasma waves)

- lasers can couple to plasmas and can generate relativistic electron plasma waves ($v_{ph} = \omega_p/k \approx c$)

- electron beams can also produce relativistic plasma waves

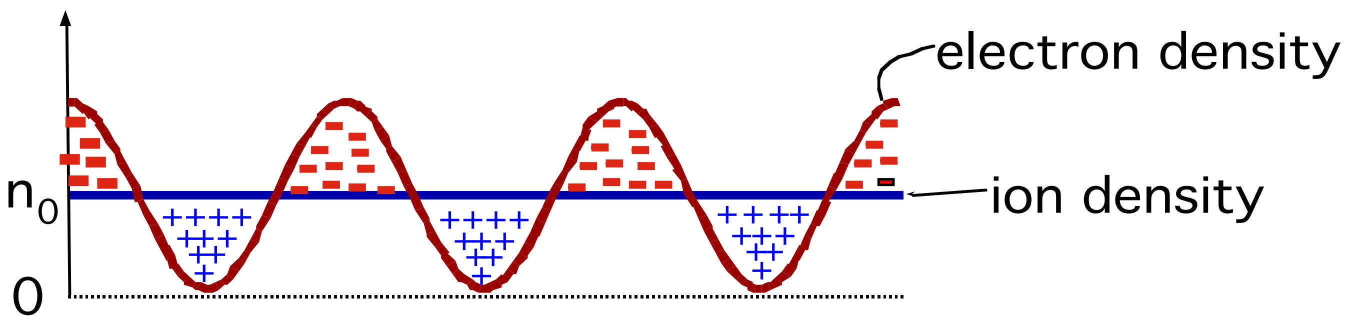

Sub 50 fsec pulses are required for good acceleration

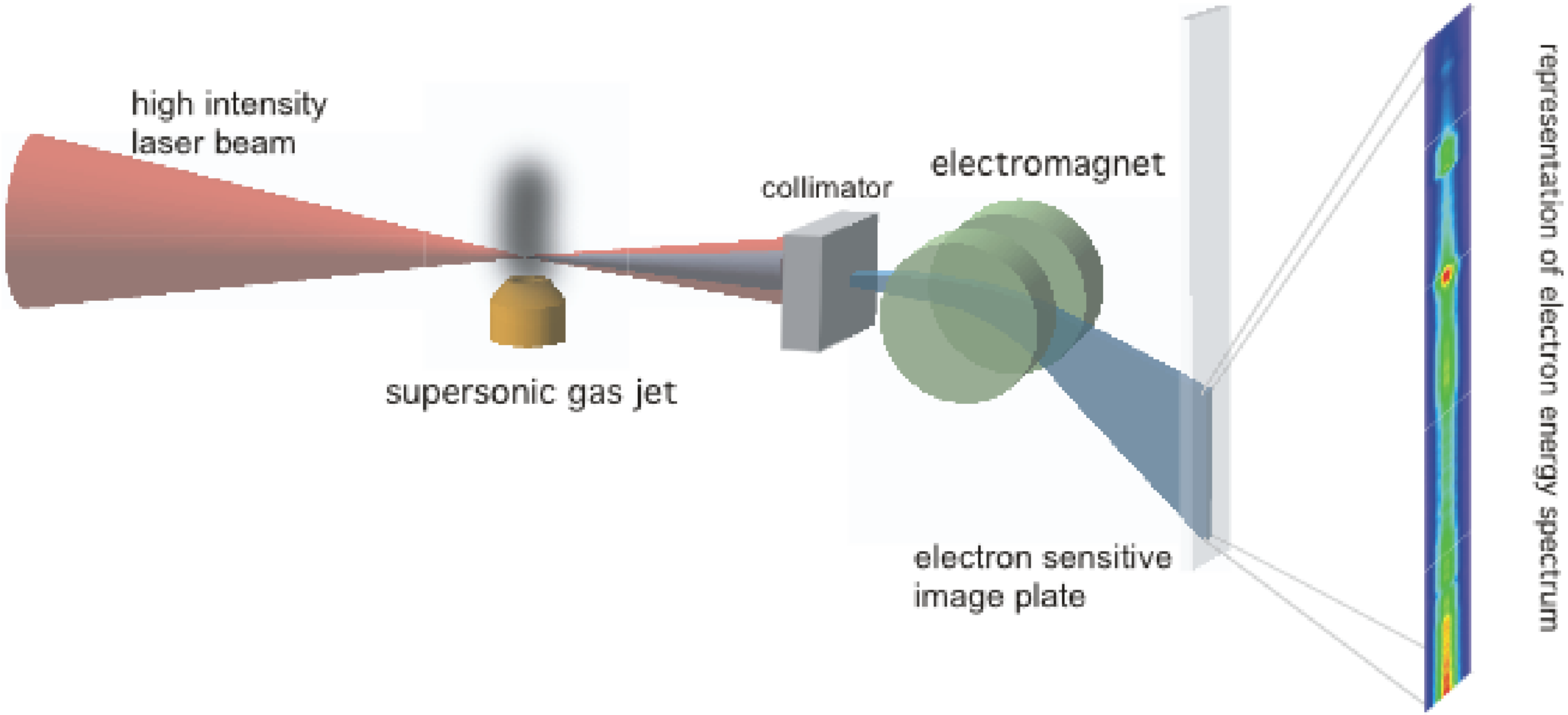

Laser wakefield acceleration

(for n ~ 10^{19} cm^{-3} the electric field is 10^4 > than conventional technology)

A short pulse of pulse length , τ

such that $\tau \approx 1/(2\pi\omega_p)$

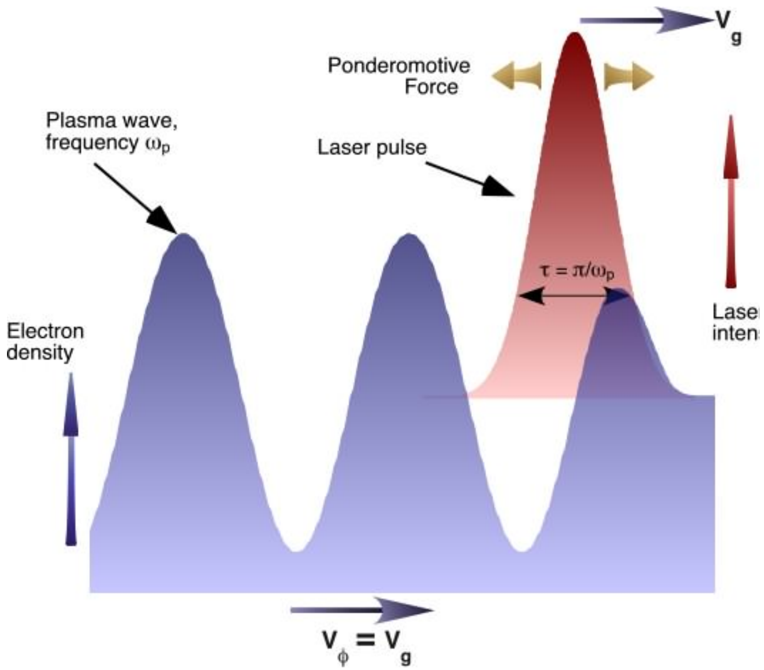

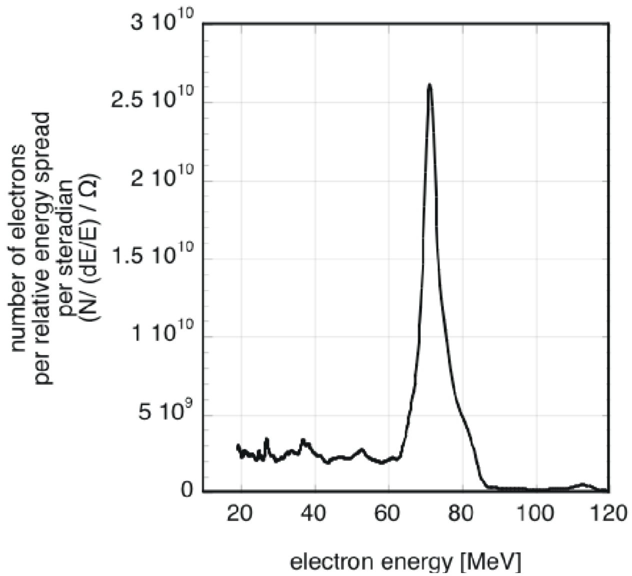

Simulations suggest that upgraded lasers to 500 TW can produce > 2 GeV beams

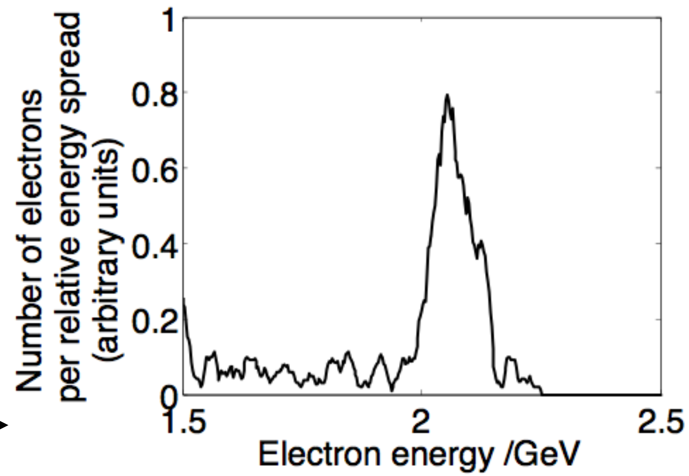

Electron beam divergence from LOA experiments

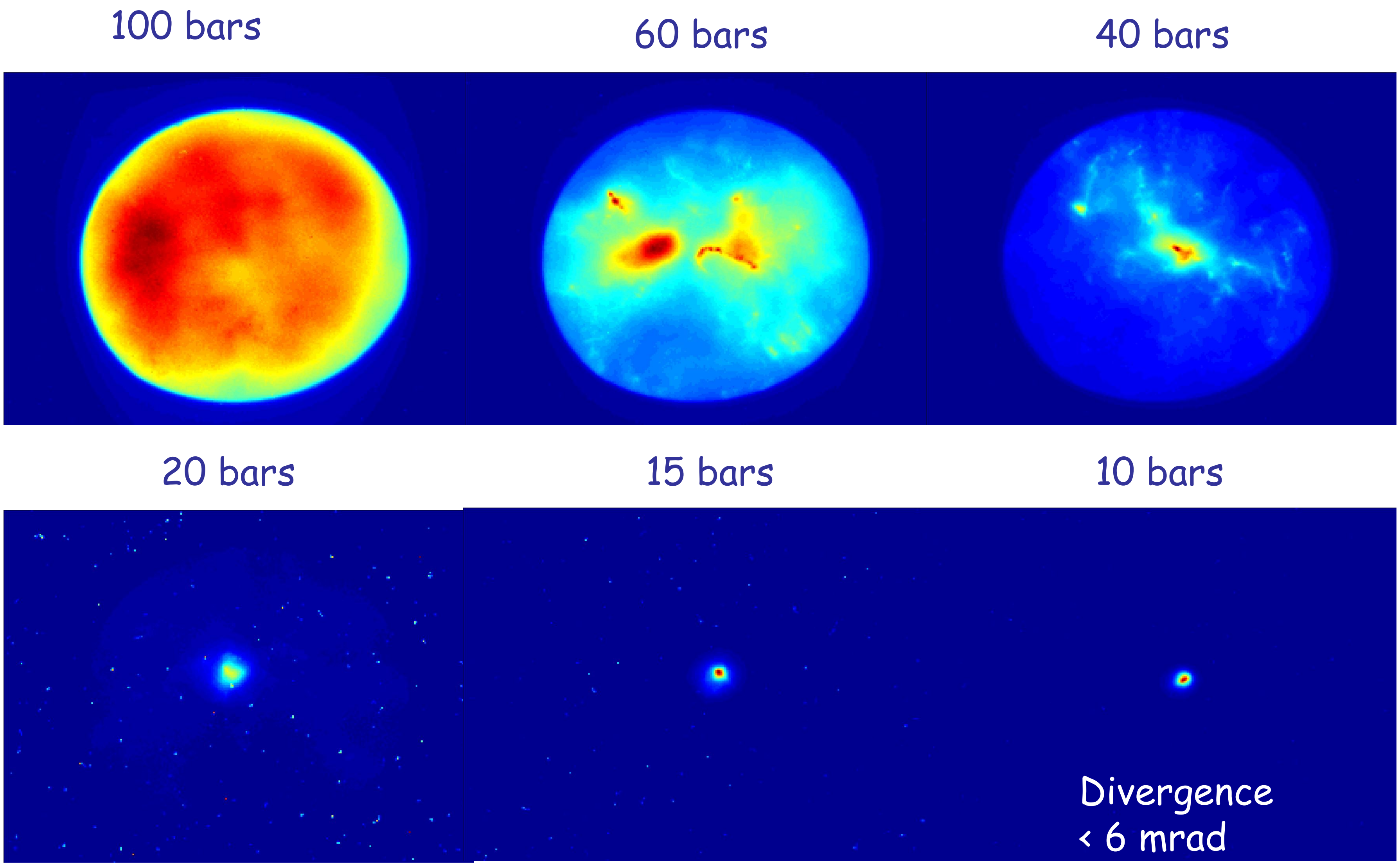

Progress in Laser Wakefield Acceleration

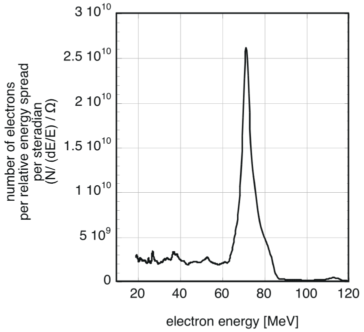

2004: Three groups demonstrate that laser wakefield acceleration can produce quality 0.1 GeV electron beams with ~15TW lasers

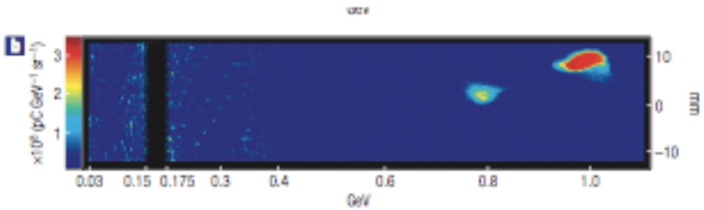

2006: Maximum energy achieved reaches 1 GeV using new external guiding technique with 40 TW laser (LBNL)

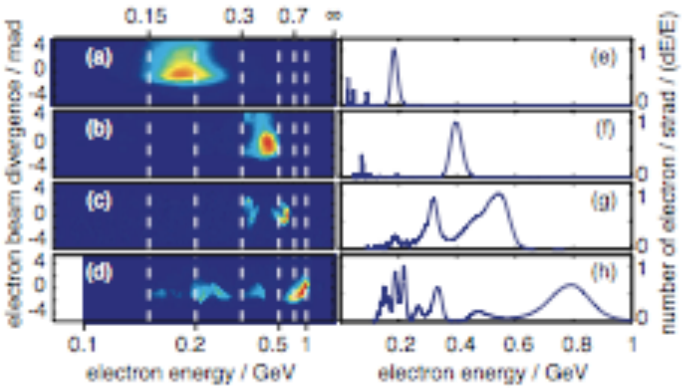

2008: Maximum energy using self- guiding also extended to 1 GeV by increasing laser power to 180 TW (Astra Gemini)

Laser Wakefield Acceleration

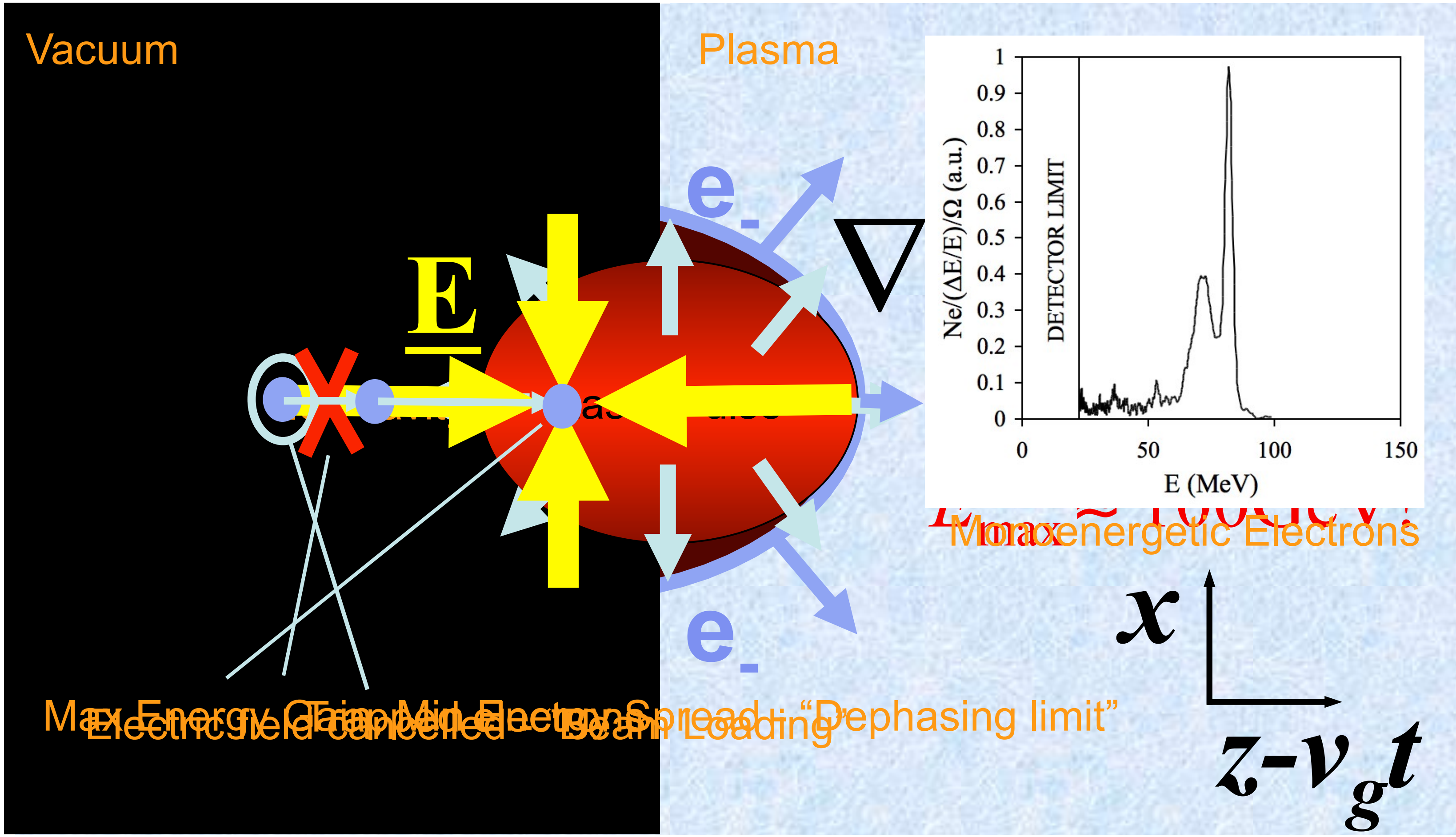

Predictions for the future

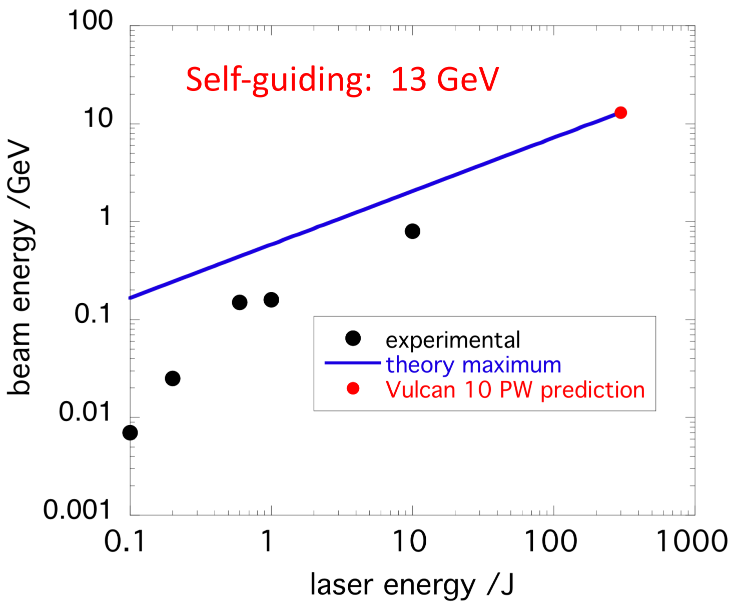

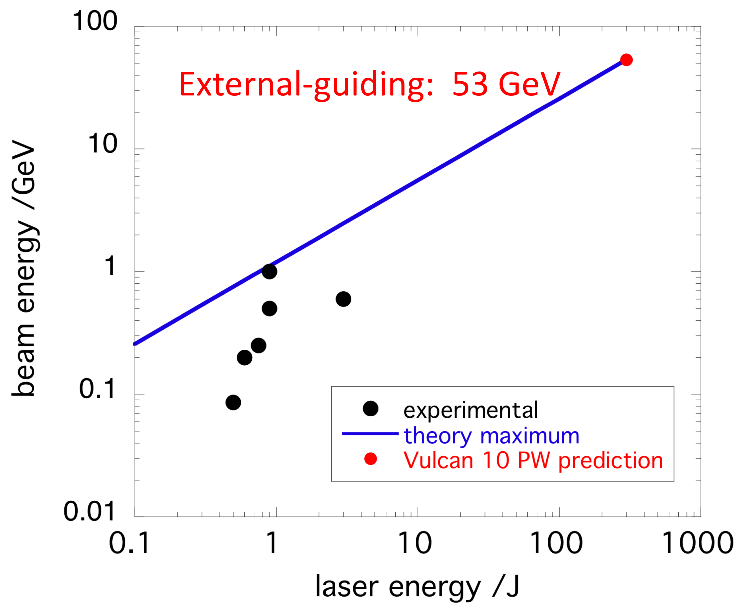

Engineering scaling laws developed from 3D modeling for both self-guided and externally-guided laser wakefield accelerators

Predictions are:

13 GeV in 10 cm for self-guiding

53 GeV in 175 cm for external guiding

Measuring the magnetic field can also give information about the e-beam (current)

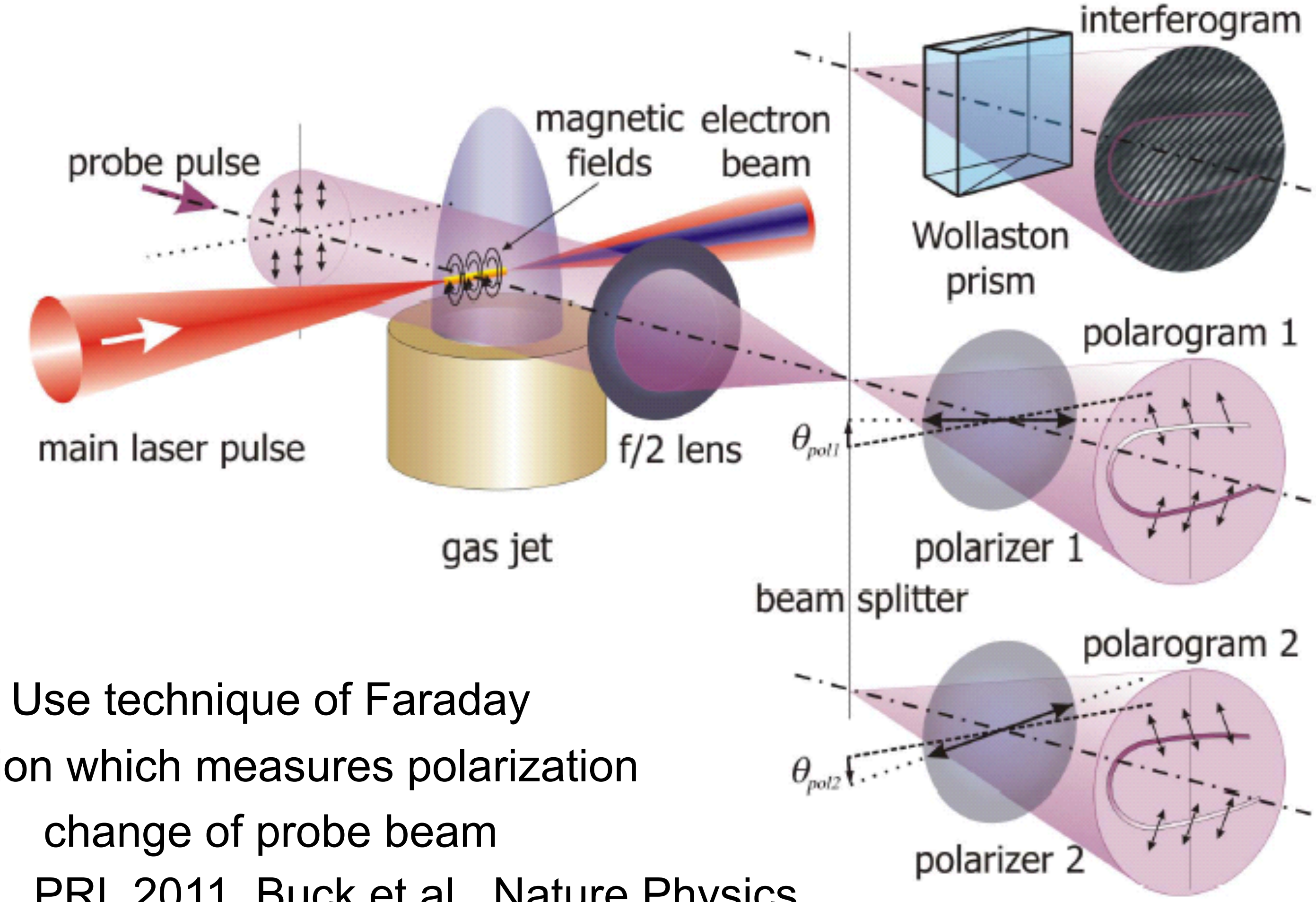

Use technique of Faraday rotation which measures polarization change of probe beam (Kaluza et al., PRL 2011, Buck et al., Nature Physics 2012)

Depolarized probe light can quantify the electron beam parameters during the interaction

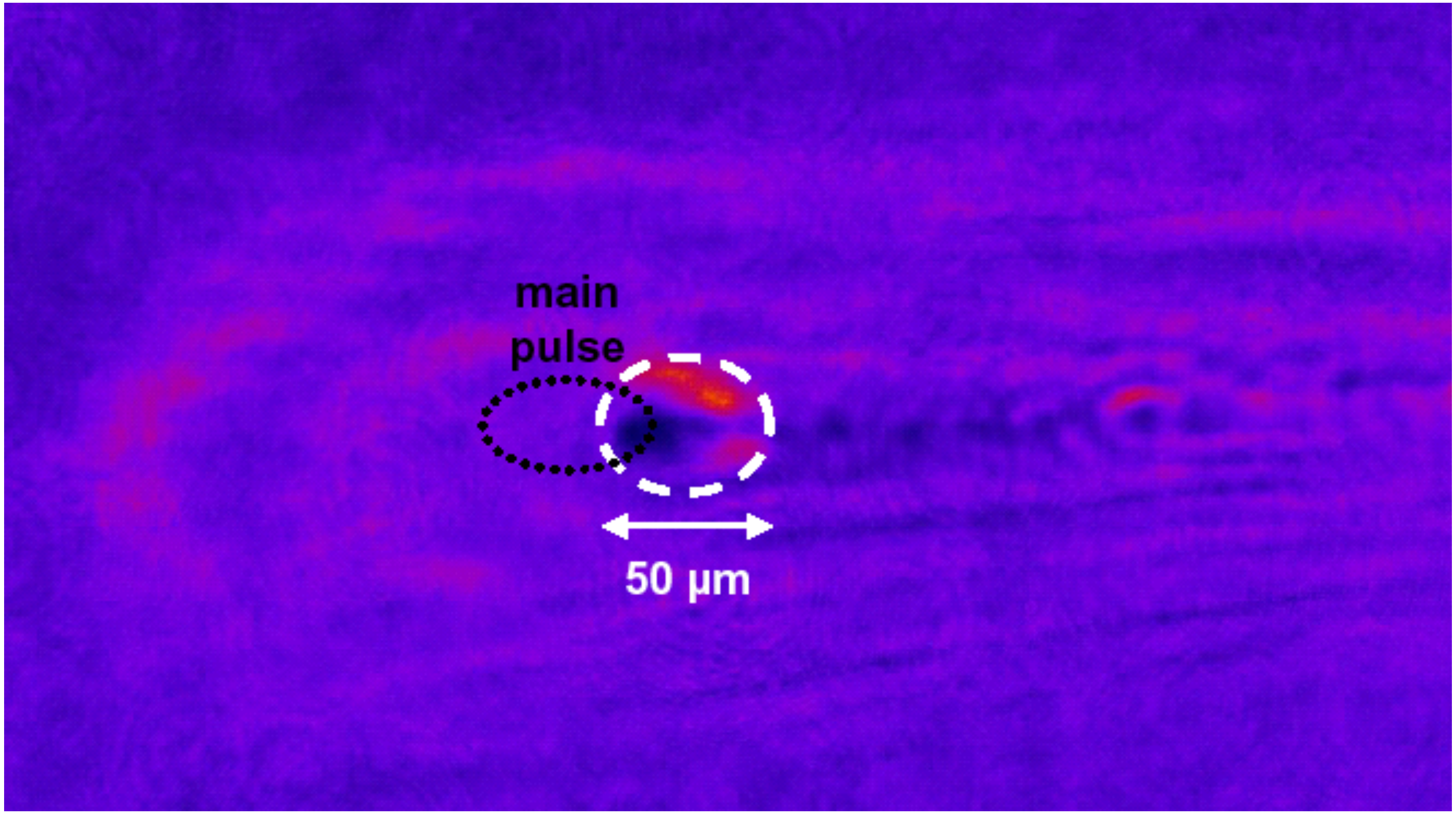

Electron beam charge is about 300 pC
- temporal evolution also measured at RAL and Jena
(Malte Kaluza et al., PRL 2011)

Reversal of intensity ratio by changing polarizer angles:

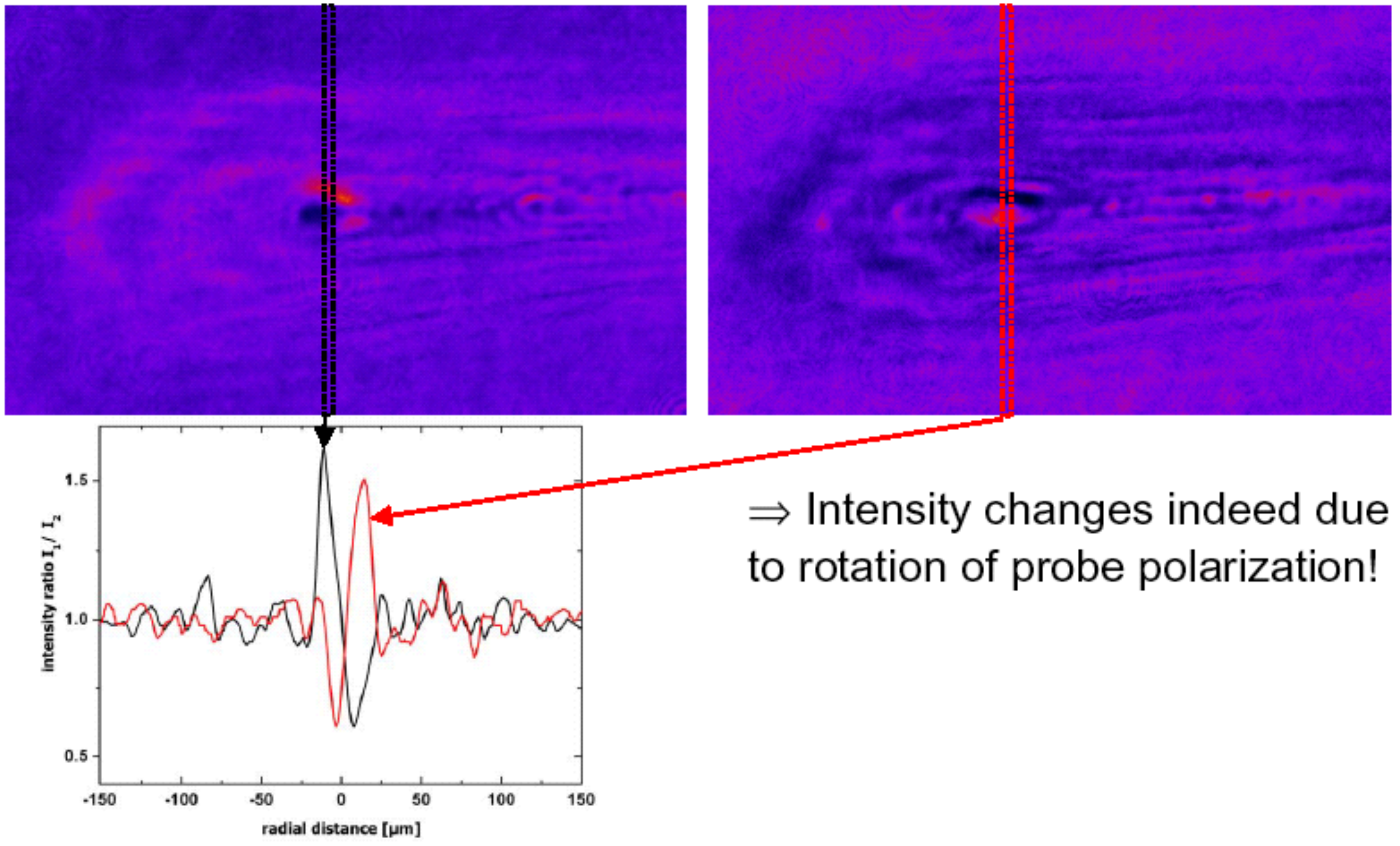

⇒ Intensity changes indeed due to rotation of probe polarization!

Temporal evolution and propagation of magnetic fields

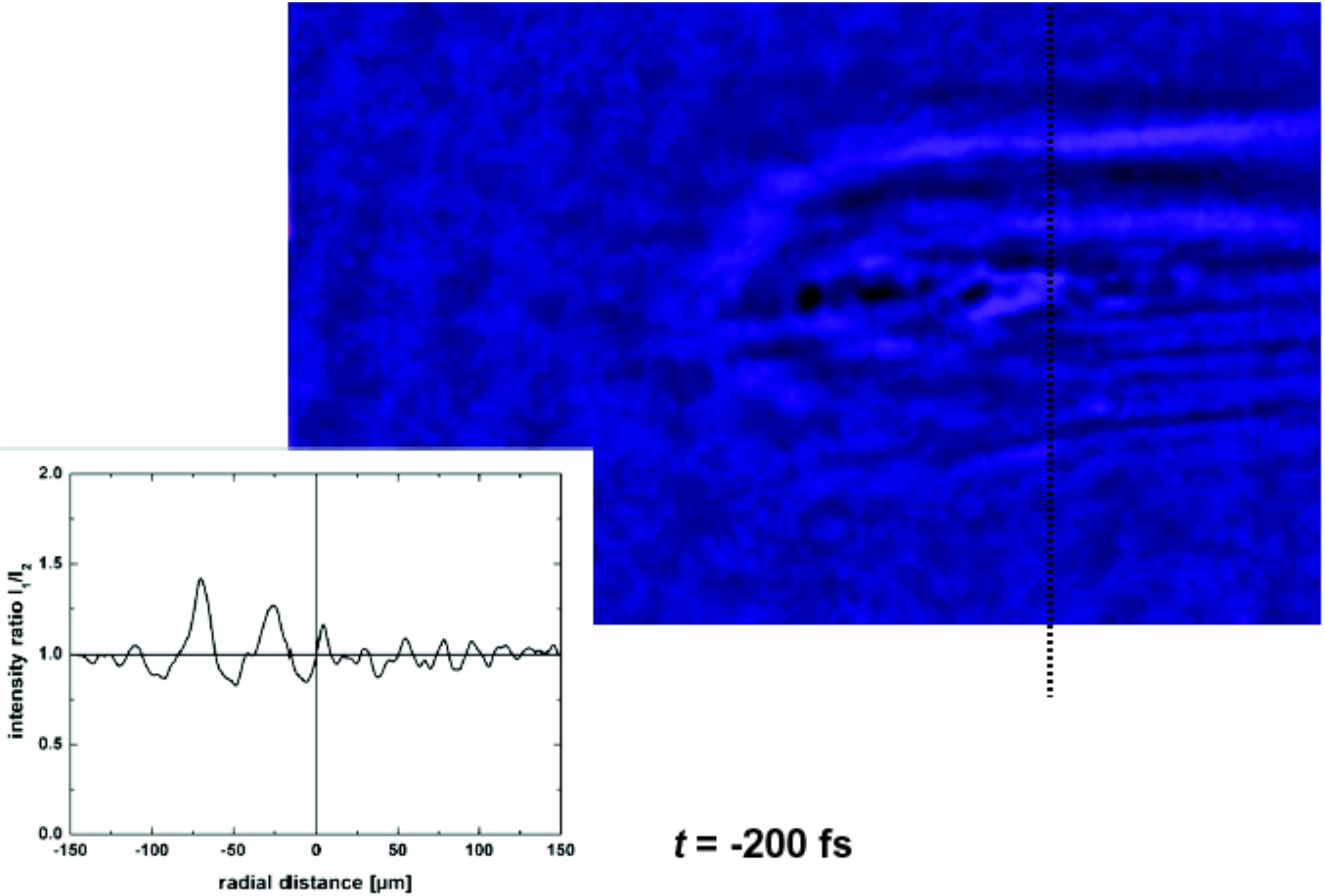

t = -200 fs

Temporal evolution and propagation of magnetic fields

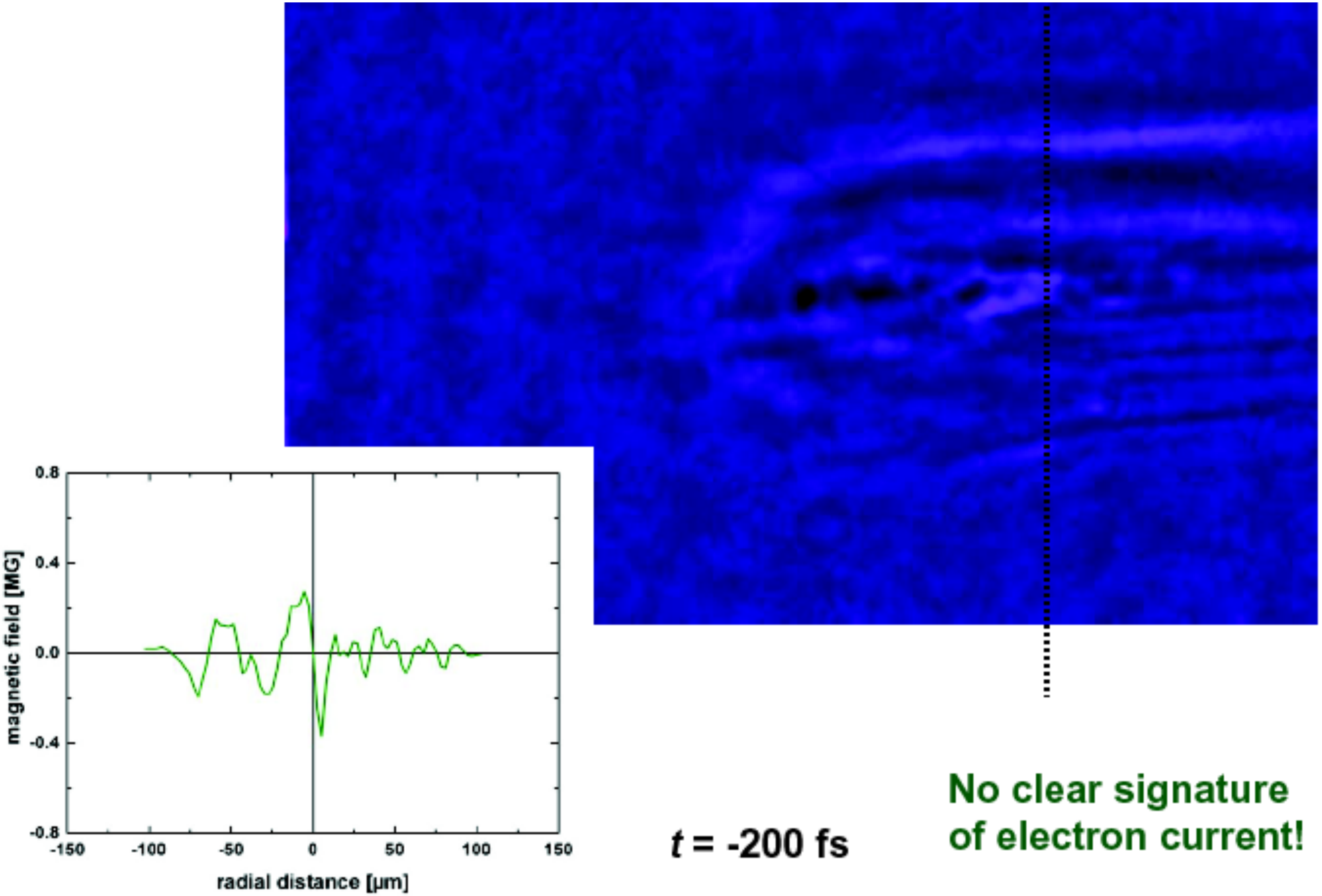

t = -200 fs

No clear signature of electron current!

Temporal evolution and propagation of magnetic fields

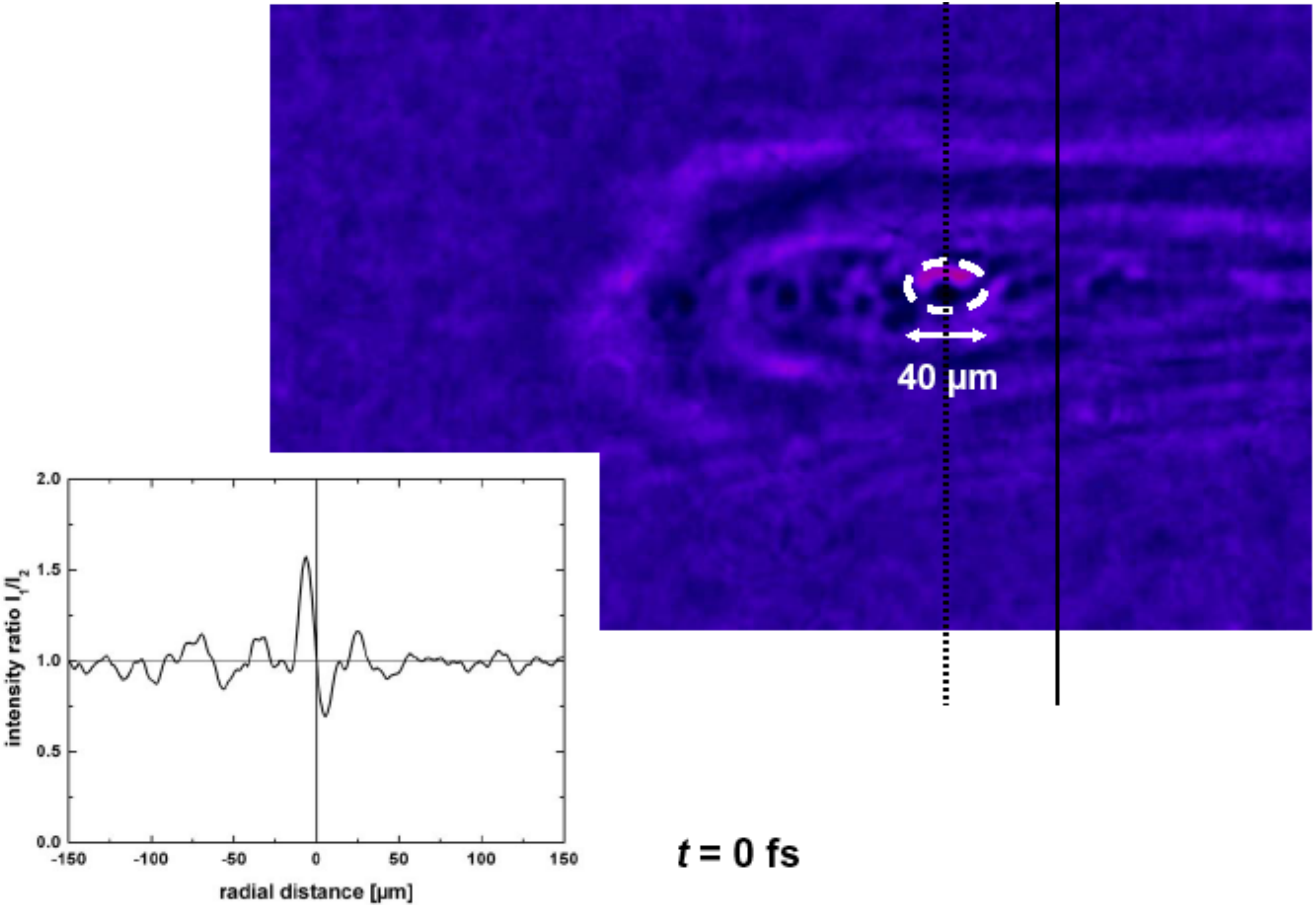

***t* = 0 fs**

Temporal evolution and propagation of magnetic fields

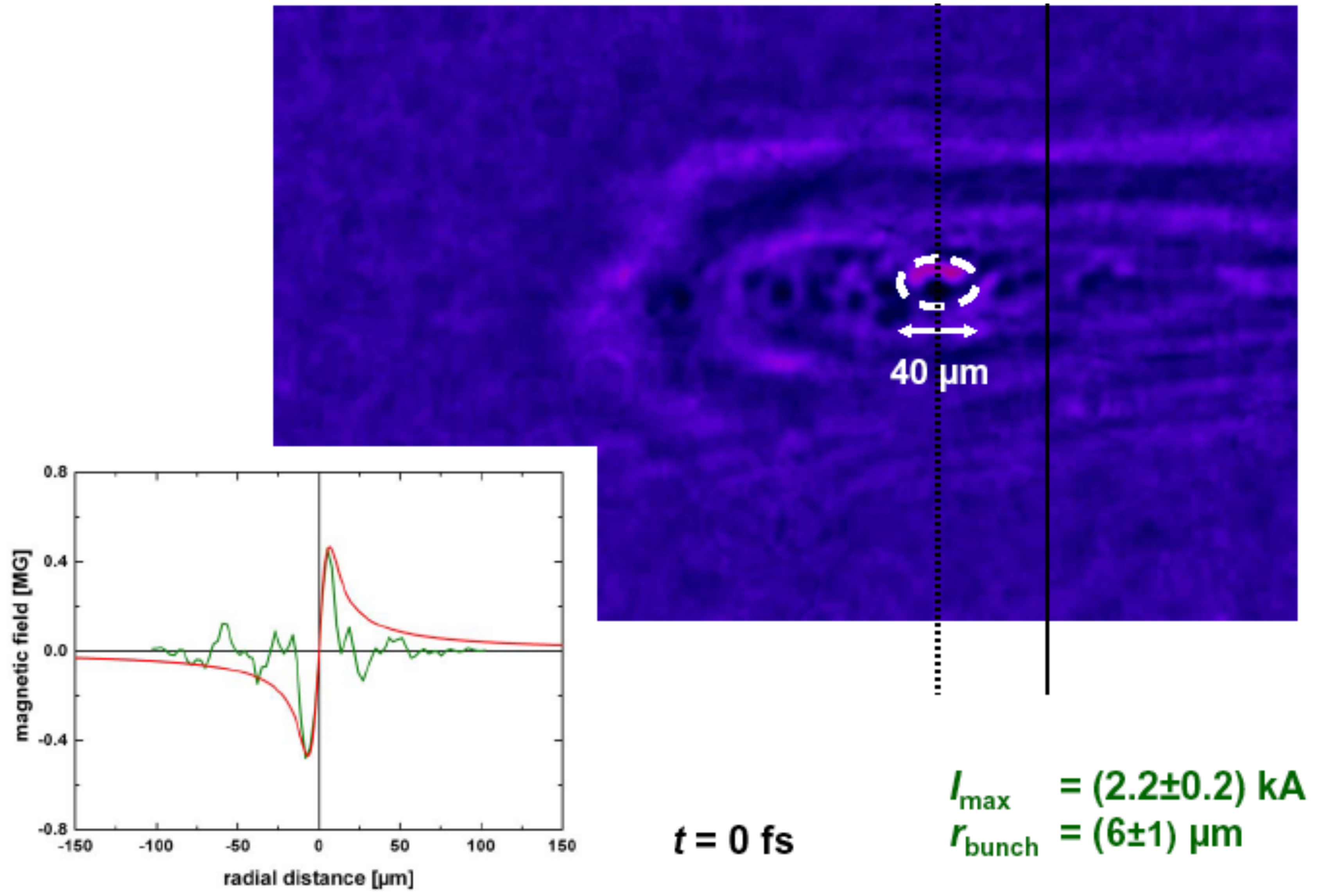

t = 0 fs

I_{max} = (2.2±0.2) kA
r_{bunch} = (6±1) µm

Temporal evolution and propagation of magnetic fields

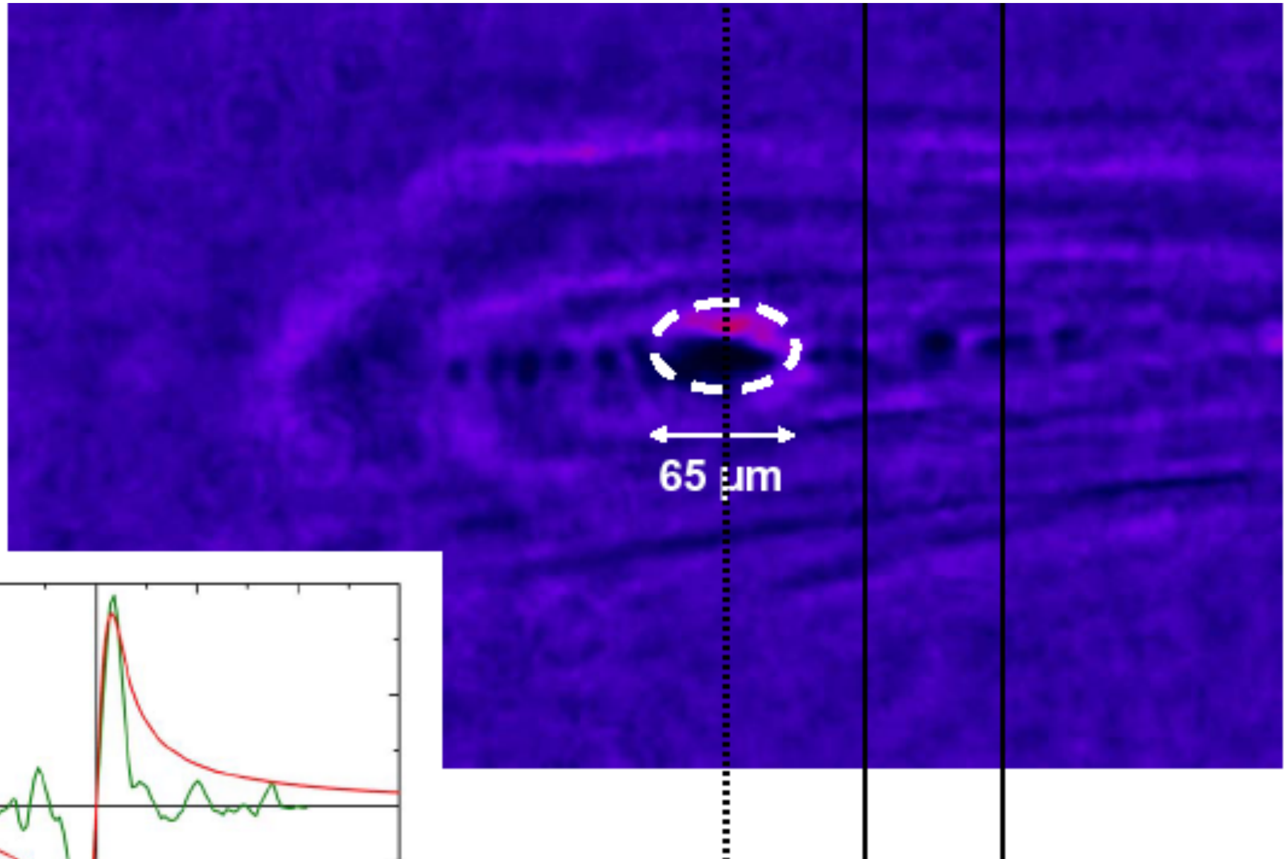

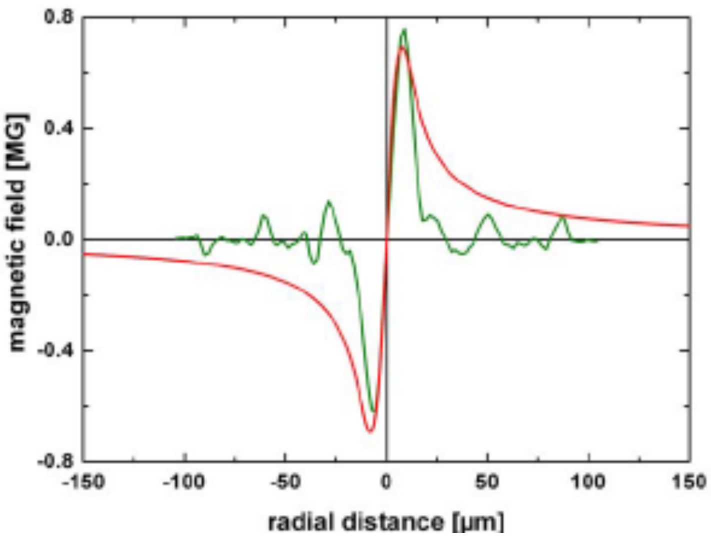

t = 200 fs

I_{max} = (3.8±0.3) kA

r_{bunch} = (7±1) µm

Temporal evolution and propagation of magnetic fields

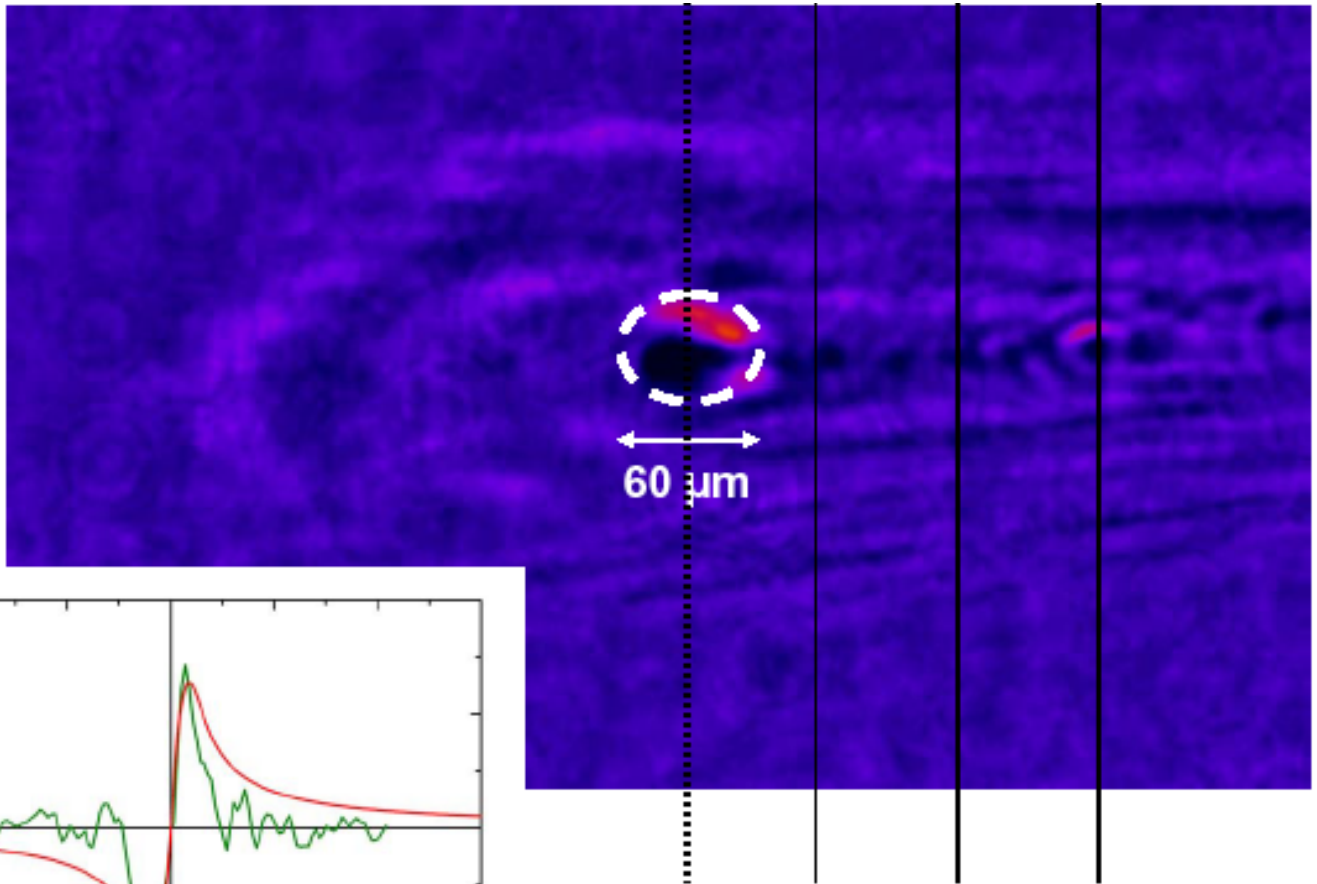

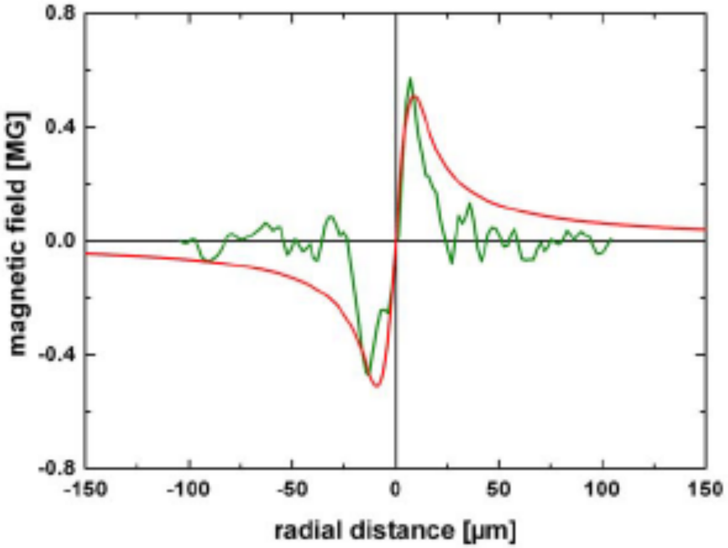

t = 400 fs

I_{max} = (3.2±0.3) kA

r_{bunch} = (8±1) µm

Temporal evolution and propagation of magnetic fields

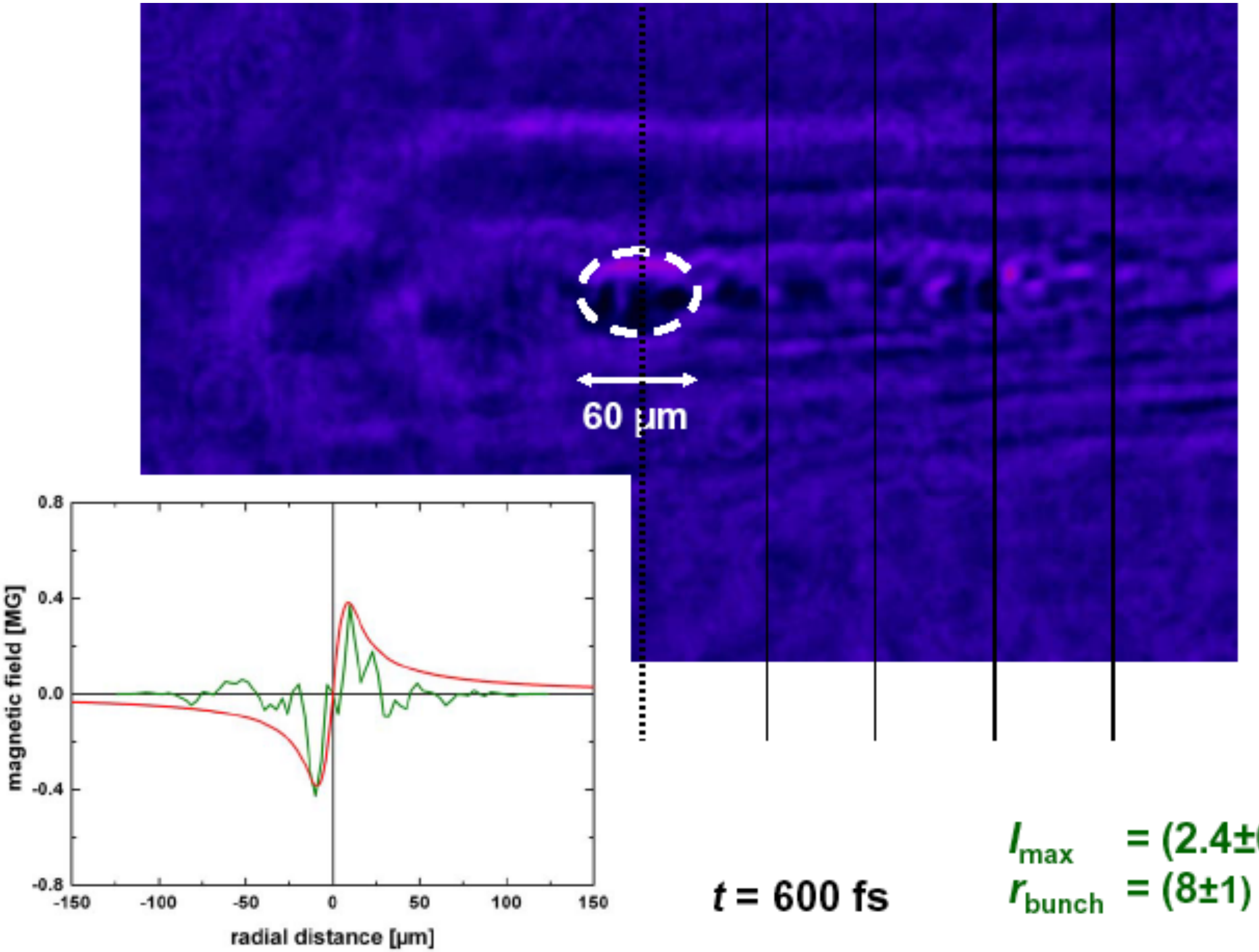

t = 600 fs

I_{max} = (2.4±0.2) kA
r_{bunch} = (8±1) µm

Temporal evolution and propagation of magnetic fields

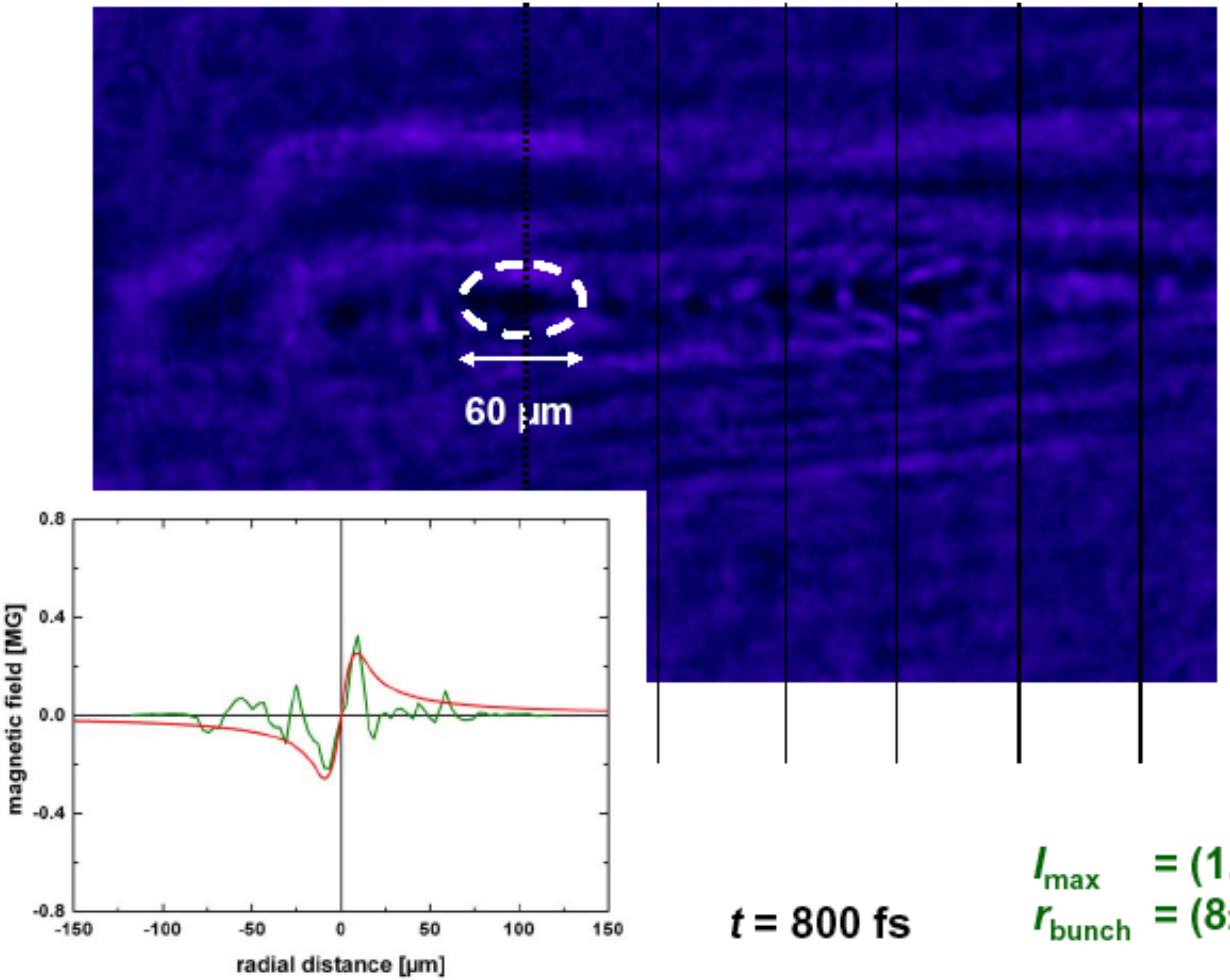

t = 800 fs

I_{max} = (1.6±0.2) kA
r_{bunch} = (8±1) µm

Temporal evolution and propagation of magnetic fields

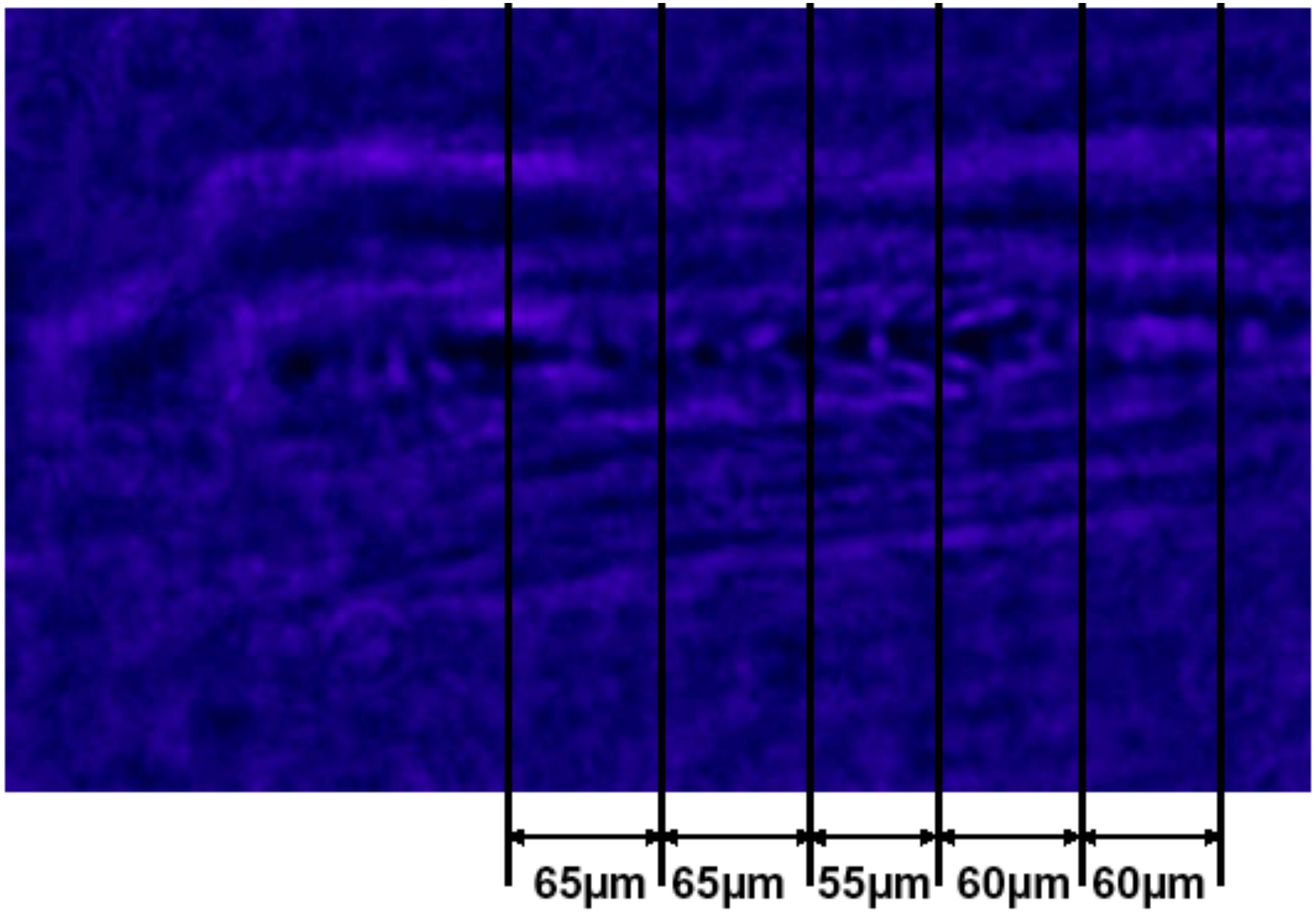

Velocity of electron current:

$\Delta t = 200\ \text{fs} \Rightarrow v_c = (3.00 \pm 0.25) \times 10^8\ \text{m/s}$

Can study Propagation Instabilities
Weibel instability / electron beam filamentation

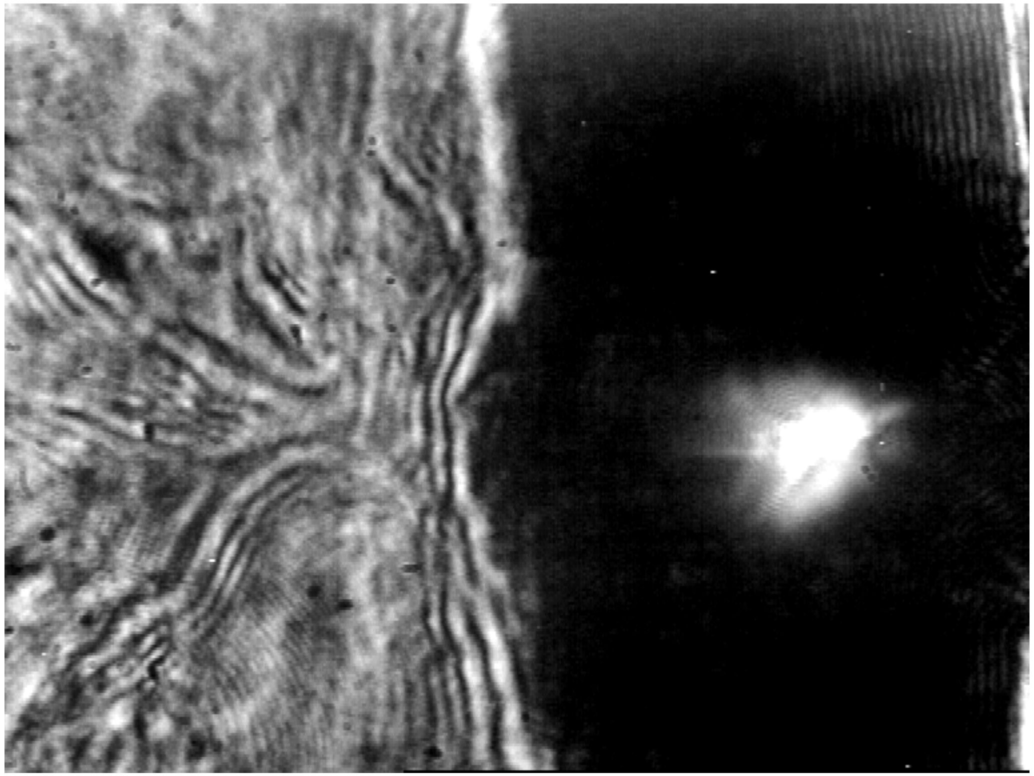

Probing time=300ps
Energy =100 J
Target= 50μm Mylar

laser

100 μm

Rear surface

Tatarakis *et al., Phys Rev. Lett.* (2003)

Investigation of the electron beam filamentation instability/Weibel (C. Huntington et al., PRL 2011))

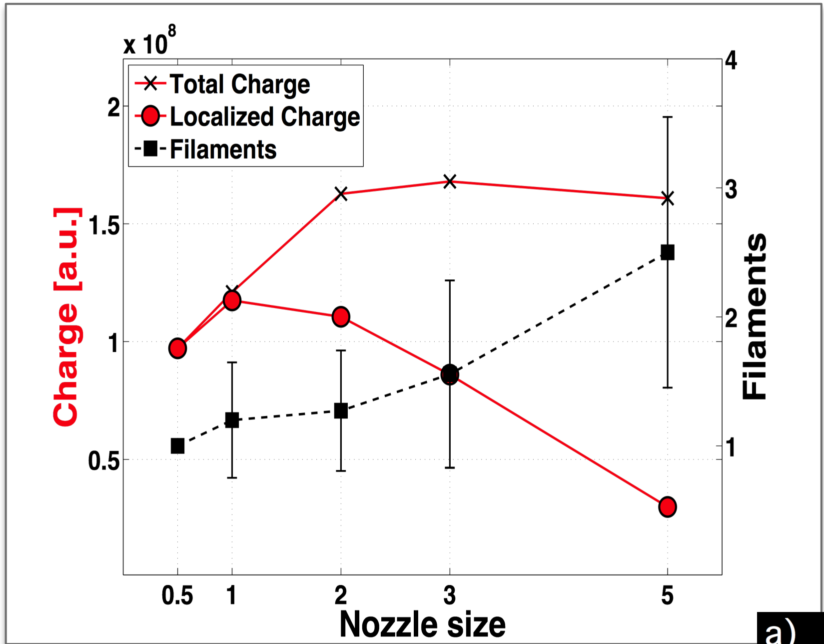

Interaction length

a) 0.5 mm
b) 1 mm
c) 2 mm
d) 3 mm
e) 5 mm

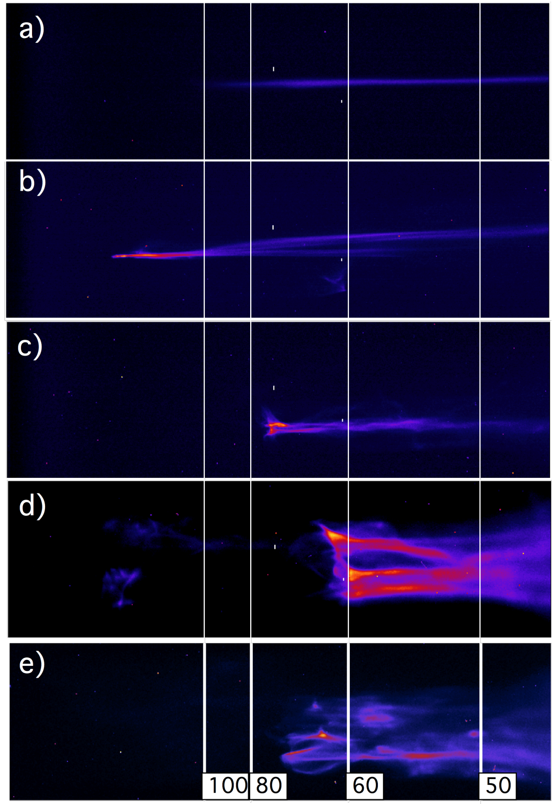

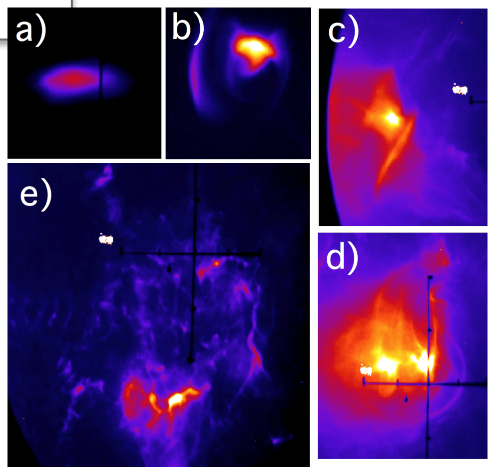

As electron beam propagates through extended distances of plasma the beam filaments due to a propagation instability

LWFA electrons as a ultrashort probe

- instead of non-relativistic protons

- LWFA electron bunches have duration of plasma oscillation period (30 fs) or less
- LWFA electrons are quasi-monoenergetic and highly-relativistic (γ ~ 200)
  - Comparable sensitivity to protons in terms of magnetic field deflections

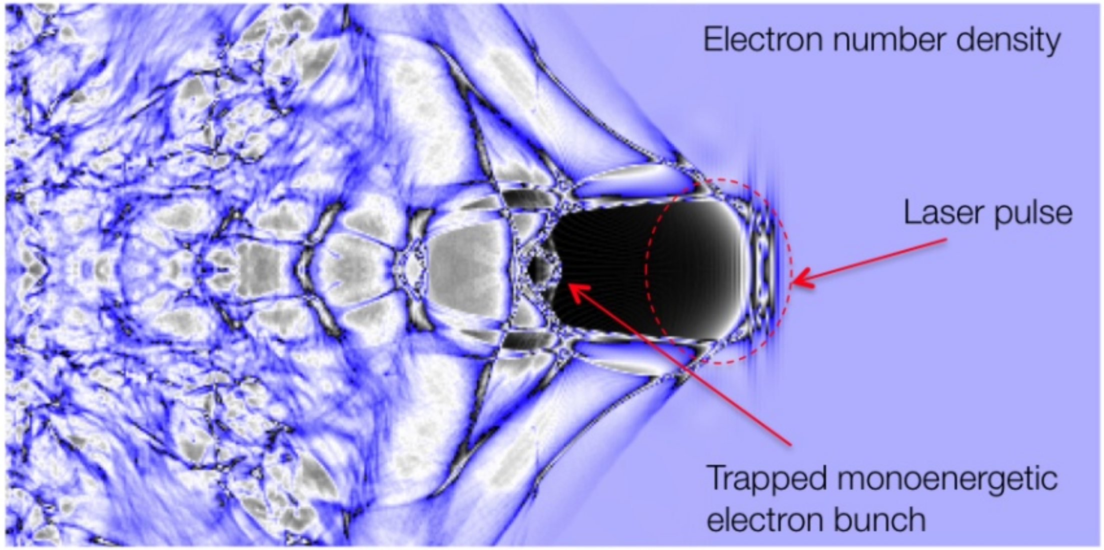

OSIRIS Paricle-in-Cell Simulation of LWFA

Probing Magnetic Fields with LWFA Electrons

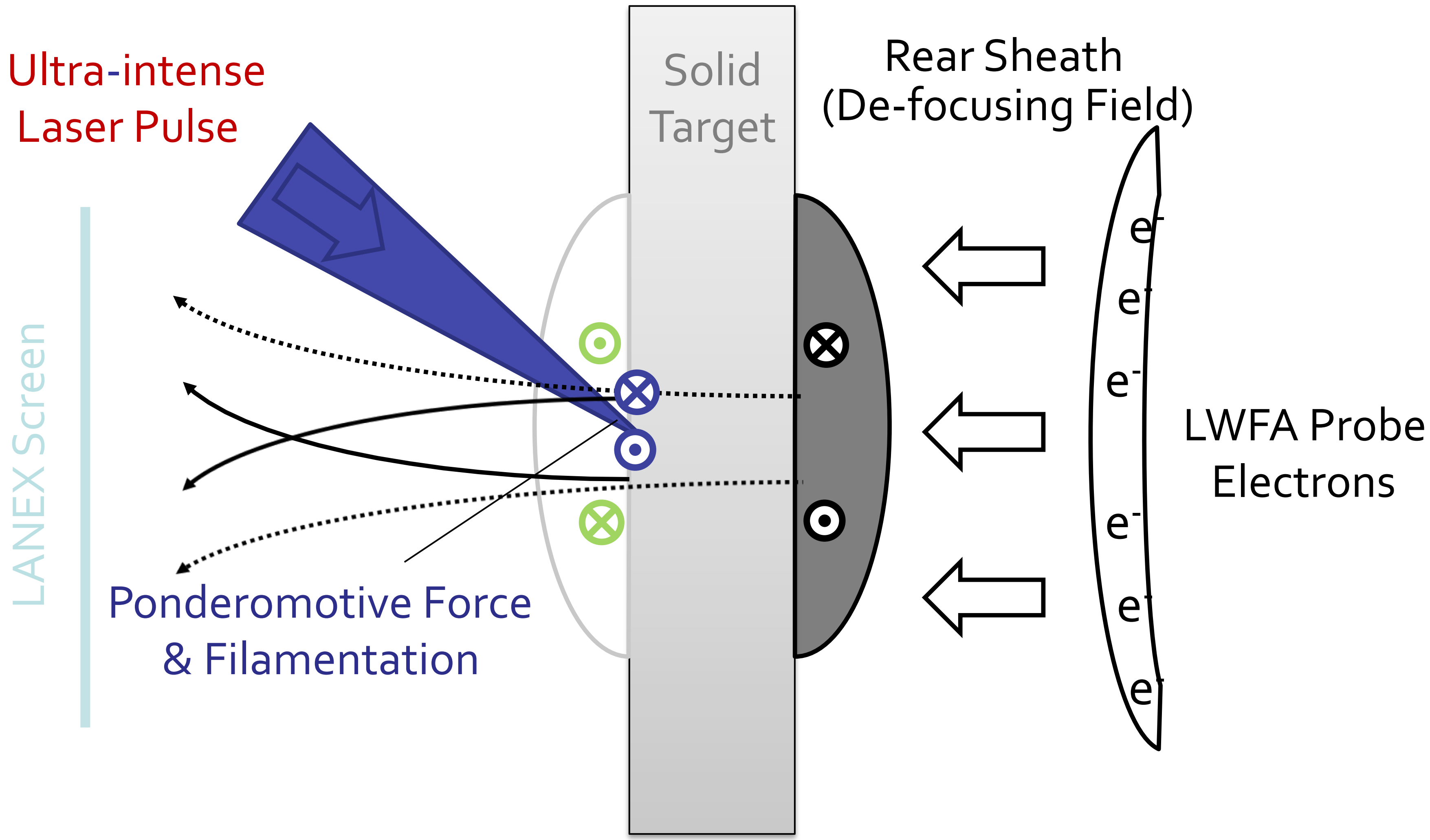

Experimental Setup

Schumaker et al., PRL (2013)

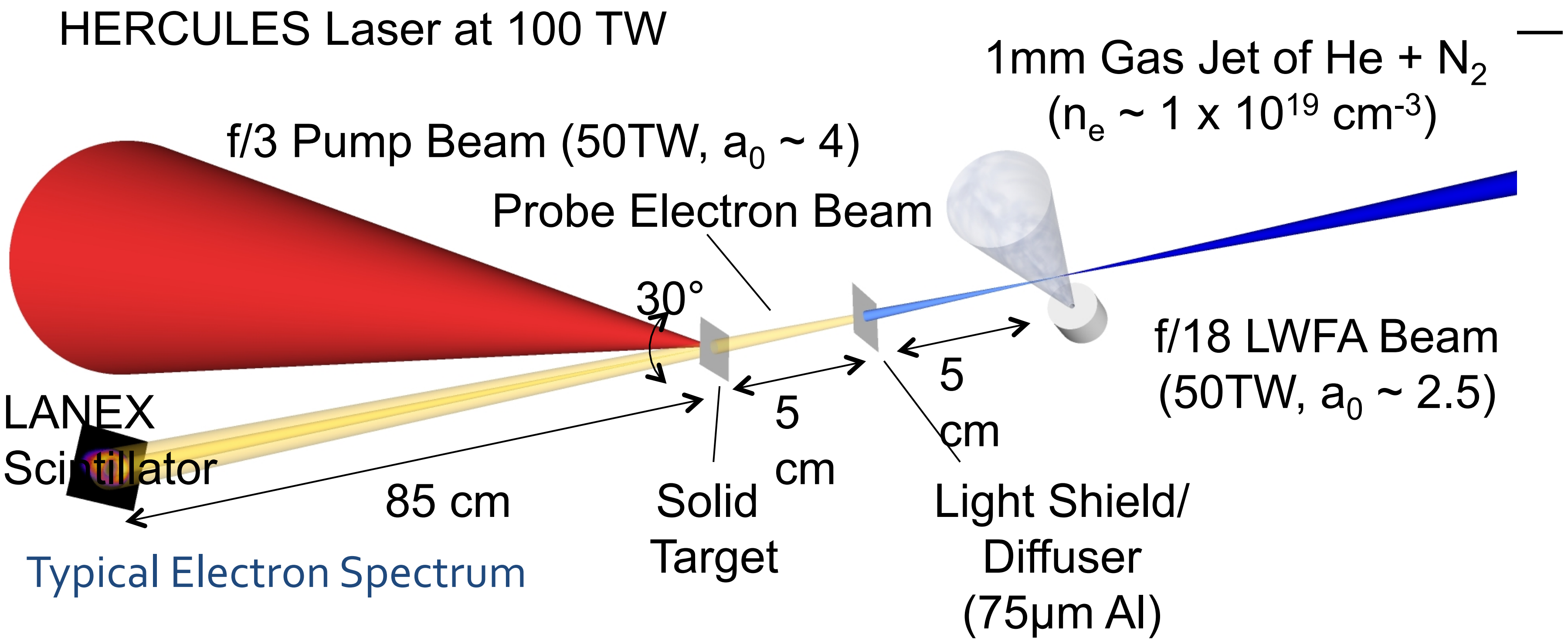

Typical Electron Spectrum

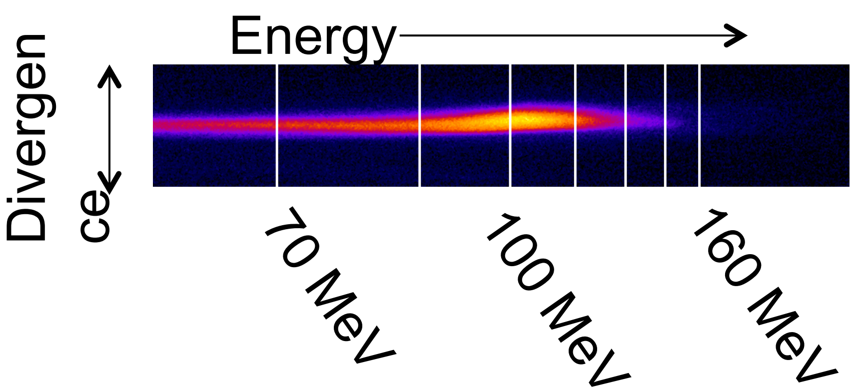

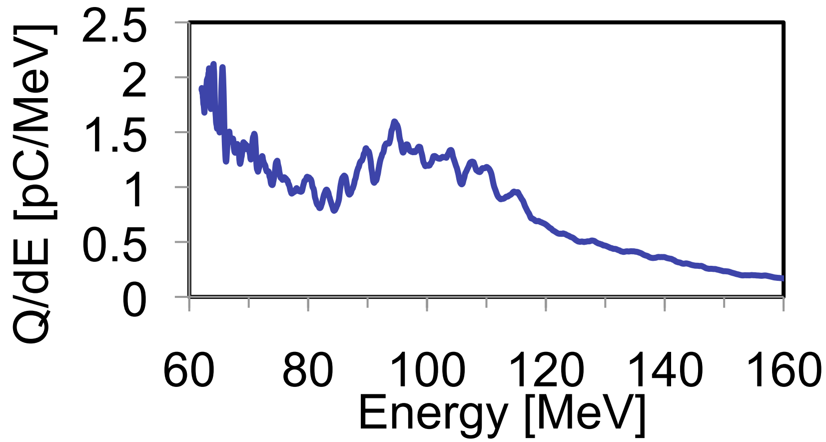

Magnetic field strength can be estimated from the deflection of electrons

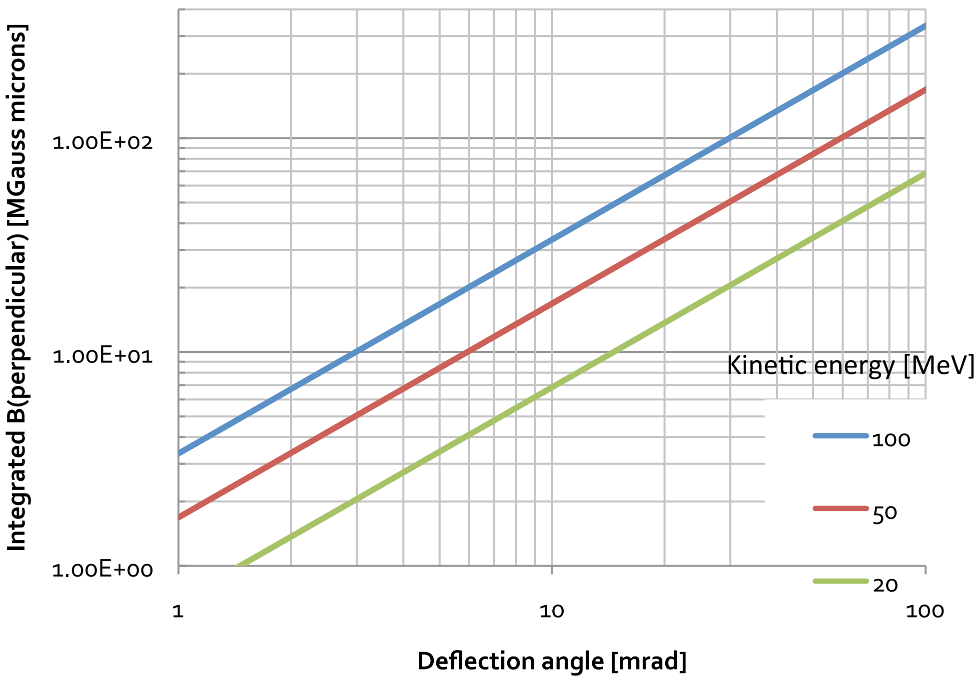

$$\int_L \mathbf{B} \times dl = \frac{m_0 c \theta_d}{e} \sqrt{\left(\frac{m_0 c^2 + \varepsilon_k}{m_0 c^2}\right)^2 - 1}$$

θ_d : *deflection angle*

ε_k : *kinetic energy*

Estimate: 60 mrad of deflection angle with 100MeV electron beam

- Integrated Magnetic Field: ~200 MGauss*µm
- Assuming : 2µm thick field w/ XPW => ~100 MGauss!

Radiographs of 10µm Al Targets

All Shots on Same Color Scale

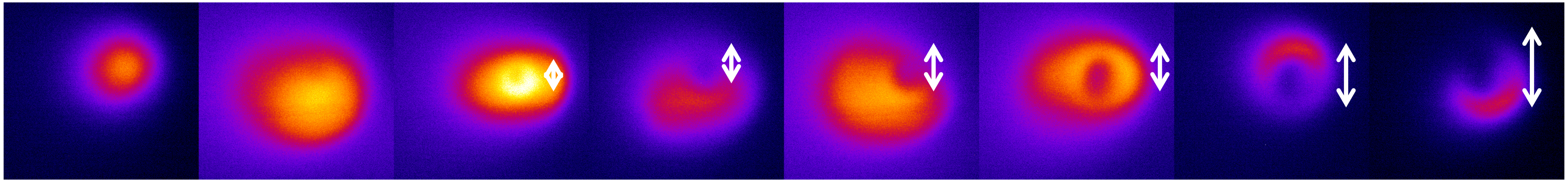

-500fs 0fs +167fs +333fs +500fs +667fs +1000fs +1333fs

- At early delay, a strong focusing structure quickly turned to blurred de-focusing

- De-focusing structure grew linearly at close to the speed of light, accounting for:
    - **Diameter** growth at ~ 2c (**Radial** growth at ~ c)

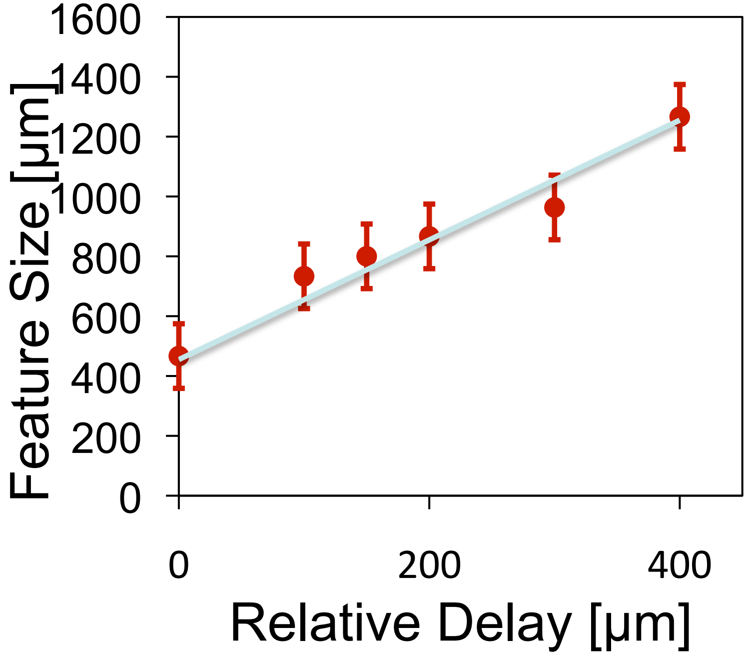

PIC Simulation of 10μm thick Al

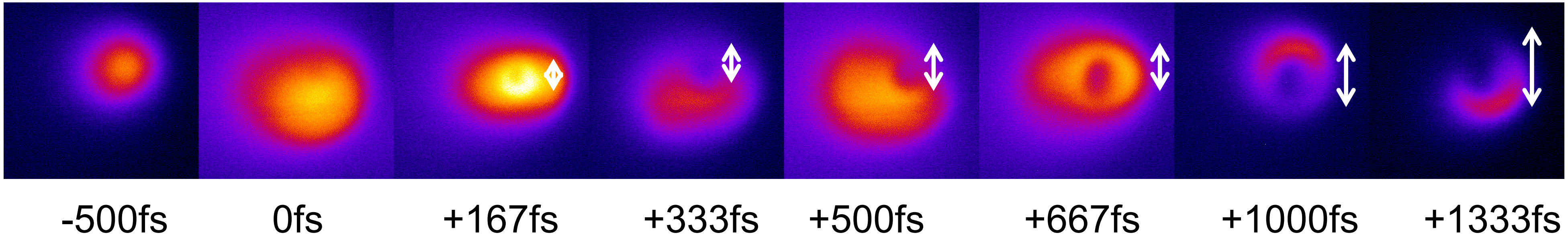

- Simulation parameters: a_0 = 6, n_e = 100*n_{crit}, τ = 34fs, w_0 = 5μm, $L_{preplasma}$ = 1μm

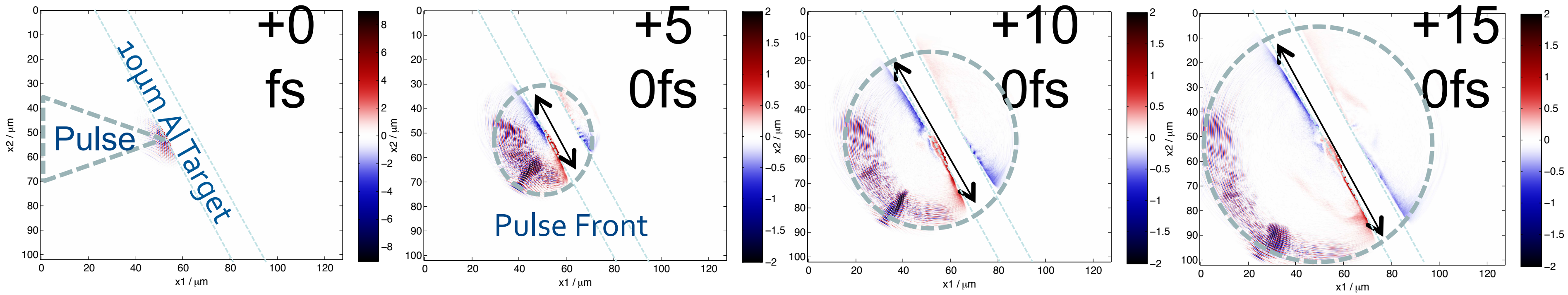

- Front surface magnetic fields are ~ 3-5 times stronger than the rear (~100 MG)
- Fields contained within 1-2μm scale length on target surface

Use short pulse laser generated plasmas to make high density positron sources (H. Chen et al.) LLNL

LLNL Titan two-beam laser

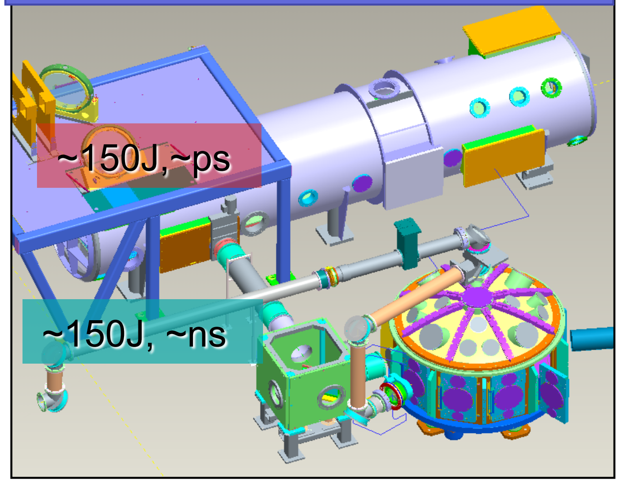

Experimental setup

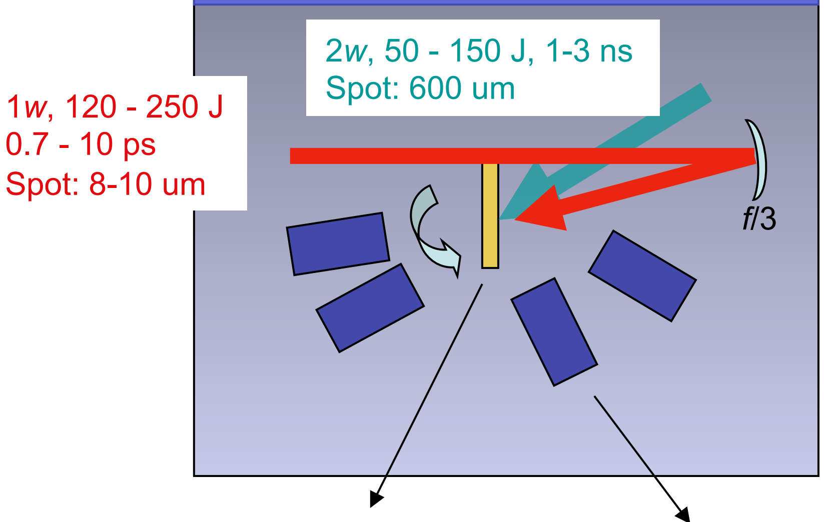

Timing for the two beams

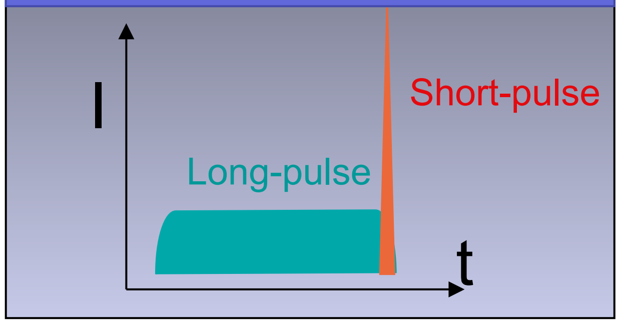

Targets

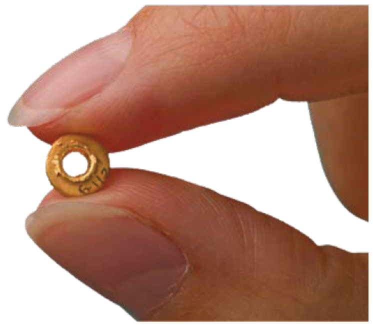

Al, Cu, Sn, Ta, Au
Thickness: 0.1 - 3.1 mm

EPP Spectrometers

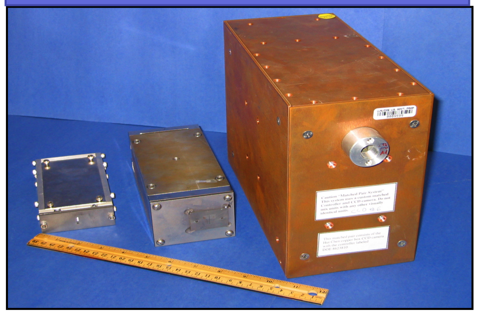

Chen et al. RSI 08

Two main processes involved in laser positron creation in the presence of high-Z nucleus

1. Direct (Trident) pair production

   $e^- + Z \rightarrow 2e^- + e^+ + Z$

   (Z: nucleus)

2. Indirect (Bethe-Heitler) pair production:

   $e^- + Z \rightarrow \gamma + e^- + Z$

   $\gamma + Z \rightarrow e^- + e^+ + Z$

   (γ: Bremsstrahlung)

Nahashima & Takabe, 2002

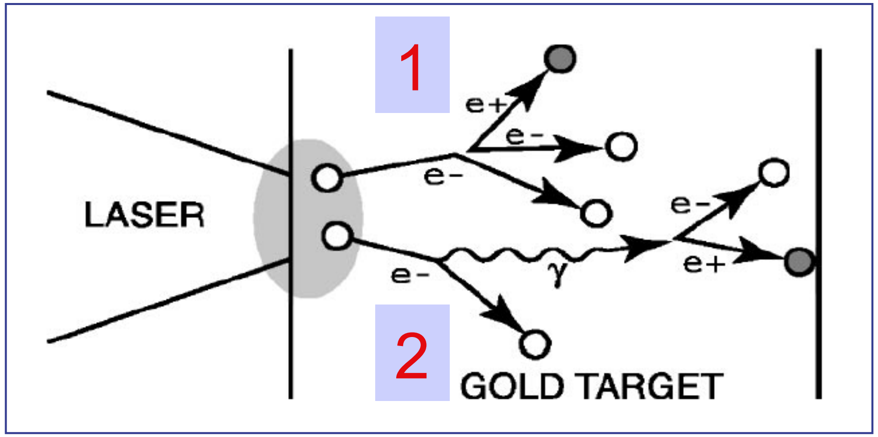

High energy (>MeV, relativistic) *e*-s are the key of both processes

Experiments on the OMEGA EP laser (~ 1 kJ) (2009, H. Chen et al.)

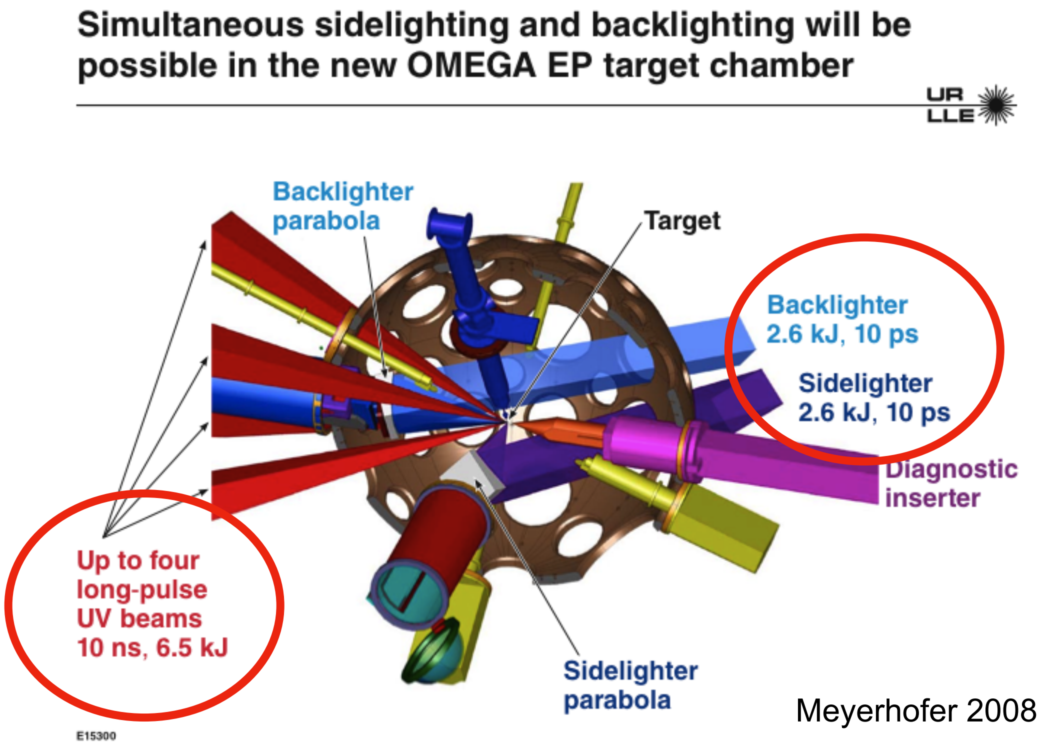

Meyerhofer 2008

EPPS positron shot #5082 (812 J, 10ps)

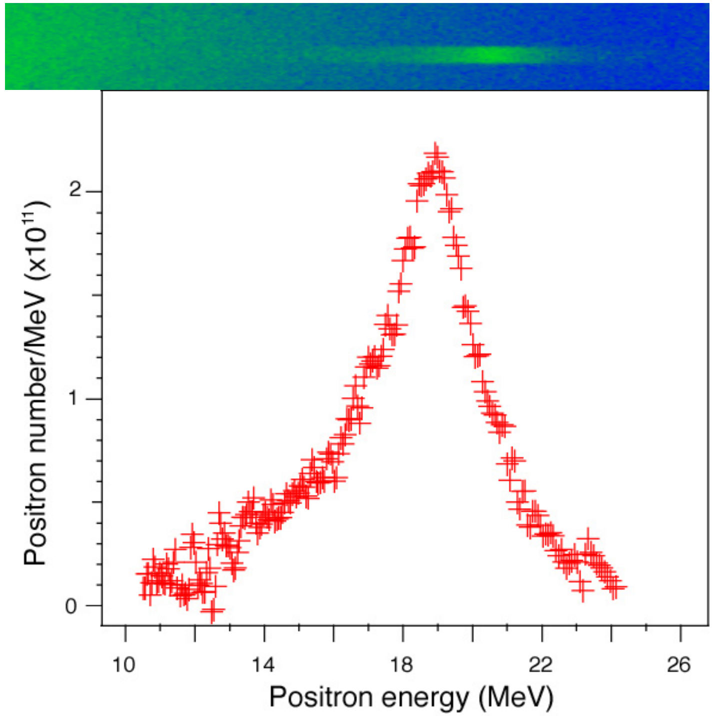

- $\sim 2\times10^{11}$ positrons
- Highest rate of positron production: $\sim 2\text{x}10^{22}$ e+/s

The electrons & positrons form a jet at the back of target, and can be controlled experimentally

Quasi-mono-energetic positrons

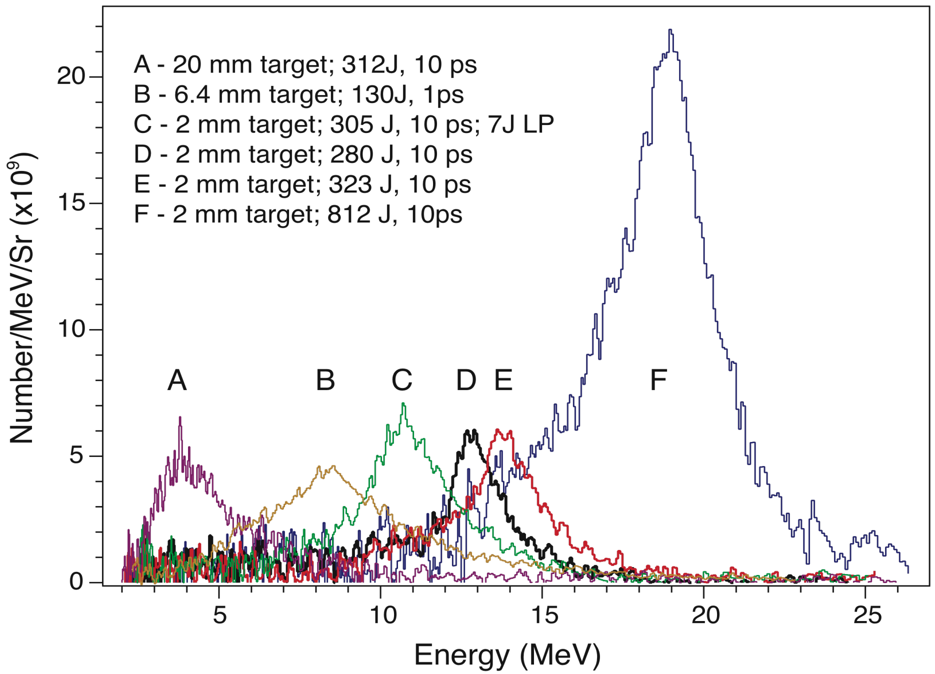

Rear e+ number vs angle

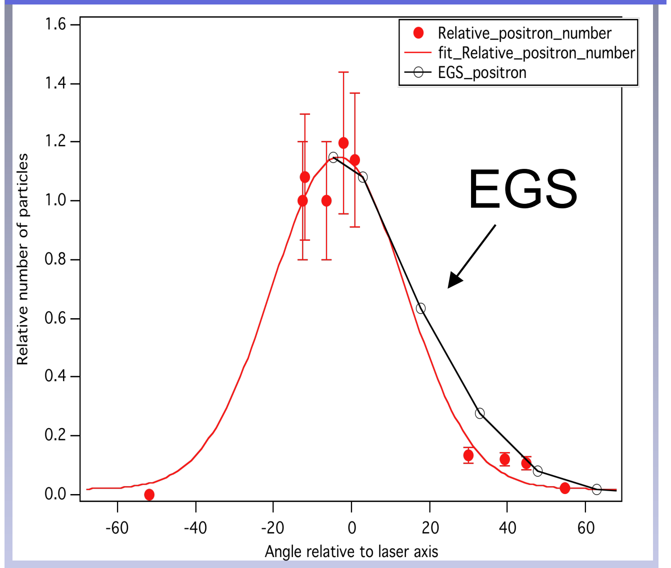

FWHM: 40.3°, center at -3.3°
EGS agree with exp. data

Hui Chen et al., PRL 2010

These properties are critical to the future laboratory astrophysics experiments on relativistic pair plasmas

Pair jets with attractive properties are made from 100 - 800 J short pulse lasers

Number of pairs:	10^{10}-10^{11}
Jet angular spread:	~20 degree
Peak energy:	4 - 20 MeV
Energy spread:	50% - 20%
Temperatures:	~3 MeV (beam direction)
	~1 MeV (transverse direction)
Energy conversion:	$>2\times10^{-4}$ (from laser energy to pair jets)

These parameters would scale up with higher laser energies

Magnetically confined MeV pair plasma?

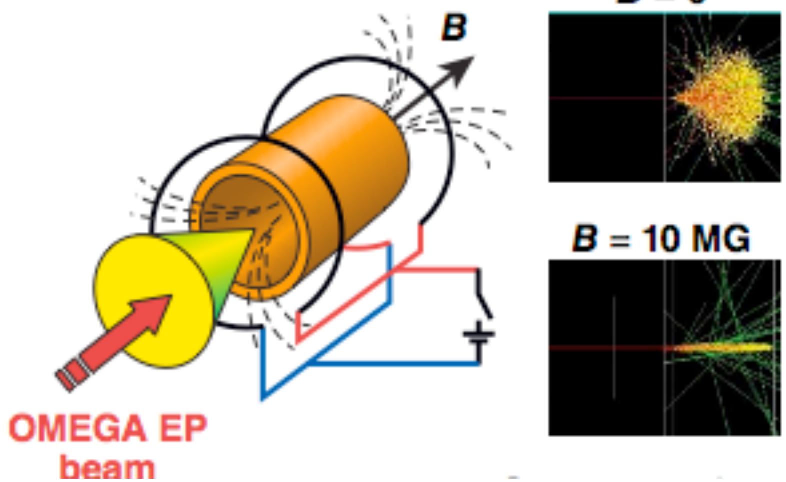

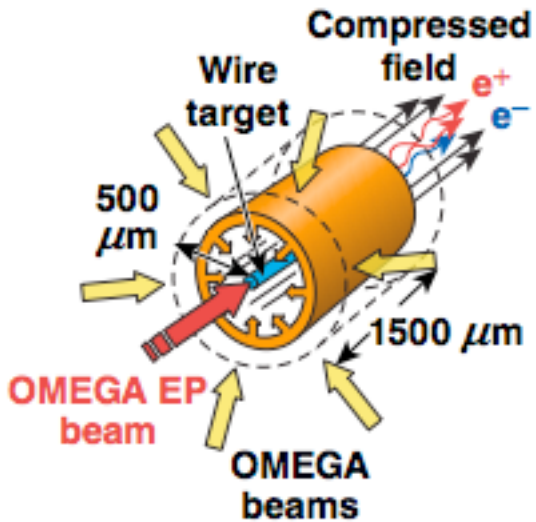

*J. Myatt *et al.*, Bull. Am. Phys. Soc. 51 (7), 25 (2006).

To be tested in an upcoming experiment
at OMEGA EP

Relativistic positrons on a bench-top experiment

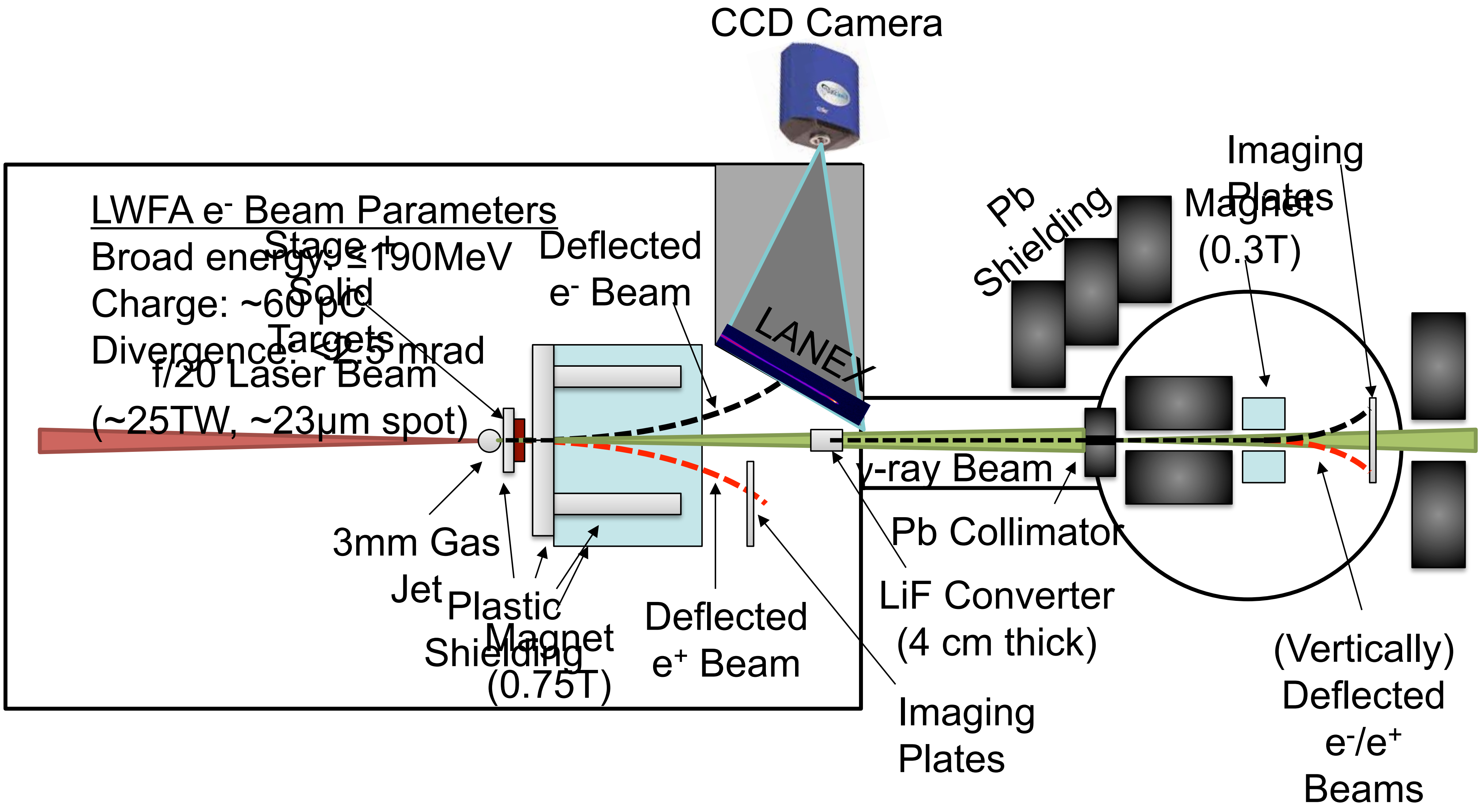

Bremsstrahlung Simulations & Expectations

Input

e^- beam

60 pC total charge
Flat spectra from 10-190MeV

Converter

2.8mm Ta ($4.7\ g/cm^2$, Z = 73)

Output

e^+ beam: 10^{-3} yield with exponential spectra to 140MeV

e^- beam

γ-ray beam: 10^{-2} yield with exponential spectra to 180MeV γ's

- Simulations were performed the with FLUKA Monte-Carlo code
- Output divergence scales as:
  - ~1/E for gamma rays
  - ~1/γ for positrons
- For relativistic beams, temporal spread is minimized

FLUKA Spectral Output

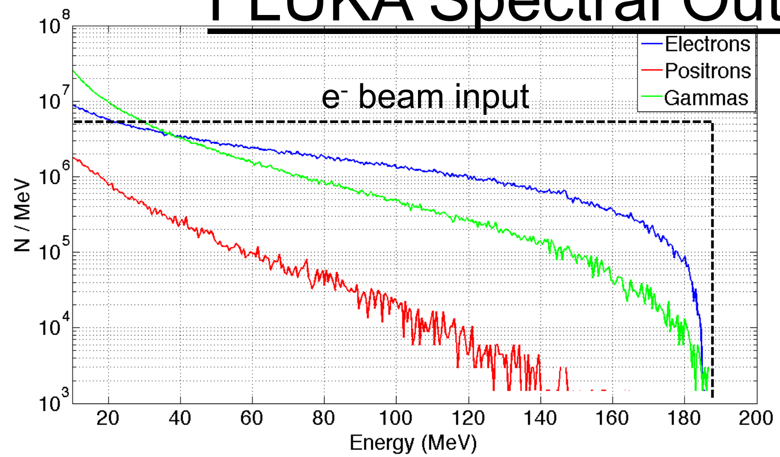

Positron Spectra from 2.8mm Ta Converter

Image Plate integrated over 10 shots

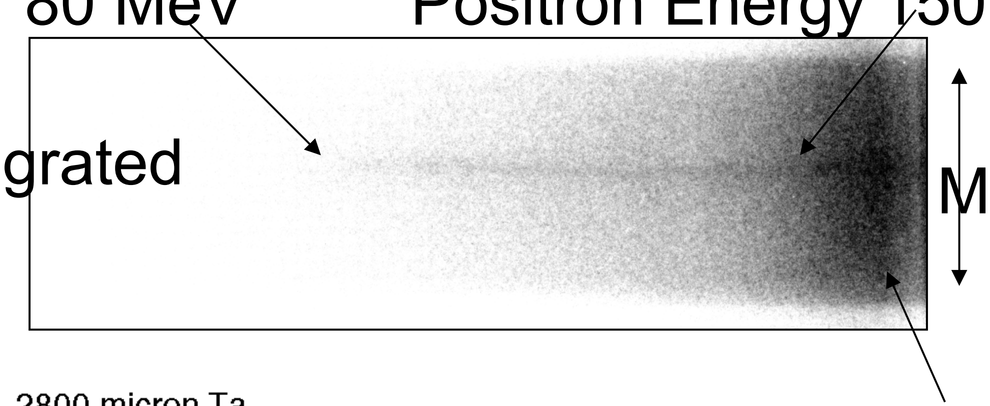

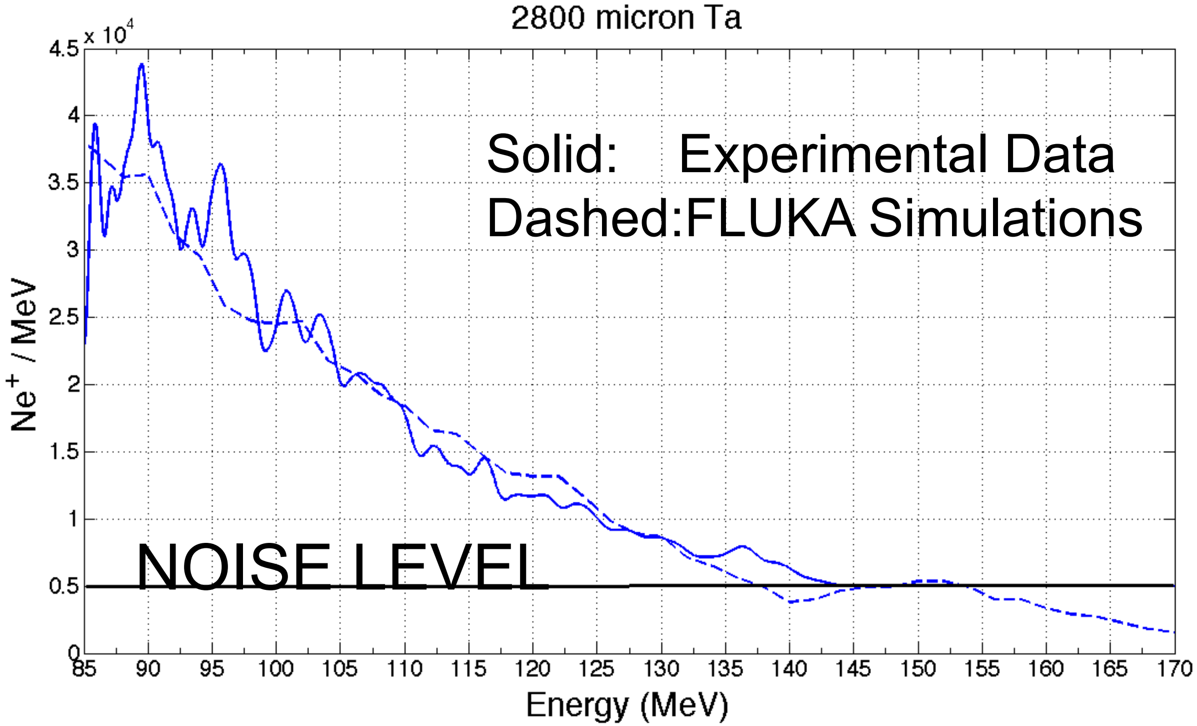

- Positron beam divergence less than 5 mrad overall
- Spectrometer has low energy cut-off of 80 MeV due to shielding in magnet

Observed Positron Yield/Dependence

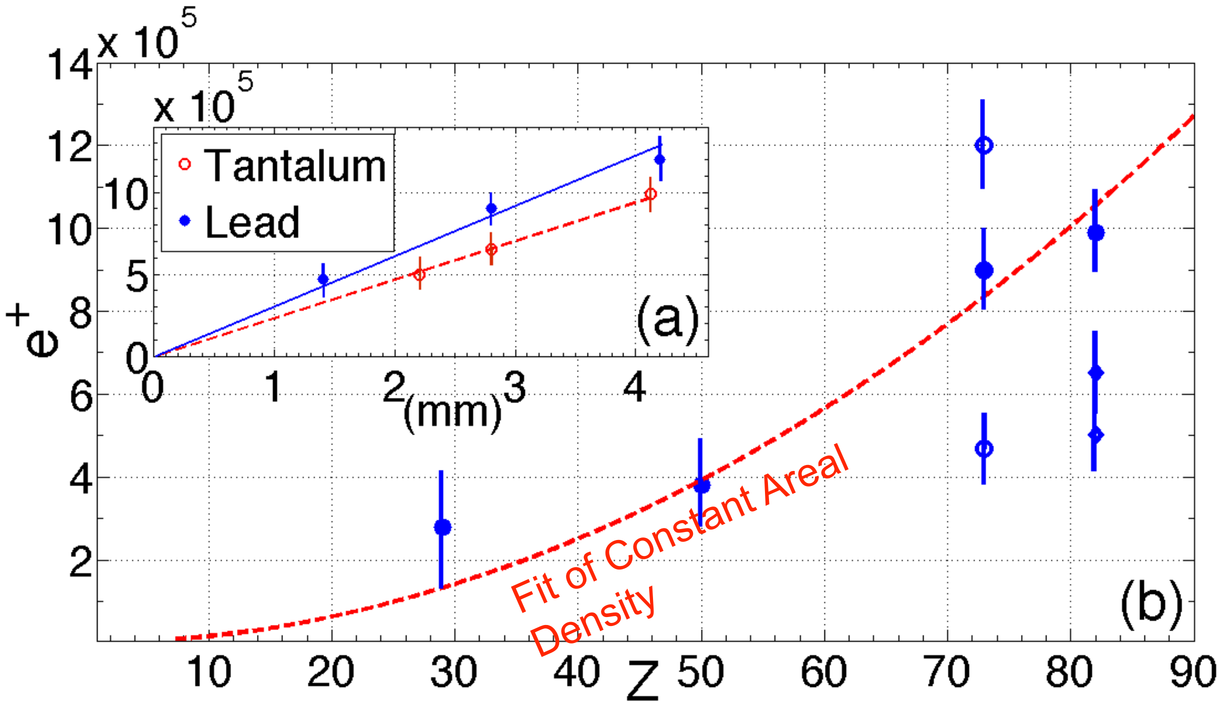

- Yield scales quadraticly with target Z, linear with thickness
  - Evidence of direct Trident process ($e^- + Z \to 2e^- + e^+ + Z$)
- Positron/laser efficiency is nearly 10^6/J at 100 MeV
  - Comparable yield to kJ-class laser experiments [1]
  - Short pulse nature and low divergence preserved

[1] Hui Chen et al. PRL (2009 & 2010)

Summary

- Ultra high magnetic fields (~ 1GGauss) are produced during high intensity (> 10^{19}W/cm^2) laser plasma interactions.

- Lower fields produced by long (nanosecond) pulses are shown to greatly affect the dynamics of the interaction (reconnection and jet formation)

- Relativistic particle beams generated in plasmas may offer a unique experimental environment for investigating plasma physics relevant for astrophysics

Acknowledgements

Center for Ultrafast Optical Science, University of Michigan Ann Arbor MI
Laboratoire d'Optiquee Appliquée (LOA), ENSTA, Palaiseau, France
UCLA/GOLP/USC (Osiris)
Department of Physics, The Blackett Laboratory, Imperial College, London, UK
Queens University Belfast, UK
Technological Educational Institute of Crete, Chania, Crete
University of California, San Diego, USA
Department of Physics, University of Alberta Edmonton, Alberta, Canada
STFC, Central Laser Facility, Rutherford Appleton Laboratory, Oxon.
Lawrence Livermore National Laboratory
LBNL
Massachusetts Institute of Technology